INVESTIGATION OF A NON-LINEAR SUSPENSION IN A QUARTER CAR MODEL

MAHMOUD HOSNI HASSANEIN SALEM

Doctor of Philosophy

ASTON UNIVERSITY

January 2018

ASTON UNIVERSITY

INVESTIGATION OF A NON-LINEAR SUSPENSION IN A QUARTER CAR MODEL

MAHMOUD HOSNI HASSANEIN SALEM

Doctor of Philosophy, 2018

Thesis Summary

This thesis presents the study of a quarter car model which consists of a two-degree-of-freedom (2 DOF) with a linear spring and a nonlinear spring configuration. In this thesis, the use of non-linear vibration attachments is briefly explained, and a survey of the research done in this area is also discussed. The survey will show what have been done by the researches in this new field of nonlinear attachments. Also, it will be shown that this topic was not extensively researched and is a new type of research where no sufficient experimental work has been applied. As an application, a quarter car model was chosen to be investigated. The aim of the Thesis is to validate theoretically and experimentally the use of nonlinear springs in a quarter car model. Design the new type of suspension and insert it in the experimental set up, built from the ground up in the laboratory.

A novel criterion for optimal ride comfort is the root mean square of the absolute acceleration specified by British standards ISO 2631-1997. A new way to reduce vibrations is to take advantage of nonlinear components. The mathematical model of the quarter-car is derived, and the dynamics are evaluated in terms of the main mass displacement and acceleration. The simulation of the car dynamics is performed using Matlab® and Simulink®. The realization of vibration reduction through one-way irreversible nonlinear energy localization which requires no pre-tuning in a quarter car model is studied for the first time. Results show that the addition of the nonlinear stiffness decreases the vibration of the sprung mass to meet optimal ride comfort standards. As the passenger is situated above the sprung mass, any reduction in the sprung mass dynamics will directly have the same effect on the passenger of the vehicle. The future is in the use of a nonlinear suspension that could provide improvement in performance over that realized by the passive, semi active and active suspension. The use of a quarter car model is simple compared to a half car model or a full car model, furthermore in the more complex models you can study the heave and the pitch of the vehicle. For the initial study of the nonlinear spring the quarter car model was sufficient enough to study the dynamics of the vehicle.

Obtaining an optimum suspension system is of great importance for automotive and vibration engineer involved in the vehicle design process. The suspension affects an automobile's comfort, performance, and safety. In this thesis, the optimization of suspension parameters which include the spring stiffness and damper coefficient is designed to compromise between the comfort and the road handling. Using Genetic algorithm an automated optimization of suspension parameters was executed to meet performance requirements specified. Results show that by optimizing the parameters the vibration in the system decreases immensely.

Keywords: Quarter Car, McPherson Suspension, Simulation, Nonlinear Dynamics, Targeted Energy Transfer, Ride Comfort, Genetic Algorithm, Optimization.

Dedication

I would like to dedicate this to my late father, my mother, wife and sons.

Acknowledgements

Firstly, I wish to express my gratitude to Dr. Xianghong Ma for her expert guidance and mentorship and for her encouragement and support at all levels. She is my mentor and I hope one day that I can repay her for all her effort. I am indebted to her.

I am indebted to Dr. Ahmed Abd El Salam for his helpful suggestions during the progress of the PhD. Also, I would like to thank Prof. El-Sayed Saber for giving me the opportunity to work with him and his assistance during my experimental work.

I would like to thank the Arab Academy for Science, Technology and Transport for giving me the opportunity to accomplish this work through the facilities of laboratory and library and for the funding of my PhD.

Finally, I would like to thank my family for their life-long love and support. I dedicate this PhD to my late Father, Hosny Salem, will never forget his support.

Table of Contents

List of Abbreviations

AGOP	Algorithm for Global Optimization Problems
CACSD	Computer Aided Control Systems Design
DADS	Dynamic Analysis and Design System
DOF	Degree-Of-Freedom
DVA	Dynamic Vibration Absorber
ER	Electro-Rheological
GA	Genetic Algorithm
HA-QCSS	Hydraulic Assisted Quarter Car Active Suspension System
HILS	Hardware-In-The-Loop-Simulation
IALR	Institute for Advanced Learning and Research
LO	Linear Oscillator
LQR	Linear Quadratic Control
MOPSO-CD	Multi-Objective Particle Swarm Optimization with Crowding Distance
NES	Nonlinear Energy Sinks
NNM	Nonlinear Normal Mode
NSGA	Non-Dominated Sort Genetic Algorithm
PERL	Performance Engineering Research Lab
PID	Proportional-Integral-Differential

PSA	Pattern Search Algorithm
PSO	Particle Swarm Optimization
RMS	Root Mean Square
SA	Simulated Annealing
SDOF	Single Degree-Of-Freedom
TET	Targeted Energy Transfer
TMD	Tuned Mass Damper
VDV	Vibration Dose Value

List of Tables

List of Figures

1 CHAPTER 1 INTRODUCTION

This chapter gives a brief description on methods to reduce vibration. It also highlights the thesis's motivation and rational, aims and objectives, main contributions and organization. This chapter starts with a brief introduction to the methodology of using a nonlinear attachment to reduce vibration and how this new application can be used on quarter car suspensions. Then it discusses the motivation and rational of this study. Next, the aims and objectives of the thesis are followed by the main contributions of this work. Finally, the thesis organization is given with a brief discussion of the contents of each chapter.

1.1 Introduction

Throughout all aspects of design engineers have been facing a critical problem of finding ways to minimize vibration, one of the solutions found is a device called a dynamic vibration absorber (DVA). If a primary system consisting of a mass-spring system which is subjected to a disturbance of harmonic excitation at a constant frequency; to reduce this vibration by attaching a secondary mass-spring system, with the right configuration response can reach a bare minimum and in some cases zero vibration. This concept was first discovered by Watts (1883) and Frahm (1909). It was shown that by adding a DVA that the vibration dramatically decreased but a DVA made up of only a mass and a spring has its disadvantages, a narrow operation region of performance if the system vibrates at different frequencies the DVA will not be able to adjust, as it is designed just for one frequency. -

To improve on this adding a damper to the DVA configuration, therefore now it consists of a mass, a spring, and a damper. The most important parameters to design a damped DVA are its tuning parameters and damping ratio. Ormondroyd (1928) and Den Hartog (1928) were the first to present a mathematical theory on the damped DVA. After that many efforts have been made to seek optimum parameters for the damped DVA. Den Hartog was the first to find an optimum solution of a damped DVA that is attached to a classical primary system, a system without damping.

Using Magneto-Rheological controllable fluid, dampers were transformed into active dampers, were the fluid can reversibly change from free-flowing, linear viscous liquids to semi-solids having controllable yield strength in milliseconds when exposed to a magnetic field. This feature provides simple, quiet, rapid response interfaces between electronic controls and mechanical systems. MR fluid dampers are relatively new semi-active devices that utilize MR fluids to provide controllable damping forces (Spencer et al. 1997). Chatterjee (2010) studied an active, stand-alone vibration absorber utilizing the state feedback taken from the absorber mass. To improve transient response featuring low peak response and fast attenuation, the design procedure utilized the mode equalization followed by the maximization of the damping. Compared

to the optimum passive absorber, the optimal active absorber can yield a wider bandwidth of operation around the natural frequency of the primary system and a lower frequency response within the suppression band. The active absorber also offers better transient response compared to the passive absorber both optimized for the best transient responses.

The vibration absorber with an active damper is an unstable system, thus providing a challenge to the control engineers or researchers. There are many efforts that have been done to develop the controller for this system, but results show that it is not feasible, for reasons including, cost, added weight or required independent energy supply as shown by Gameel H. (2011). Therefore, research in nonlinear vibration absorber is being investigated due to promising initial results.

Using nonlinear vibration absorbers causes an interesting phenomenon where vibrational energy transfers from the primary system that is initially induced by a force to a carefully designed passive nonlinear sink where the energy is transmitted and diminishes in time due to damping dissipation and this is called Nonlinear targeted energy transfer – TET. The nonlinear energy transfer phenomenon can be utilized for design of engineering systems with vibration and shock absorption abilities.

1.2 Motivation and Rational

The suspension affects an automobile's comfort, performance, and safety. The suspension system suspended the automobile's body a short distance above the ground and maintains the body at relatively constant height to prevent it from pitching and swaying. To maintain effective acceleration, braking, and cornering the components of good handling, the suspension system must also keep all four tyres firmly in contact with the ground.

Nonlinear suspensions have the potential to increase vehicular comfort, performance, and safety. Active suspension requires an accurate suspension model for the controller to predict the suspension's response, unlike the nonlinear model we are using. It requires no controller or any additional power supply. Computer based quarter-car test models are often employed in vehicle dynamics studies as simplified and well-understood systems for such uses as testing new control strategies, designing new suspension systems, and analysing ride dynamics. When available, quarter-car rigs are used to obtain relevant experimental data. A quarter-car test rig is an experimental platform which attempts to replicate the dynamics of one corner of a car. Having an accurate computer model of the test rig used is very valuable since it gives the researcher

more flexibility in experimenting with various scenarios in the virtual world, helps design experiments, and helps perform extensive analysis.

In this study, the focus was on modelling and testing a McPherson strut suspension which was created by Earle (1953). The quarter-car test rig was designed to accommodate a multitude of different suspensions on a chassis of a Hyundai Verna 2014. Also, to study different parameters on experimental rig, masses can be added to simulate different sprung masses. Two degree of freedoms model is used in this thesis, a simplified model of McPherson was found to be sufficient enough for our work to estimate the dynamics applied to the quarter-car rig's sprung mass.

First goal was to identify the quarter-car rig parameters. The quarter car is to be tested on a standard bump at different speeds, and sprung mass loads. The optimization of suspension parameters which include the spring stiffness and damper coefficient is designed to compromise between the comfort and the road handling. The mathematical model of the quarter-car is derived, and the dynamics are evaluated in terms of the main mass displacement and acceleration. The approach starts with the development of a fast and accurate vehicle model in Matlab® and Simulink® combined for testing the parameters and concludes by automated optimization of suspension parameters using genetic algorithm (Davis (1991)), to meet performance requirements specified. Results show that by optimizing the parameters the vibration in the system and adding the nonlinear spring will completely change how the system reacts to bumps.

1.3 Thesis Aims and Objectives

The aim of the thesis is to design a nonlinear suspension based upon the methodology of nonlinear energy transfer. The main objectives of the research involved in this may be summarised as follows:

1. Carry out a detailed review on existing suspension models and various techniques used to decrease vibration of the passenger and increase comfort. State the advantages of the new suspension and disadvantages of previous suspensions.

2. The mathematical model of the quarter-car is derived, and the dynamics are evaluated in terms of the main mass displacement and acceleration. The approach starts with the development of a fast and accurate vehicle model in Matlab® and Simulink®.

3. Study and examine the use of nonlinear attachment phenomenon. Linear components produce constant distributions of energy that decrease the possibility of energy transfers from one mode to another while using nonlinear connections increased the energy transfer in different modes.

4. Design a physical spring that will be able to produce a nonlinear coefficient of stiffness. Obtain the equation of motion of the nonlinear spring and apply them to the mathematical model of the quarter car model. Create a nonlinear attachment, build different prototypes. Perform various compression tests on the new specimens and acquire the most suitable one for a nonlinear effect.

5. Build a quarter car experimental rig based upon the McPherson strut suspension, investigate the current parameters of the model of the car used. Perform tests on rig using sensors, to obtain an analytical proof that the experimental follows the dynamic simulation model.

6. Optimize the suspension parameters which include the nonlinear spring stiffness and damper coefficient using Genetic Algorithm. Apply the optimization model to the experimental work. Therefore, obtaining the least vibration possible at the sprung mass.

7. Apply new prototype spring into the experimental rig and obtaining results using accelerometers on the sprung mass.

8. Compare the final readings of the nonlinear model with a linear model. Discuss the finding from this type of suspension set up.

1.4 Main Contributions

The spring is mechanical part that produce a vibration phenomenon. Building on the basic design of a passive spring, a new type of spring is to be investigated and designed. A new approach to car suspensions is using a nonlinear spring that can be retrofitted to nearly all commercial cars, instead of active suspension that require a lot of control and electrical components. First, the theory of a nonlinear attachment is thoroughly investigated. To build upon this theory an experimental rig is built form the ground up. Various prototype of the nonlinear springs is designed and tested.

Obtaining the optimum parameters for the experimental rig based upon a Hyundai Verna, using genetic algorithm, to obtain the best comfort for the passenger. The genetic algorithm approach concentrates on decreasing the the root mean square of the absolute acceleration, a novel criterion for optimal ride comfort specified by British standards ISO 2631-1997. After installing the appropriate nonlinear spring to the quarter car rig, results were obtained and analysed to further prove that this new type of suspension is a different approach to designing suspensions in the car industry.

1.5 Thesis Organization

This thesis comprises of seven chapters. The thesis has been organized in the following fashion:

- **Chapter 1 Introduction**

This chapter starts with an introduction to the methodology of using vibration absorbers consisting of a nonlinear attachment and how this new application can be used on quarter car suspensions. Then it discusses the motivation and rational of this study. Next, the aims and objectives of the thesis are followed by the main contributions of this work. Finally, the thesis organization is given with a brief discussion of the contents of each chapter.

- **Chapter 2 Literature Review**

In Chapter 2, the published works related to the research of this thesis are reviewed. It includes: 1. Quarter car modelling and optimization history. 2. Different applications to control vibration. 3. Study of targeted energy transfer, which introduced the primary study of the principle of this research. 4. Nonlinear energy pumping. It is the core technique for investigation of targeted energy transfer. 5. A review of different types of nonlinear experimental applications has been reviewed to help the design process.

- **Chapter 3 Methodology of a Nonlinear Attachment**

In this chapter, the theory of nonlinear attachments is explained briefly. Applying it to equation of motions of a vibration absorber to further understand this methodology. Energy analysis is computed and compared to linear model showing the advantages of this new type of attachment. Finally choosing the quarter car as a new application.

- **Chapter 4 Mathematical Model of Quarter Car Suspension System**

A theoretical nonlinear suspension has been developed in this chapter. The energy transfer that occurs is based on complex and non-linearity of the spring stiffness. In this chapter, the theoretical model of a quarter car has been researched. The approach starts with the development of a fast and accurate vehicle model in Matlab® and Simulink® combined for testing the parameters.

- **Chapter 5 Genetic Algorithm**

In Chapter 5, the genetic algorithm is briefly explained. This optimization technique is used to obtain the optimum suspension parameters using Genetic Algorithm, to meet performance requirements specified. The data obtained from the new parameters are analysed and compared to the passive system. In the end of the chapter, a conclusion has been made.

- **Chapter 6 Experimental Set up**

In this chapter, a quarter car experimental setup is developed complying to the simulation model in Chapter 4. Normal suspension model is used initially for preliminary testing. The rig has been tested with different types of nonlinear spring prototypes. The simulation results have been gathered and discussed. The experimental results have been validated by comparing them with the results from the theoretical model. New parameters obtained from the genetic algorithm have been presented and used in the equations of motions and the results are discussed. Finally using the new nonlinear spring, the experimental data has been validated by the simulation results and show the improvement of using this new type of suspension.

- **Chapter 7 Conclusions and Future Work**

The conclusions have been presented as well as the limitations that have been drawn or found during the works in this research. The limitation in the research has been discussed in this chapter. Further study and research has been suggested.

2 CHAPTER 2 LITERATURE SURVEY

2.1 Introduction

The survey in this chapter is divided into two sections. The first section describes the modelling of the front quarter car suspension system, multiple researches in this field study the passive, semi-active and active suspension system of the quarter car. Another important purpose of studies on active suspension system is to achieve force control with different technique using different software. The second section investigates the literature review on the phenomenon of energy transfer through a nonlinear connection. There are many methods that can be used to analyse targeted energy transfer, in this section the different configurations and methods will be explained along with a review of the past research implemented using them.

2.2 Literature Review on Modeling of a Quarter Car Suspension

Suspension system, system that connects the wheels of the automobile to the body, in such a way that the body is cushioned from jolts resulting from driving on uneven road surfaces. The suspension affects an automobile's comfort, performance, and safety.

The suspension system suspended the automobile's body a short distance above the ground and maintains the body at relatively constant height to prevent it from pitching and swaying. To maintain effective acceleration, braking, and cornering the components of good handling, the suspension system must also keep all four tyres firmly in contact with the ground

The automotive suspension system is designed to compromise between the comfort as the road handling can be improved by using the electronically controlled suspension system.

Basically, there are three types of car suspension system; passive, semi-active and active suspension system. A passive suspension system includes the conventional springs and shock absorbers. Such system has an ability to store energy via spring and to dissipate in via damper. To achieve a certain level of compromise between road holding, load carrying and comfort, its parameters are generally fixed. (Patil et al. (2014))

A semi-active suspension system provides controlled real-time dissipation of energy. A mechanical device called active damper is fixed in parallel with a conventional spring. It does not provide any energy to the system.

Active suspension system has an ability to store, dissipate and to introduce energy to the system. The

hydraulic actuator is connected in parallel with a spring and absorber. While, sensor of the body is located at different points of the vehicle to measure the motions of the body. It may vary its parameters depending upon operating conditions. The active suspension is equipped with sensors, which are linked to a powerful computer system, which has information about the vehicle and its response to different road conditions.

Automotive manufacturers started to try to improve their current passive suspension and experimented using the principle of active and semi-active suspensions started to be increasingly employed in high-end luxury cars as they improve comfort and stability despite their high price and power consumption (Ren et al. (2007)). The semi-active was first introduced by Karnopp and Crosby in the early 1970s, (Crosby et al. (1974)) based on the well-known skyhook control. The damping coefficient is varied by variety of methods but still the suspension system can only dissipate the road forces and can't add additional force to the system. With the right control system, the passive suspension's compromise can be reduced resulting in a smart system making cars comfortable regardless of the road they are driven on.

The early studies on active suspensions performed by Hrovat (1997) included numerous approaches such as modal analysis, eigenvalue assignment, model order reduction, nonlinear programming, multi-criteria optimization, and optimal control. Classic control methods have also been considered, such as root locus, Bode diagrams, and Nichols plots. Before applying any of those control techniques well-defined, linear model for the system is a necessity. To design the controller, linearization of the system is a must. The main obstacle for commercialization of such systems is the significant power requirement. To reduce the cost associated with the required power, practical active suspension designs generally function as a low-bandwidth system that requires 4 kW of peak power for road vehicle applications.

The system process information obtained from the sensors and then sends a signal to provide and appropriate response in the actuator. The computer system and actuator will keep the car level on a smooth surface. However, if the vehicle were to encounter an irregularity in the road surface or a bend, then the signals from the sensors will enable the computer system to calculate the change in load in that actuator and cause response to compensate for the change in load. Drivers are not aware of any minor change in road conditions, since the time for the sensors to detect the change and the actuator to respond is a matter of milliseconds. The active suspension system must support the car, provide directional control during car handling and provide effective isolation of passengers or payload from road disturbances. Figure 2.1 shows the passive, semi-active and active car suspension system.

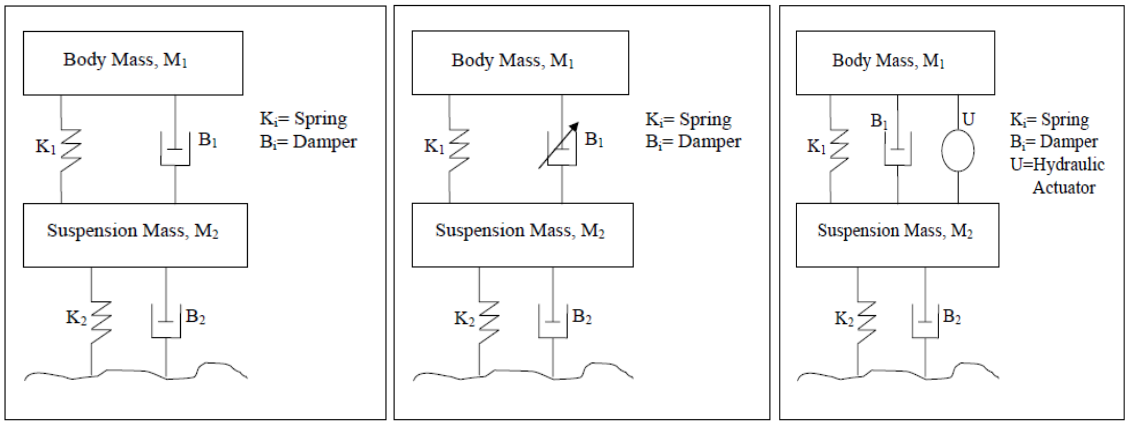

(a) Passive **(b) Semi-Active** **(c) Active**

Figure 2.1 Suspension System Classifications

As passengers spend more time in their vehicles comfort has become one of the major aspects of choosing one's vehicle. Car manufacturers are competing to provide the utmost level of comfort by modifying their suspension systems to cope up with the road bumps and potholes. The input over which the vehicle design engineers and vehicle drivers have the least amount of control is the excitations arising from road roughness and road bumps which affect the vehicle ride comfort, it is.

There are three different types of potholes which are smooth, non-smooth and statistical potholes (Pazooki, et al. (2012)).

Choi et al. (2001) performed field test to evaluate performance characteristics of a semi-active electrorheological suspension system associated with skyhook controller. They demonstrated that ride comfort and steering stability of the vehicle were improved. Pazooki, et al. (2012) showed that semi-active systems have advantages over active systems, including low power requirements, simplicity, ease of implementation and low-cost.

Omar et al. (2017) designed a fully active electro-hydraulic and passive automotive quarter car suspensions experimental test-rigs. Investigation of the active performance compared against the passive is performed experimentally and simulated numerically utilizing SIMULINK's Sims cape library. Both systems are modelled as single-degree-of-freedom to simplify the validation process. Position sensors for sprung and unsprung masses are installed to obtain the experimental results. The road input is introduced by a cam and a roller follower mechanism driven by 1.12 kW single phase induction motor with speed reduction

assembly. The active hydraulic cylinder was the most viable choice due to its high power-to-weight ratio. The control that was used is a proportional-integral-differential (PID) type. Applying the controller on the electro-hydraulic suspension improved the ride comfort significantly, as shown by the results; 24.8% sprung mass vibration attenuation is achieved.

Bello et al. (2014) constructed a state space model for 2 DOF quarter car using full state feedback controller numerically via Simulink. For step input of 0.1 m, the sprung mass acceleration and displacement of the active system has been reduced by 80% and 11% respectively compared to the passive system which shows an improvement in the ride comfort, also, the rattle space usage was reduced by 92.5% compared to the passive suspension system. The settling time in all cases was about 2 s.

Bello et al. (2015) and Venkateswarulu et al. (2014) modeled a nonlinear 4 DOF half vehicle model containing an active suspension system model. The controller used for the active suspension was a PID controller. The constructed model ignored nonlinearities in the hydraulic actuator as their effect was minimal and was created numerically using Matlab/Simulink. A sinusoidal road input disturbance was introduced to the system, results show that a 52.29% and 57.47% reduction in front and rear suspension deflection by using the active suspension compared to the nonlinear passive model. It was concluded that regardless of the power consumption of the active system, it had better performance.

Fayyad (2012) and Kumar et al. (2007) and Elattar et al. (2016) designed a PID controller for a Quarter car model to improve the ride comfort and road holding ability. Kumar found that ride comfort was improved by 78.03% and suspension travel has been reduced by 71.05% with active system while Fayyad showed numerically that for the step input of 80 mm, the sprung mass displacement has been reduced by 25% while compared to passive one both experimentally and numerically. Elattar compared between PID and PDF controllers and showed that although both showed improved performance, PDF has more potential.

Gobbi and Mastinu (2001) presented Multi-Objective Programming and Monotonicity analysis-based optimization method for finding the trade-off for conflicting performance requirements such as discomfort, road holding and working space. A 2 DOF quarter car model running on random road profile was used. The optimal settings of the vehicle suspension parameters such as tyre stiffness, spring stiffness, and damping were derived numerically.

Choi et al. (2008) and Yao et al. (2001) discussed the design and control of the Magnetorheological (MR) dampers via several techniques while utilizing Hardware-in-the-loop-Simulation (HILS) methodology. And a semi-active suspension utilized is the Electro-rheological (ER) damper system.

Zhao et al. (2017) derived the equation of motion of a 3-DOF (degree-of-freedom) model of quarter-car consisting of the suspension, driver and cushion, from which he obtained the driver RMS (root-mean-square) acceleration response under random excitation generated by road irregularities. The driver RMS acceleration values are calculated from the measured data and from the analytical formulae of the 3-DOF and is compared to the classical 2-DOF mode. The results show the analytical formula for the 3-DOF model provides a more reasonable approximation of the real response of the test car. Also studied was the effects of vehicle parameters on the driver RMS acceleration are studied. Finally, to provide critical foundations for the selection of the cushion damping, the optimal damping ratio of driver-cushion system is deciphered from the analytical formula. This formula can be used in preliminary design for the driver-cushion system.

Shirahatti et al. (2008) studied a passenger car optimizing the car parameters using a passive and active to meet the criterion of road comfort according to ISO 2631-1997 standards. Many objectives such as maximum bouncing acceleration of seat and sprung mass, root mean square (RMS) weighted acceleration of seat and sprung mass as per ISO2631 standards, jerk, suspension travel, road holding, and tyre deflection are minimized subjected to a few constraints. The constraints arise from the practical kinetic and comfortability considerations, such as limits of the maximum vertical acceleration of the passenger seat, tyre displacement and the suspension working space. The genetic algorithm (GA) is used to solve the problem and results were compared to those obtained by simulated annealing (SA) technique and found to yields similar performance measures. Both the passive and active suspension systems are compared in time domain analyses subjected to sinusoidal road input. Results show passenger bounce, passenger acceleration, and tyre displacement are reduced by 74.2%, 88.72% and 28.5% respectively, indicating active suspension system has better potential to improve both comfort and road holding.

Cui et al. (2017) researched a quarter car with nonlinear active suspension on a rough road. According to the relative motion principle, the study of the effect of the rough road is a force is affected by the noise. The model has been simulated including a random rough excitation force. By an appropriate transform, the model is transformed into a lower triangular system, which can be used as back stepping method. Then a controller is designed such that the mean square of the state converges to an arbitrarily small neighbourhood of zero by tuning design parameters. The simulation results illustrate the effectiveness of using the controller. Therefore, concluding that the active suspension system offers better riding comfort and vehicle handing to the passengers.

Nagarkar et al. (2016) modelled a nonlinear quarter car suspension–seat–driver model for optimum design. This model consisted of a quadratic tyre stiffness and cubic stiffness in suspension spring, frame, and seat cushion with 4 degrees of freedom driver model. The system is modelled and optimized to the comfort and

health criterion comprising of Vibration Dose Value (VDV) at the head, frequency weighted RMS head acceleration, crest factor, amplitude ratio of head RMS acceleration to seat RMS acceleration and amplitude ratio of upper torso RMS acceleration to seat RMS acceleration along with stability criterion comprising of suspension space deflection and dynamic tyre force. ISO 2631-1997 standard was adopted to assess ride and health criterions. Suspension spring stiffness and damping and seat cushion stiffness and damping are the design variables. Non-dominated Sort Genetic Algorithm (NSGA-II) and Multi-Objective Particle Swarm Optimization – Crowding Distance (MOPSO-CD) algorithm are implemented for optimization. Simulation result shows that optimum design improves ride comfort and health criterion over classical design variables. Optimization of the car suspension–seat–driver system is successfully implemented using NSGA-II and MOPSO-CD with penalty function algorithms. The MOPSO-CD algorithm takes less computation time as compared to NSGA-II for optimization. Numerical simulations are presented for optimum design variables of a quarter car suspension–seat–driver system obtained by implementing NSGA-II and MOPSO-CD algorithms. Results of a quarter car travelling over a Class C road (average road) at speed 80 km/h are presented to show its performance. For class C road, RMS head acceleration and VDV at head increase with increase in speed. Simulation result shows that optimum design variables improve ride comfort and health criterions over classical design variables.

For the models with Agharkakli et al. (2012) obtained a mathematical model for the passive and active suspensions systems for quarter car model. Current suspensions use passive components consisting of a spring and damping coefficient with fixed rates. To be a functioning suspension it must improve handling and increase passenger comfort. Passive suspensions only offer compromise between these two conflicting criteria. Active suspension is an improvement to traditional design as it can choose between handling and comfort which do not go hand by hand by directly controlling the suspensions using force actuators. The purpose is to design a controller which will improve performance of the system compared to passive suspension. A Linear Quadratic Control (LQR) technique is implemented to the active suspensions system for a quarter car model at different types of road profiles. The performance of the controller is compared with the LQR controller and the passive suspension system. Suspension travel in active case has been found reduced to more than half of their value in passive system. By including an active element in the suspension, it is possible to reach a better compromise than is possible using purely passive elements. Though it is a complicated process and require electrical and control components.

Verros et al. (2005) presents a methodology for optimizing the suspension damping and stiffness parameters of nonlinear quarter-car models subjected to random road excitation. The investigation starts with car models involving passive damping with constant or dual-rate characteristics. Then, examining the car models where the damping coefficient of the suspension is selected so that the resulting system approximates

the performance of an active suspension system with sky-hook damping. Verros investigated the effect of road quality and the effects related to wheel hop. The results show a critical comparison is performed between vehicles with passive linear or bilinear suspension dampers and those obtained for cars with semi-active shock absorbers.

Taffo et al. (2016) investigated a two-degrees-of-freedom nonlinear quarter-car model with time-delayed feedback control. Time delay has destabilizing effects in mathematical models. In this work a system was explored where a time delay can be both stabilizing and destabilizing. The critical control gain for the delay-independent stability region and critical time delays for stability switches are derived using the generalized Sturm criterion. There is a small parameter region for delay-independently stability of the system. Once the controlled system with time delay is not delay-independently stable, the system may undergo stability switches with the variation of the time delay. These stability switches correspond to Hopf bifurcations that occur when the time delays cross critical values. Properties of Hopf bifurcation such as direction and stability of bifurcating periodic solutions are determined by using the normal form theory and centre manifold theorem. The numerical simulations support the theoretical analysis and can provide critical conditions that can guide through the process of the design of vehicles with significant reduction of vibration to increase the passengers ride comfort.

Bououden et al. (2016) proposes the Takagi-Sugeno fuzzy approach to design a robust nonlinear multivariable predictive control for nonlinear active suspension systems. The controller design is converted to a convex optimization problem with linear matrix inequality constraints. The stability of the control system is achieved using terminal constraints, the terminal constrained is Constrained Receding-Horizon Predictive Control algorithm to maintain a robust performance of vehicle systems. A quarter-car model with active suspension system is modelled and numerically employed to illustrate the effectiveness of the proposed approach. The obtained results are compared with model predictive control in terms of robustness and stability and show that using this method.

A half car model (front and rear) is used to study the heave and pitch motions (Moran and Nagai, 1994; Vetturi et al., 1996; Campos et al., 1999). Four degree-of-freedom model allows the study of the heave and pitch motions with the deflection of tyres and suspensions. The full car model requires a more complex analysis while the half-car model is relatively simple to analyse and the response of the system is easily obtained using Matlab simulation (Oueslati and Sankar, 1994). Therefore, many researchers often use it. A more complex model is the full vehicle model which is a four wheel model with seven degree-of-freedom done for studying the heave, pitch and roll motions (Ikenaga et al., 2000).

Rao et al. (2008) studied a four degree-of-freedom half-car model traversing at constant velocity a random road and used a semi-active controller for the response. The suspension spring is assumed to be hysteretic nonlinear and modelled by the Bouc–Wen model but is considered a standard normal helical spring. The design of the spring in this work in the same as the conventional spring. Statistical linearization technique is used to derive linearize the equation of motion. Suspension stroke, road holding, and control force are the parameters used to optimize the response of the vehicle. The RMS values of the suspension stroke, road holding, and control forces are computed using the spectral decomposition method. The results for the equivalent linear model obtained by the spectral decomposition method are verified using Monte Carlo simulation. It is shown that the control results produced a better vehicle performance.

Lin et al. (2004) researched a nonlinear back stepping design scheme, which is developed for the control of half-car active suspension systems to improve the opposing effects to ride quality and suspension travel. Vertical and angular displacements of a vehicle body are the factors that ride quality depend on. The design of active suspensions must have the ability to minimize heave and pitch movements to guarantee the ride comfort of passengers. The study shows an improvement of trade-off between ride quality and suspension travel through comparative simulations.

2.3 Literature Review on Quarter Car Experimental Rigs

In this chapter, a background of the current state-of-the-art in vehicle testing rigs and the controls they utilize is reviewed. The chapter begins with a survey of the current test rig technology and some of the issues or deficiencies found with them. This will lay the groundwork for defining the new requirements of the quarter-car rig design presented in this thesis. This section will show that all the work done on semi-active or active dampers with different types of controllers. None of the work done before is based upon nonlinear spring attached to the experimental rig.

The rig used in this thesis is based on the McPherson strut suspension therefore the historical and the applications will be reviewed. This configuration has several advantages. The McPherson strut suspension, designed in the late 1940s by Earl Steele Macpherson, was first used on the 1949 Ford Vedette (Gilles (2004)). As such, it is a relatively new suspension configuration. Mantaras et al. (2004) states that the clear majority of current small- and medium-sized cars use this configuration. The McPherson strut suspension configuration consists of a lower control arm and telescopic strut attached to the body of the car and to the wheel carrier, which is also called an upright. It is often the case that the primary spring and damper are co-linear with the strut's line of translation.

Gillespie (1992) points out that its inherent L-shape aids with the packaging of transverse engines. Likewise, as Daniels (1988) notes, its three mounting points can be widely spaced, thereby allowing this configuration to be made structurally efficient. Daniels also notes that camber angle change with suspension travel is small. A final advantage is the ease with which the strut can be replaced. Nevertheless, this type of suspension configuration also has some disadvantages. From a packaging standpoint, although beneficial for transverse engines, this configuration's high installation height limits the designer's ability to lower the hood height (Gillespie (1992)). From a performance standpoint, Daniels notes that the effect of the rolling force increases the further the body rolls due to the roll center migration incurred with this suspension. Daniels also notes that roll center migration on a double wishbone suspension creates no serious problem (Daniels (1988)). Another performance compromise Milliken et al. (1995) mentions is that McPherson strut suspensions lose negative camber when the suspension travels upward.
Despite these disadvantages, manufacturers such as Porsche and BMW use this suspension to great effect in their road racing efforts. Likewise, consumer car makers such as Toyota and General Motors use them effectively on their passenger vehicles.

There are several examples of prior work on correlating experimental and dynamically simulated suspensions. Trom et al. (1987) developed a multibody dynamics model of a mid-sized passenger car with front McPherson strut suspension in Dynamic Analysis and Design System (DADS) software. Dynamic simulations with this model are compared to corresponding experimental data.

Park et al. (2003) used model data from Salaani et al. (2001) to create a full vehicle ADAMS simulation. This work addressed how to refine kinematic steering and suspension models using measurement data. Ozdalyan et al. (1998) developed an ADAMS suspension model to replicate a Peugeot 605 McPherson strut suspension that provides insight into how suspension parameters change in relation to each other. The wheel rate, camber angle, caster angle, steer angle, and track change with suspension travel is predicted in ADAMS and compared to the same experimentally-measured values obtained from the Peugeot.

Rahnejat (1998) discusses the formulation and analysis of a simplified multibody dynamics 2D McPherson strut suspension model. Gillespie (1992) develops a linear quarter-car model to describe vehicle response properties such as sprung mass isolation and transmissibility. Inman (2017) develops a base excitation model that can be used to represent a quarter-car suspension. Five semi-active control policies are tested on a full-scale 2 degree-of-freedom quarter-car system incorporating a magneto-rheological damper in Goncalve's (2001) experimental study. Mantaras (2004) presents a set of kinematic constraints used to model a 3D McPherson strut suspension.

Patil et al. (2016) developed a prototype of light passenger quarter car to be experimented upon to achieve improved vehicle ride characteristics. A hydraulic assisted quarter car active suspension system (HA-QCSS) is designed and compared to a passive suspension system with the objective to analyse vehicle ride characteristics. A hydraulic actuator has been selected for active damping in active suspension system because of its high power-to-weight ratio. The simulation model of the two degree of freedom model is simulated using MATLAB. The details of the test set-ups development for the passive and hydraulic assisted quarter car active suspension system (HA-QCSS), MATLAB analysis and experimental analysis results are shown. The results show considerable improvement in vehicle ride characteristics over the conventional passive system

Ahmadian et al. (2000) studied the performance of three semi-active control policies, the skyhook control, ground hook and hybrid control. The three performances are tested using a single suspension fitted with a semi-active suspension consisting of a magnetorheological damper that is tuned for this study. The three semi-active control policies are explained and the results of a series of experiments with each control policy are presented. Using transmissibility plots of the test results confirm effects of each control policy. Skyhook control showed the most significant reduction in the transmissibility of the sprung mass, as compared to the passive damper. Similarly, the ground hook control substantially reduces the unsprung mass transmissibility. When the sprung mass transmissibility decreases it results in improving the ride comfort, less wheel hop, therefore resulting in better road holding ability and improved vehicle stability. A hybrid control combined the effect of skyhook and ground hook, indicate that it holds the promise of achieving a semi-active control policy that can be slowly adapted to the driving condition and vehicle dynamics for better vehicle stability and ride comfort.

Lauwerys et al. (2005) presents a design of a robust linear controller for an active suspension mounted in a quarter car test-rig. Unlike most active suspension control design methods, this approach can be used using a simplified linear model, unlike the nonlinear which is very time consuming to derive. Computer Aided Control Systems Design (CACSD) software tools were used for the linear techniques well obtaining a fast control design approach, applicable to almost any active suspension system. Linear black box models are identified using frequency domain identification techniques, while robust linear control design techniques ($H\infty$ and μ-synthesis) account for the model uncertainties introduced by the linear model approximation of the nonlinear dynamics. Although this linear approach is over simplified, the results shows that the desired performance is achieved in simulation as well as on the experimental test-rig.

Burton et al. (1995) analysed and controlled a model of a prototype self-levelling active suspension system for road vehicles. Self-levelling systems is a better approach than fully active designs which are currently

regarded as impractical due to the cost and fuel-consumption penalties. Disturbances affecting the automotive suspension systems are due to the irregularities in road surface elevation and dynamic (inertial) forces resulting from driving manoeuvres such as steering and braking. Analysis of the suspension system is done for a linear and nonlinear dynamic modelling of a quarter car for which a suitable controller is designed. The analytical work is supported for both the active and passive suspensions by experimental results taken from a full-scale hydraulically powered quarter-car suspension test rig.

Andersen Erik (2007) modelled and simulated a linear and a non-linear quarter-car suspension model based upon the McPherson strut. Due to the angles inserted in the equations of motion they are consider a nonlinear equation. Both models' dynamic response is developed using Lagrange multiplier which is customary to multibody dynamics so that the same numerical integrator can be used to compare their respective performances. The response of these models to an excitation of a band-limited random tyre displacement time array is then simulated using a Hilber-Hughes-Taylor integrator. The models are constructed to match the dynamic response of a state-of-the-art quarter-car test rig that was designed, constructed, and installed at the Institute for Advanced Learning and Research (IALR) for the Performance Engineering Research Lab (PERL) based upon a front left McPherson strut suspension from a 2004 Porsche 996 Grand American Cup GS Class race car. Using the experimental rig, their optimal parameters are obtained by performing system identification. The performance of both models using their respective optimal parameters is presented and the results show that the experimental rig has been simulated and modelled correctly.

Thite et al. (2017) studied the influence of the series stiffness on the effective suspension damping both experimentally and numerically. A frequency domain analysis of two-degree of freedom Zener quarter car model is to find the relation between effective damping coefficient and the limiting value of damping ratio for a given series stiffness which is very complex. A four-post experimental rig set-up is used to validate the results by measuring transmissibility's, giving damping ratios for varying shock absorber settings. A closed form solution, based on a simplified partial model, of optimal damping coefficient, which is a nonlinear function of stiffness, shows good agreement with numerical simulations of the complete system. The nonlinearities in shock absorbers also influence the outcome. These findings can be a great value at early design stage.

The literature review of the modelling of a quarter car shows us that a clear majority of the researchers used semi-active and active suspension with different types of controllers. A lot of the work stated the complexity to using the controller, and that it requires an accurate model of the vehicle model. The requirement of an external power supply also was a hardship in the design of the overall vehicle. Therefore, using a new passive suspension with new nonlinear mechanical properties is the focus of our thesis. The advantages of

a passive system are its simplicity, low cost and the ability to mass produce it. Further investigation of the new research of nonlinear attachment will be shown in the next section.

2.4 Literature Review of Non-linear Attachment Analysis

This section reviews three main parts: Non-linear Attachment Analysis, Targeted Energy Transfer and practical implementation of this theory. There are many methods that can be used to analyse targeted energy transfer, in the following subsections the different configurations and methods will be explained along with a review of the past research implemented using them.

The phenomenon of energy transfer through a nonlinear connection was researched by Gendelman (2001) who investigated the dynamics of a two-DOF system consisting of a damped linear oscillator (LO) which is the primary system that was connected to a weakly coupled nonlinear damped attachment. Comparisons between linear and nonlinear DVA showed that through using systems with linear components produce constant distributions of energy that decrease the possibility of energy transfers from one mode to another while using nonlinear connections increased the energy transfer in different modes. An advantage of using nonlinear connections that is not limited to one resonant frequency, it can work for various frequencies therefore it is more efficient than a linear connection that only works with one frequency.

For the vibration absorber to absorb the initial energy inserted into the LO, a nonlinear normal mode (NNM) localized to the nonlinear attachment must satisfy the condition that the energy is above a critical threshold. As a result, TET occurs and a significant portion of the imparted energy to the LO gets passively absorbed and locally dissipated by the essentially nonlinear attachment, which acts as nonlinear energy sink (NES).

A different nonlinear attachment was considered in Gendelman et al. (2001) and Vakakis and Gendelman (2001) were the nonlinear oscillator (the NES) was connected to ground using an essential nonlinearity. This configuration is depicted in Figure 2.2.

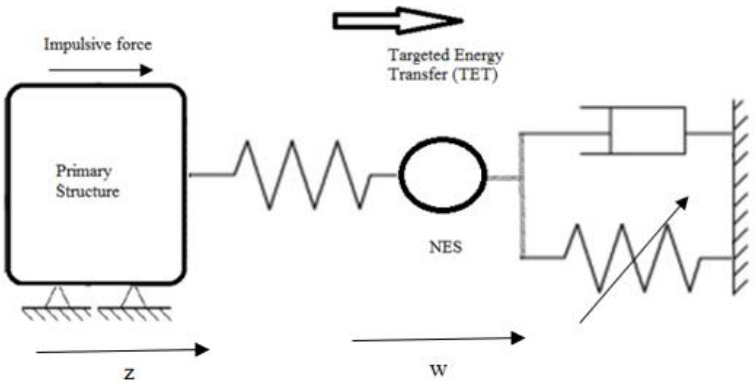

Figure 2.2 Configuration I: Impulsively Loaded Primary Structure Weakly Coupled to a Grounded NES.

TET was defined as the one-way irreversible channelling of vibrational energy from the initially excited primary system to the attached NES.

To improve on the configuration (referred to as NES Configuration I) where heavy nonlinear attachments were used which is considered a limitation to actual applications. To further improve the configuration Gendelman et al. (2005) introduced a lightweight and ungrounded NES configuration II which led to a more efficient nonlinear energy pumping from the LO to which it was attached. This alternative configuration is depicted in Figure 2.3.

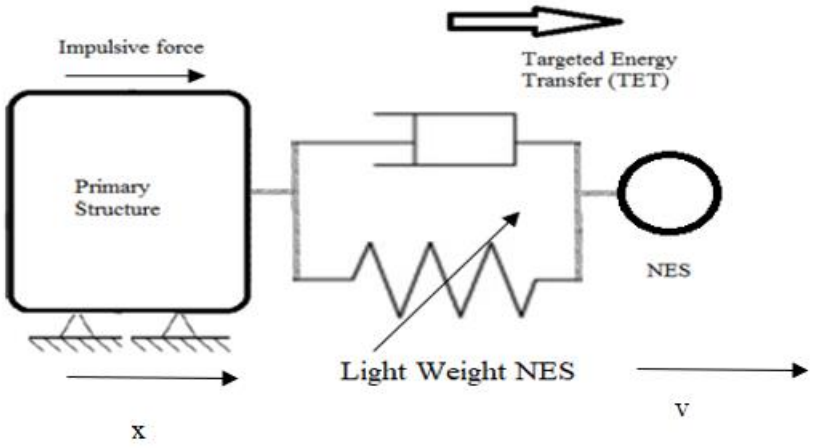

Figure 2.3 Configuration II: Impulsively Loaded Primary Structure Connected to an Ungrounded and Lightweight NES.

Through the substitution of variables in the equations of the two NES configurations related by Kerschen et al. (2005) we can show that Configuration II nearly resembles a primary system with an attached grounded NES of Configuration I to show this, we consider the simplest possible system with an NES of Configuration II, namely a SDOF LO with a SDOF ungrounded nonlinear attachment,

$$\ddot{x} + x + C(x - v)^3 = 0 \tag{2.1}$$

$$\varepsilon\ddot{v} + C(v - x)^3 = 0 \tag{2.2}$$

(Config. II NES).

where

$$\varepsilon = \frac{m_2}{m_1} \qquad C = \frac{k_2}{m_1} \tag{2.3}$$

In the above system, the light weight of the NES is ensured by requiring that $0 < \varepsilon \ll 1$; ε being the ratio between secondary mass and main mass. While x & z being the motion of the primary system (LO) and v & w being the motion of the NES. Through the change of variables,

$$\boldsymbol{x = \varepsilon(z - w)} \tag{2.4}$$

$$\boldsymbol{v = \varepsilon z + w} \tag{2.5}$$

The above system is expressed as

$$\boldsymbol{\varepsilon(1 + \varepsilon)\ddot{z} + \varepsilon(z - w) = 0} \tag{2.6}$$

$$\boldsymbol{(1 + \varepsilon)\,\ddot{w} + \varepsilon(w - z) + \frac{C(1 + \varepsilon)4}{\varepsilon} w^3 = 0} \tag{2.7}$$

(Config. I NES).

After investigating the equations, we see that equation (2.7) corresponds to a linear primary system composed of a mass with no grounding stiffness linearly coupled to an NES of Configuration I. Comparing the two systems shows that an ungrounded NES (Config. II) with small mass ratio ε, is equivalent to a grounded NES (Config. I) with large mass ratio (1 + ε) / ε. This result shows that using the NES Configuration II is more efficient because you can use lighter vibration absorbers therefore it is more applicable, while the NES Configuration I requires a much heavier mass and is relatively unpractical to be used as a vibration absorption device.

2.5 Targeted Energy Transfer Methodologies Survey

To analyse TET researchers considered different methodologies to observe energy transfer from the two connected structures. Vakakis (2001) studied a 2-DOF system with nonlinear attachments and showed that these attachments can be designed to act as passive sinks of unwanted vibrations generated by external impulsive excitations. He proved that the dynamical phenomenon of energy pumping from a vibrating

system to the attached nonlinear sink can be achieved. Gendelman et al. (2003) analytically studied the degenerate bifurcation structure of the free periodic solutions of an essentially nonlinear system in 1:1 internal resonance. Vakakis and Rand (2004) discussed the resonant dynamics of the same undamped system and concentrated their study on the influence of damping on the resonant dynamics and TET phenomena in the damped system.

A suitable tool for analysing energy was shown in the superposition of a frequency-energy plot (FEP) depicting the periodic orbits of the underlying Hamiltonian system, to the wavelet transform (WT) spectra of the corresponding weakly damped responses represents exchanges and transfers taking place in the damped system where introduced by Kerschen et al. (2005).

A procedure for designing passive nonlinear energy pumping devices was developed in Musienko et al. (2006). To further improve on this Koz'min et al. (2007) employed global optimization techniques of optimal transfer of energy from a linear oscillator to a weakly coupled grounded nonlinear attachment.

Lee et al. (2006) focused on the dynamics of the underlying Hamiltonian system, producing periodic orbits of a nonlinear system on a frequency-energy plot (FEP). The plot showed a backbone curve with periodic orbits satisfying the condition of fundamental (1:1) internal resonance; secondly it also showed a countable infinity of subharmonic branches, with each branch corresponding to a different realization of a subharmonic resonance between the LO and the NES.

To study the TET dynamics using a different method Gendelman (2004) computed the damped NNMs of a LO coupled to an NES using the invariant manifold approach which resulted in that the rate of energy dissipation in this system is closely related to the bifurcations of the NNM invariant manifold. To further this research Panagopoulos et al. (2007) analysed how initial conditions determine the specific equilibrium point of the slow flow dynamics that is eventually reached by the trajectories of the system.

Manevitch et al. (2007a, 2007b), Quinn et al. (2008) and Koz'min et al. (2008) studied the conditions and parameters that should be monitored to obtain maximum TET at the least time where most of the vibration energy of the LO gets transferred and locally dissipated by the NES.

Cataldo et al. (2013) concentrated his research on three uncertain parameters of the nonlinear system, the nonlinear stiffness and the two dampers. Then a sensitivity analysis was performed, considering different levels of energy dispersion, and obtained in conclusion of the influence of the uncertain parameters in the robustness of the system.

A must for TET is to have damping, without it the system can only exhibit nonlinear beat phenomena where the conserved energy gets continuously exchanged between the linear primary system and the nonlinear attachment and no TET can occur.

2.5.1 Practical Implementation

All the previous studies were theoretical; to take the research to another level experimental work must be investigated. Considered a new research the first experimental report of nonlinear energy pumping was provided by McFarland et al. (2005a), providing evidence that energy pumping can be used in practical applications. To further expand experimental work Cochelin et al. (2006) used nonlinear energy pumping in acoustic applications.

In Kerschen et al. (2006a), he approached the energy exchanges in the damped system based on the topological structure and bifurcations of the periodic solutions of the underlying undamped system. Results show that TET can be obtained by two distinct mechanisms, namely fundamental and subharmonic TET. Also found a third mechanism, which relies on the excitation of so-called impulsive periodic and quasi-periodic orbits, is necessary to initiate either one of the TET mechanisms through nonlinear beating phenomena. These impulsive orbits were studied using different analytic methods in Kerschen et al. (2008). These theoretical findings were validated experimentally in McFarland et al. (2005b).

Z. Nili Ahmadabadi (2011) realized that TET using an NES with hysteretic nonlinearity can be achieved, investigating the effect of an attached nonlinear energy sink on energy suppression of a cantilever beam under shock excitation. Grounded and ungrounded configurations of NES are studied, and the NES performance is optimized through variation of different parameters. The results show through vibration control and optimizing the system parameters TET occurs and up to 89% of the energy is dissipated of the ungrounded system energy imposed by shock excitation.

Alternative designs of linear oscillators coupled to NESs were also researched, by increasing the range at which nonlinear vibration absorbers can work research of multi-degree-of-freedom NESs were first introduced in Tsakirtzis et al. (2005).

Passenger ride comfort requires that the vertical motion of the main mass and the root mean square of the acceleration reach a minimum specified by British standards ISO 2631-1997 (1997). Faheem et al. (2006) investigated the response of quarter and half-car models to road excitation. They studied the time response to a step road input and the frequency response of the sprung and unsprung masses. Unaune et al. (2011)

simulated the time response of a quarter-car model to a step input with passive elements suspension. They investigated the effect of mass ratio, stiffness ratio and damping coefficient ratio on the sprung-mass dynamics.

Hessling (2008) quoted that comfort changes with car speed and improper design of road humps leading to a risk of injury. He listed the tools of dynamic measurement systems used in the measurement of vehicle dynamics when crossing a speed hump. Garcia-Pozuelo et. al. (2014) developed a simulation program using MATLAB considering the vehicle dynamics, hump geometry and vehicle speeds. Their proposed tool was expected to provide useful information to set guidelines for the proper design and installation of speed humps.

Christine Vehar (2008) studied a generalized nonlinear spring synthesis methodology for prescribed load-displacement functions. Four spring examples, J-curve, S-curve, constant-force, and linear, demonstrated the effectiveness of the methodology in generating planar spring designs having distributed compliance and matching desired load-displacement functions. Two fabricated designs validated nonlinear spring responses, while demonstrating the applicability of nonlinear springs. By examining various nonlinear spring designs, several interpretations were provided for how a spring's shape, topology, and loading (i.e. axial and bending) influence its response.

Ando et al. (2010) and Amri et al. (2011) researched the use of nonlinear springs, its effects were studied in vibration energy harvesters and results showed that they function for a wider range bandwidth.

Zhao, D. (2016) presents the study of a two-degree-of-freedom nonlinear system consisting of two grounded linear oscillators coupled to two separate light weight nonlinear energy sinks of an essentially nonlinear stiffness for the aim to design the application of a tremor reduction assessment device. Series connection and parallel connection structure systems have been designed to run the tests. The results of theoretical model show a large decrease in vibration while in the experiment set up he was not able to achieve near results due to the hardship of designing the nonlinear spring.

As seen above there has not been immense research practically in this field and a large spectrum is still available for future investigation in practical applications. Also, most of the practical implementation was not able to obtain very good results. Research shows that no work using nonlinear attachments has been done on quarter car suspensions or any vehicle design. Therefore, this will be the focus of this thesis.

2.6 Literature Review on Genetic Algorithm

The genetic algorithm (GA) is a general purpose, population-based search algorithm in which the individuals in the population represent samples from the set of all possibilities, whether they are solutions in a problem space, strategies for a game, rules in classifier systems, or arguments for problems in function optimization. The individuals evolve over time to form even better individuals by sharing and mixing their information about the space (Tanese R. (1989)).

Genetic algorithms have been used to solve difficult problems with objective functions that do not possess simple properties such as continuity, differentiability, satisfaction of the Lipschitz Condition. GA can solve nonlinear, multi-modal, non-convex problems (Davis (1991) Goldberg (1989) Holland (1975) Michalewicz (1994)). These algorithms maintain and manipulate a family or population of solutions and implement a survival of the fittest strategy in their search for better solutions. This provides an implicit as well as explicit parallelism that allows for the exploitation of several promising areas of the solution space at the same time. The implicit parallelism is due to the schema theory developed by Holland (1975), while the explicit parallelism arises from the manipulation of a population of points-the evaluation of the fitness of these points is easy to accomplish in parallel.

Genetic algorithms search the solution space of a function using simulated evolution, i.e. the survival of the fittest strategy. In general, the fittest individuals of any population tend to reproduce and survive to the next generation thus improving successive generations. However inferior individuals can by chance survive and reproduce Genetic algorithms have been shown to solve linear and nonlinear problems by exploring all regions of the state space and exponentially exploiting promising areas through mutation crossover and selection operations applied to individuals in the population.

3 CHAPTER 3 METHADOLOGY OF NONLINEAR ATTACHMENT

3.1 Introduction

In this chapter, a numerical model is developed of a main mass attached with a nonlinear attachment based up on the literature review in Chapter 2. Theoretical model is simulated on Matlab/Simulink, energy analysis is performed on the model. Investigation of this new theory is carried out, to further understand and show the advantages of the nonlinear attachment.

3.2 Simulation of Nonlinear attachment

To study the capacity of targeted energy transfer, a simple design of a system is required. In Figure 3.1 a primary system (Linear Oscillator - LO), coupled to an ungrounded attachment (NES Configuration II) through a pure cubic stiffness which lies in parallel to a viscous damper is simulated and equation of motions are shown in equations 3.1-3.5. Where m_1 is the primary mass and m_2 is the nonlinear energy sink mass. k_1 is the spring stiffness of the linear oscillator and k_2 is the nonlinear spring stiffness of the energy sink. Included also in the equations of motion, c_1 and c_2 are the damper coefficients of the linear oscillator and energy sink. x and v are the displacements of the linear oscillator and energy sink, respectively.

The coefficient of stiffness of a conventional spring obtains a linear slope, while the nonlinear spring will produce a curved coefficient. The study will show how this new curved slope changes the dynamics of the governing equation model of a two degree of freedom model.

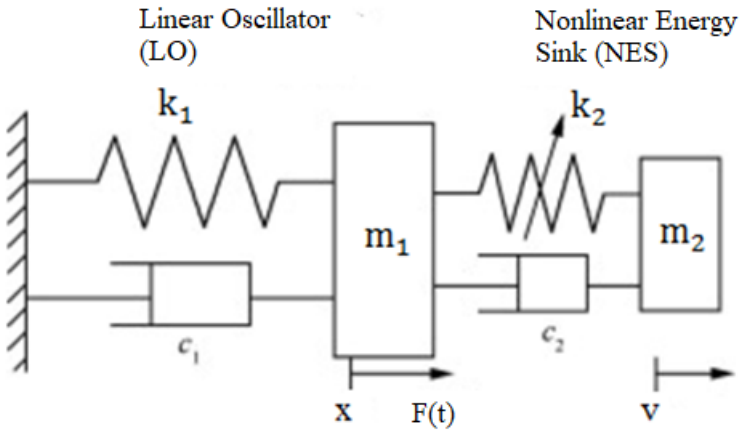

Figure 3.1 The Two-DOF System with Essential Stiffness Nonlinearity.

$$m_1\ddot{x} + c_1\dot{x} + c_2(\dot{x} - \dot{v}) + k_1x + k_2(x - v)^3 = 0 \tag{3.1}$$

$$m_2\ddot{v} + c_2(\dot{v} - \dot{x}) + k_2(v - x)^3 = 0 \tag{3.2}$$

Substituting

$$\ddot{x} + \lambda_1\dot{x} + \lambda_2(\dot{x} - \dot{v}) + w_0{}^2x + C(x - v)^3 = 0 \tag{3.3}$$

$$\varepsilon\ddot{v} + \lambda_2(\dot{v} - \dot{x}) + C(v - x)^3 = 0 \tag{3.4}$$

Where

$$\varepsilon = \frac{m_2}{m_1} \quad w_0{}^2 = \frac{k_1}{m_1} \quad C = \frac{k_2}{m_1} \quad \lambda_1 = \frac{c_1}{m_1} \quad \lambda_2 = \frac{c_2}{m_1} \tag{3.5}$$

Using lightweight NES is very important because it adds to the advantage of not having to make major modifications to the mechanical or structural system to which they are attached.

The system we are using is to be initially at rest, with an impulse of magnitude X applied to the LO; this is equivalent to initiating the system with initial conditions $\dot{x}(0) = X$, $x(0) = \nu(0) = \dot{\nu}(0) = 0$ and no external forcing.

Numerical integration of the system is carried out for varying values of the impulse X and fixed parameter $\varepsilon = 0.1$, $w_0^2 = C = 1$, $\lambda_1 = \lambda_2 = 0.004$. Note that weak damping is chosen to better highlight the different dynamical phenomena that occur in this system. The parametric values where used in an initial test to analyse the nonlinear targeted energy transfer. To obtain data we used Matlab Simulink to simulate the system as seen in figure 3.2.

A quantitative measure of the capacity of the NES to passively absorb and locally dissipate impulsive energy from the LO can be obtained by computing the following energy dissipation measures (EDMs) as shown as equation 3.6:

$$\boldsymbol{E_{NES}} = \frac{\boldsymbol{\lambda_2 \int_0^t [\dot{v}(\tau) - \dot{x}(\tau)]^2 dt}}{\boldsymbol{\frac{X^2}{2}}} \tag{3.6}$$

To obtain the energy dissipated we used Matlab Simulink to simulate the equation 3.6 as seen in figure 3.2. Using this equation it can show how much energy is being dissipated from the primary mass to the nonlinear energy sink. Proving that the nonlinearity in the spring will have a new effect to the vibration absorber.

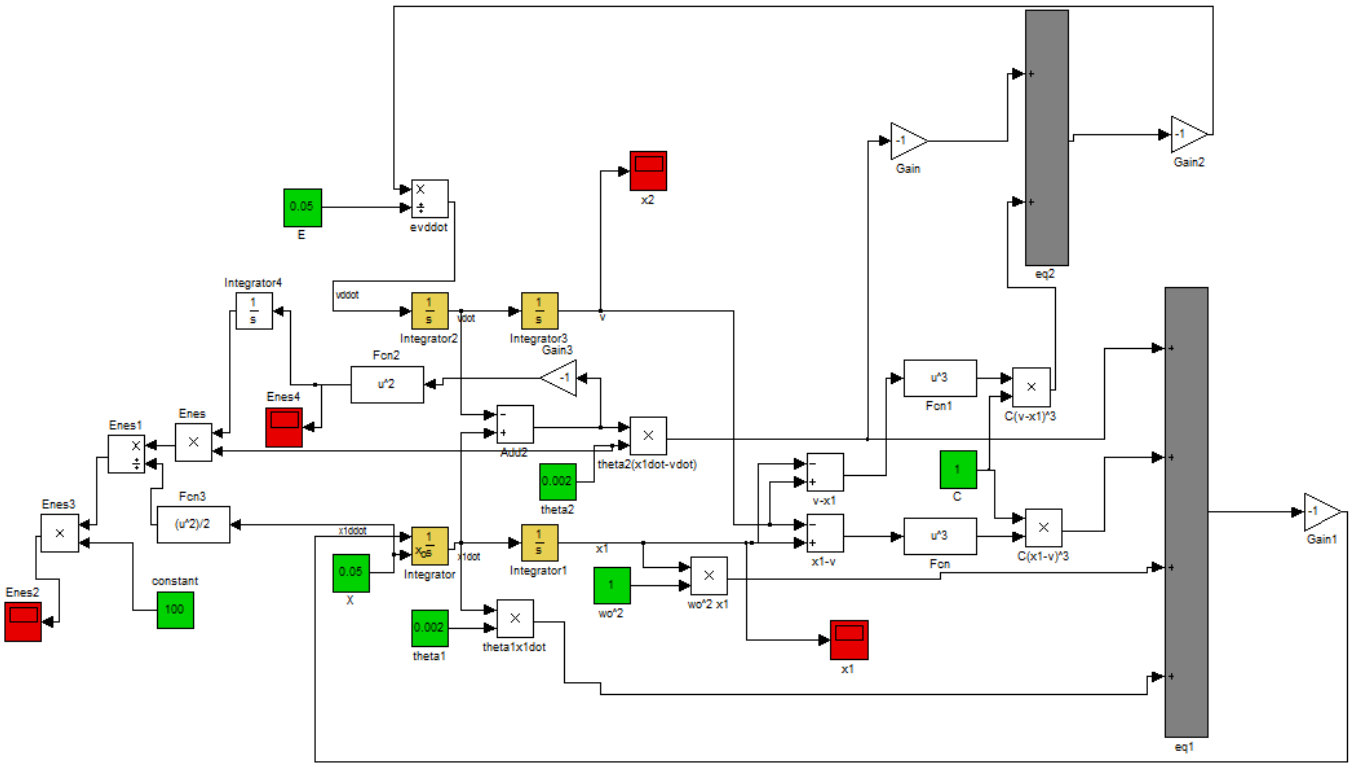

Figure 3.2 Matlab Model of The System

As we can see from Figure 3.3 the dependence of the NES absorption on the impulse of magnitude X, shows that the NES is most effective at intermediate levels of energy, where it dissipates as much as 90% of the input impulsive energy.

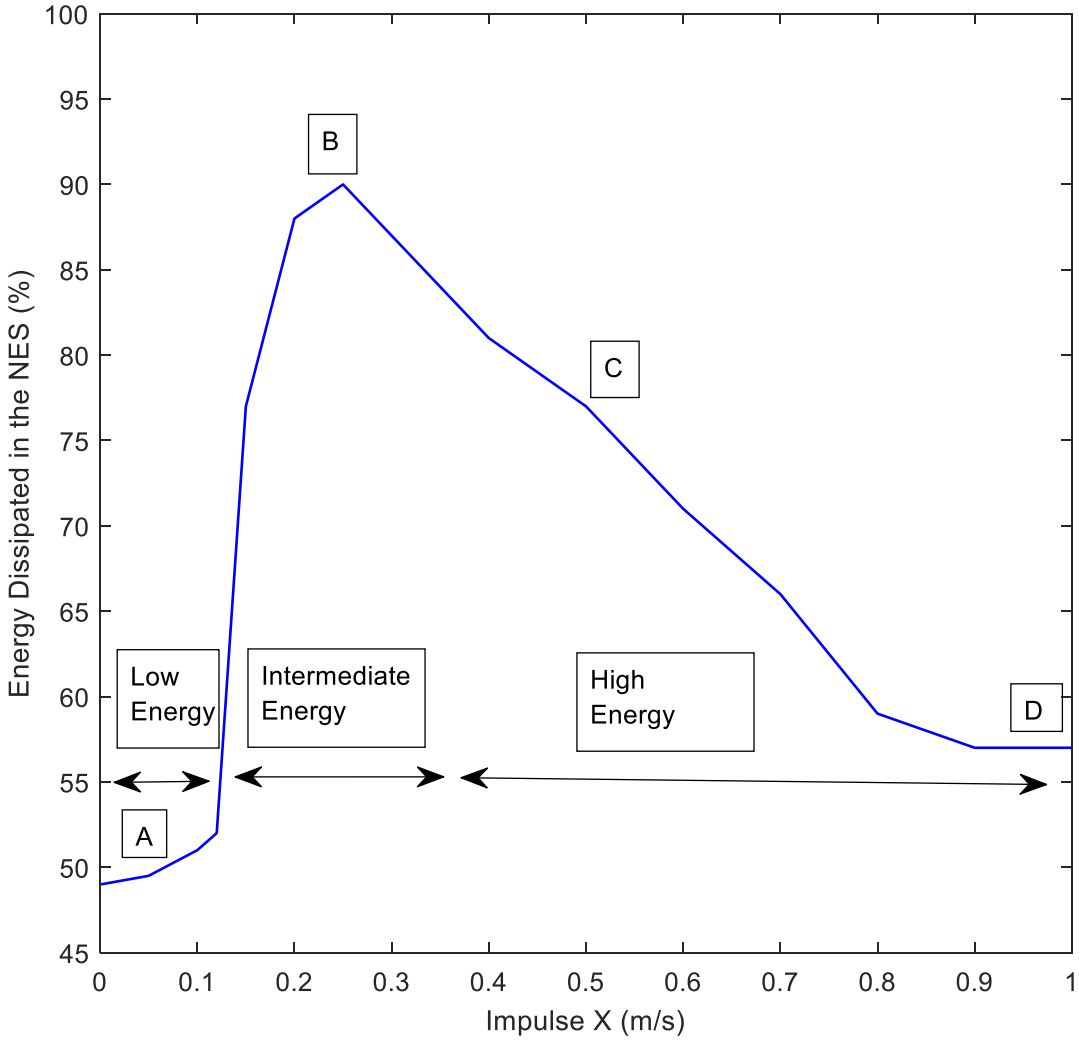

Figure 3.3 Percentage of Impulsive Energy Eventually Dissipated in the NES as a Function of the Magnitude of the Impulse. (Vakakis A.F. 2009)

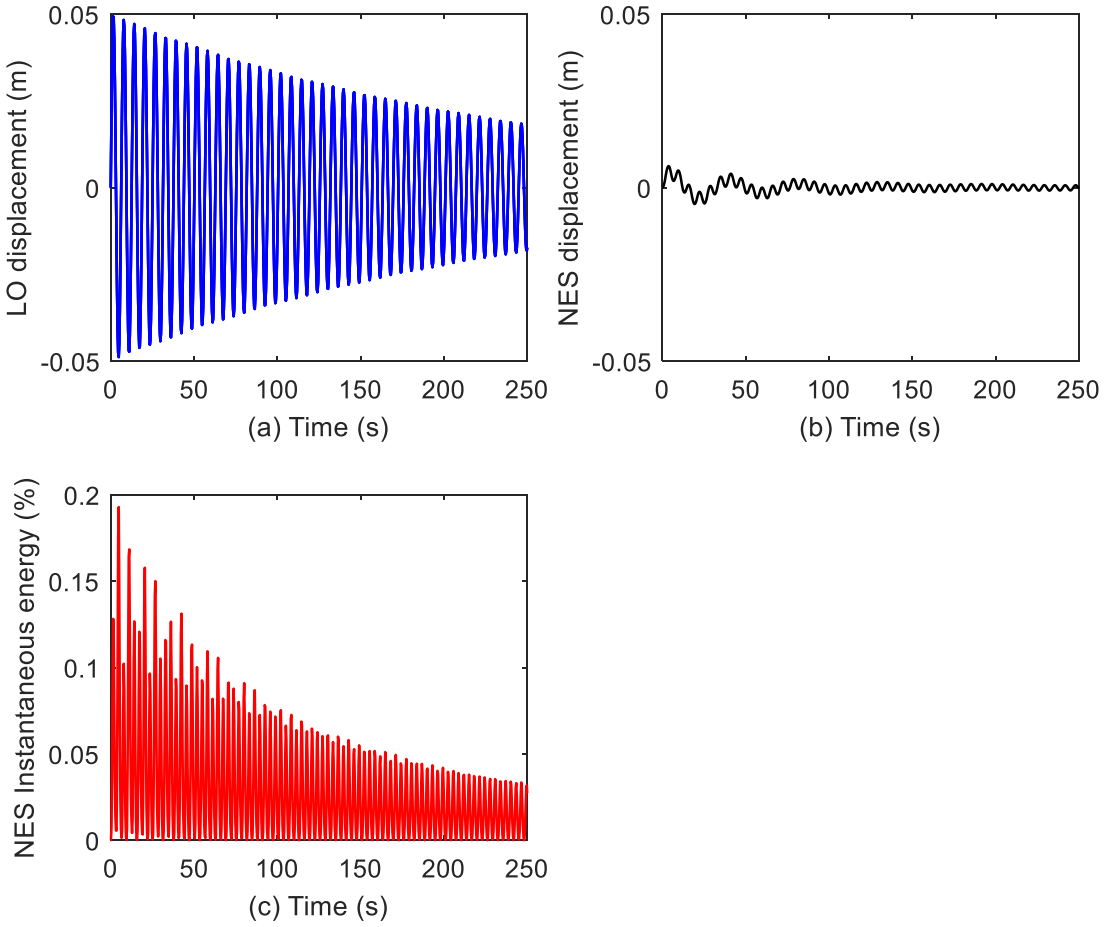

Figure 3.4 Transient Dynamics of the Two-DOF system (low energy level; X = 0.05): (a) LO Displacement; (b) NES Displacement and (c) Percentage of Instantaneous Total Energy in the NES.

Also, there consists a range at which the input energy has no effect on energy dissipated by the NES. To show this an input impulse of X=0.05 is simulated in the model corresponding to point A. As seen in figure 3.4 the amplitude of the LO possesses much higher amplitude than that of the NES. The NES undergoes small oscillations and most of the impulsive energy remains localized to the LO. This becomes apparent when we compute the percentage of instantaneous total energy stored in the NES as shown in equation 3.7,

$$\boldsymbol{D(t)} = \frac{\boldsymbol{\varepsilon \dot{v}(t) + \left(\frac{C}{2}\right)[x(t) - v(t)]^4}}{\boldsymbol{\dot{x}^2(t) + w_0{}^2 x^2(t) + \varepsilon \dot{v}^2(t) + \left(\frac{C}{2}\right)[x(t) - v(t)]^4}} \tag{3.7}$$

this is depicted in Figure 3.4c. No energy transfer occurs from the LO to the NES in this case, and the response remains localized mainly to the LO. This explains why a relatively small portion of the input energy (44%) is dissipated by the NES at this low-energy.

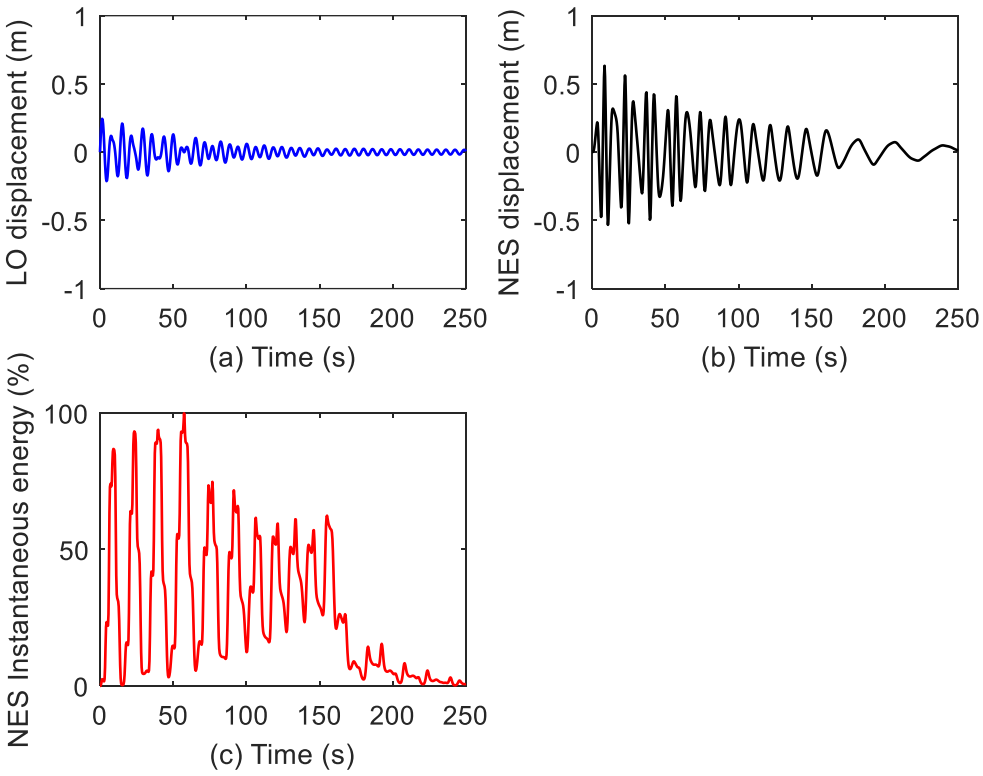

Figure 3.5 Transient Dynamics of the Two-DOF System (intermediate energy level; X = 0.25): (a) LO Displacement; (b) NES Displacement; (c) Percentage of Instantaneous Total Energy in the NES

For impulse X = 0.25 (point B in Figure 3.3) we observe a completely different dynamical behaviour. As seen in Figure 3.5 the NES has a higher amplitude compared to that of the LO. Looking at the NES frequency we observe an extreme variation in the NES frequency which indicates the strongly nonlinear nature of its oscillation. Despite this energy is entirely stored in the LO, it quickly flows back and forth between the two oscillators. After t = 15 s, 87% of the instantaneous total energy is stored in the NES, but this number drops down to 3% immediately thereafter. Even so this as much as 90% of the total input energy is dissipated by the damper of the NES. An important advantage of this new nonlinear model that no priori tuning of the

NES parameters was necessary to achieve this result due to the variation of the frequency of the NES due to damping dissipation that plays the role of tuning.

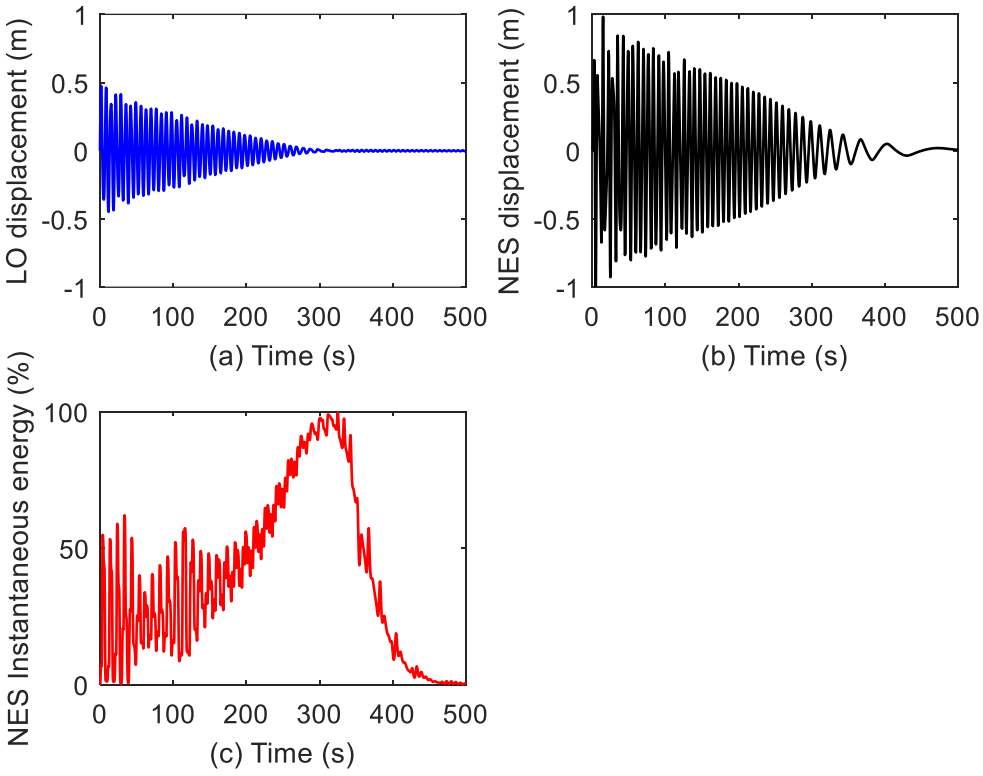

Figure 3.6 Transient Dynamics of the Two-DOF System (moderate-energy level; X = 0.5): (a) LO Displacement; (b) NES Displacement; (c) Percentage of Instantaneous Total Energy in the NES and (d) Superposition of Both Displacements During Nonlinear TET.

Further increasing the impulse to X = 0.5, results shown in Figure 3.6 (point C in Figure 3.3). Motion is still mainly in the NES and in the initial stage of the motion until approximately t = 15 s, a nonlinear beating phenomenon takes place as in the previous case. Thereafter this continuous energy exchange between the two oscillators takes place, an irreversible energy flow from the LO to the NES occurs, nonlinear energy pumping is triggered, and TET is realized. At t=300s the transient nature of the resonance capture is clear in Figure 3.6(c). Overall, 87.6% of the total input energy is dissipated by the NES in this case.

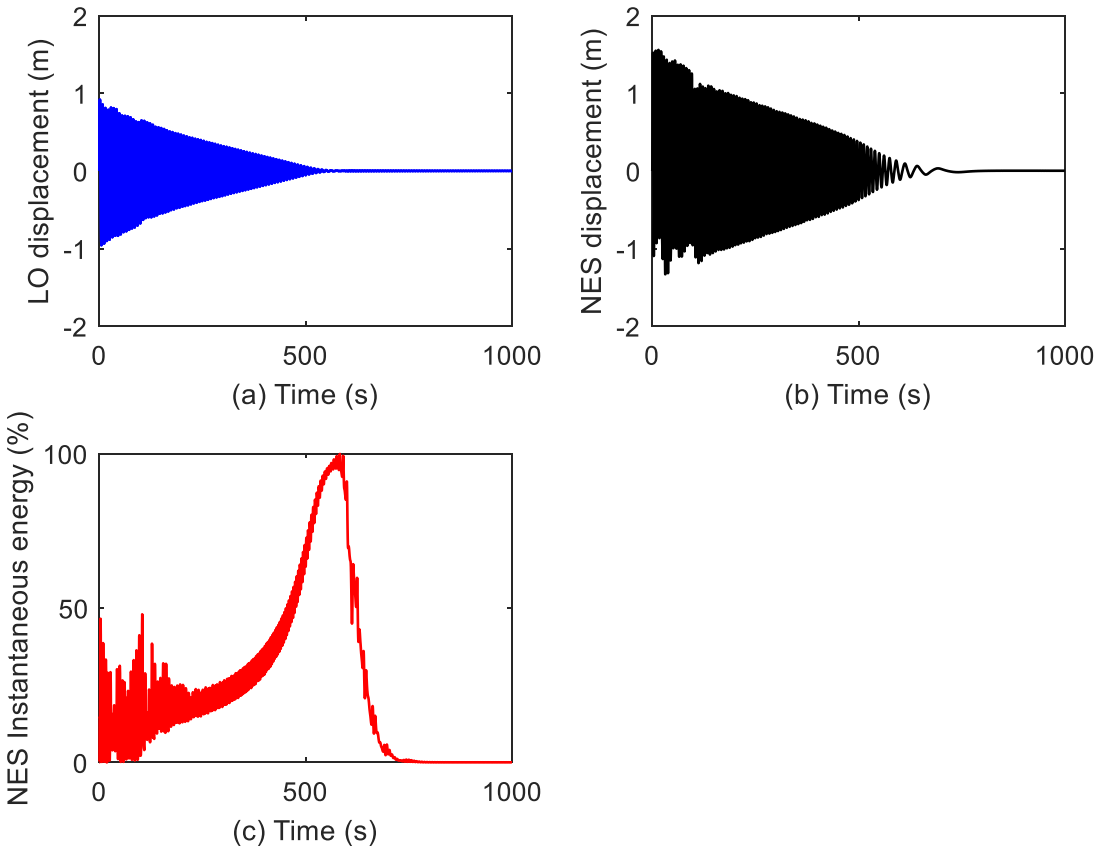

Figure 3.7 Transient Dynamics of the Two-DOF System (high-energy level; X = 1): (a) LO Displacement; (b) NES Displacement and (c) Percentage of Instantaneous Total Energy in the NES.

At a higher impulse at X = 1, Figure 3.7 (point D in Figure 3.3), nonlinear beating phenomenon dominates the early regime of the motion. After t =4s a weaker but faster energy exchange is observed, since 32% of the total energy is transferred. The irreversible energy transfer from the LO to the NES is slower compared to the previous simulation but still TET occurs.

Therefore, energy dissipation is less efficient than at the moderate-energy regime, and only 50% of the total input energy is dissipated by the NES.

To fully understand the advantages, we compare the SDOF NES and the classical linear TMD configurations. To further research the capacities of for the two vibration absorptions an additional series of

simulations were performed. To simulate different model parameters, we study by varying (i) the spring constant k_1 of the LO (and therefore the natural frequency of the LO, ω_0), and (ii) the magnitude X of the impulse applied to the LO.

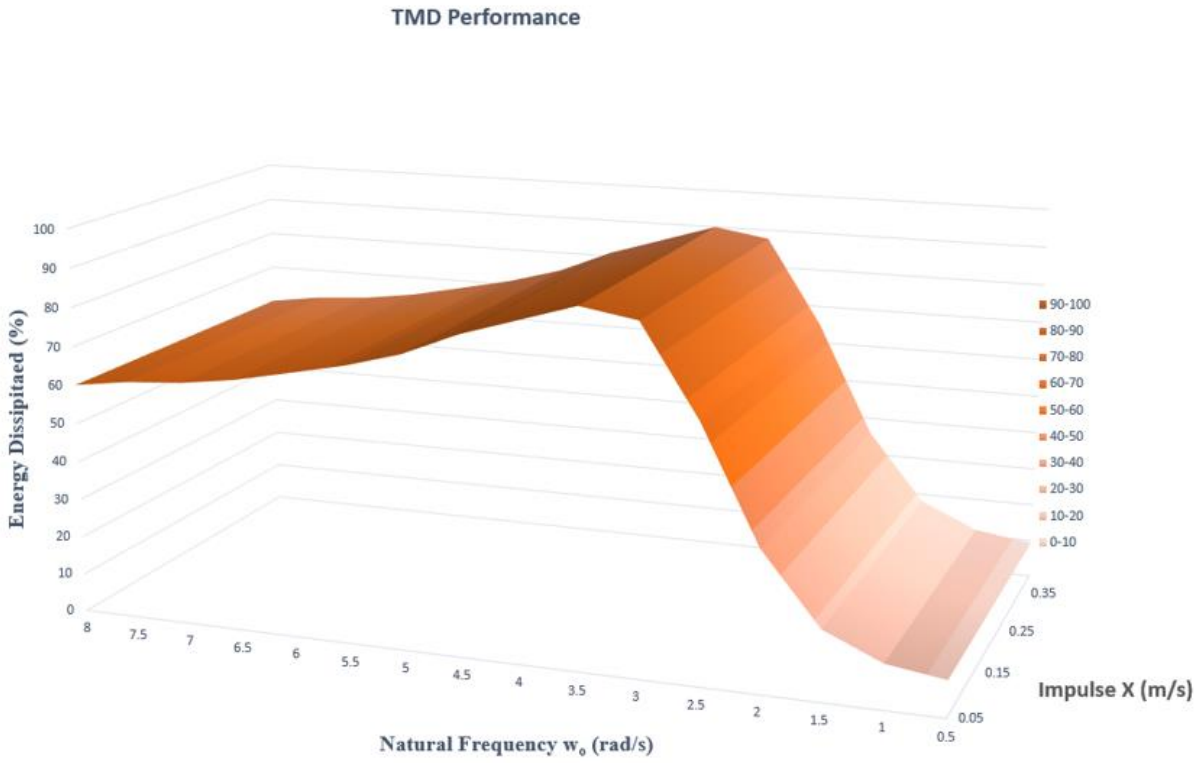

Figure 3.8 TMD Performance.

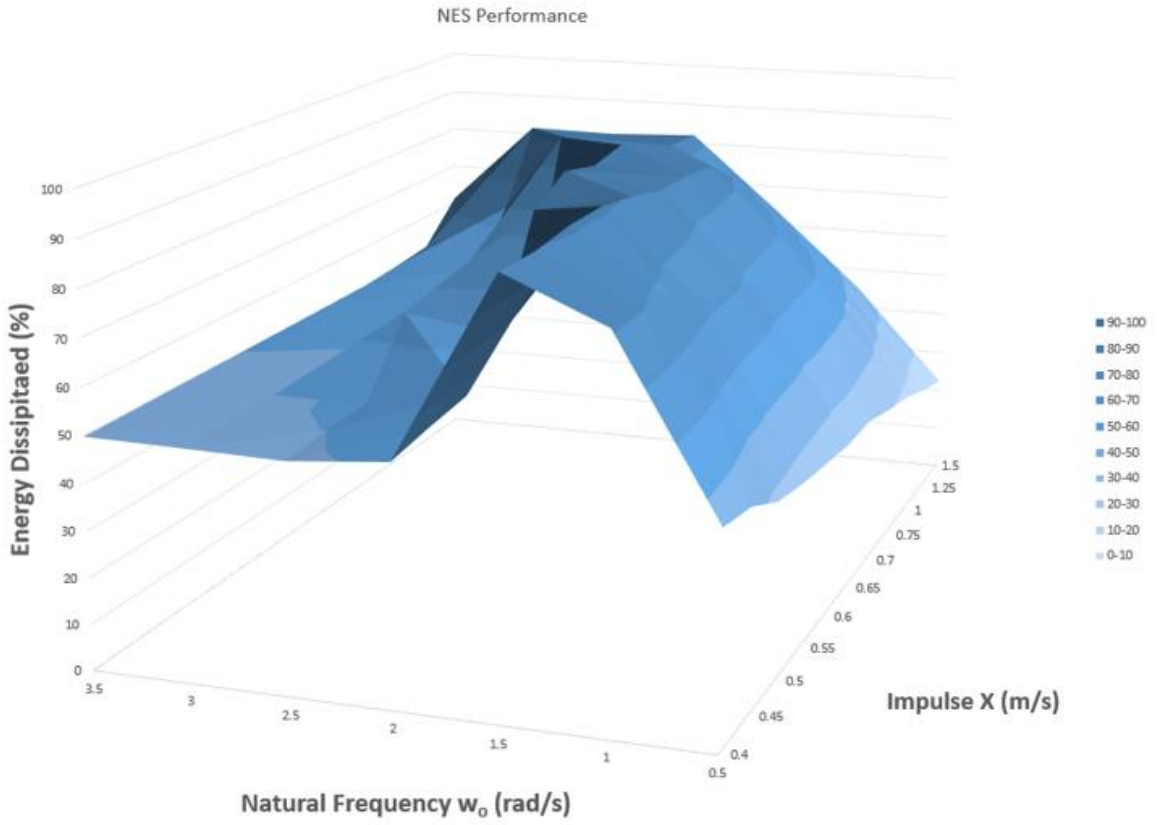

Figure 3.9 NES Performance.

The three-dimensional plots in Figures 3.8 and 3.9 displays the energy dissipated by the TMD and the SDOF NES, respectively, as functions of parameters ω_0 and X. Due to the linear superposition principle, we can see that the TMD does not depend on the impulse magnitude. There is a specific value of ω_0 for which the energy dissipation in the TMD is maximum (90 % of the total input energy). Only a change in the frequency content of the LO response decreases the TMD performance, showing that the TMD is only effective when it is tuned to the natural frequency of the LO. Unlike the TMD, the NES performance depends mainly on the impulse magnitude, which is a limitation of this type of nonlinear absorbers. This is confirmed in Figure 3.9. This figure indicates that the effectiveness of the NES is not significantly influenced by changes in the natural frequency of the LO. More precisely, for values of ω_0 beyond a critical threshold there exists impulse magnitude for which the NES dissipates a significant amount of the total input energy. Moreover, there are alternative mechanisms by which the NES can induce TET in this system.

3.3 Conclusion of Nonlinear Attachment

In conclusion, even though the performance of the TMD is not affected by the level of total energy in the system, it is limited by its inherent sensitivity to uncertainties in the natural frequency of the primary system. In contrast, if the energy is above a critical threshold, the SDOF NES is capable of robustly absorbing transient disturbances over a broad range of frequencies. Hence, the NES may be regarded as an efficient passive absorber, possessing adaptivity to the frequency content of the vibrations of the primary system. This is due to its essential stiffness nonlinearity, which precludes the existence of any preferential resonance frequency.

3.4 Design of Conical Springs

3.4.1 Introduction

Conical springs usually have been presented in books with a linear equation of motion. Wahl (1963) has derived the load deflection relation of the coil cylindrical spring. Timoshenko (1966) extended this relation to a conical spring, but only its linear behavior.

The first research about the nonlinearity of a conical was done Rodriguez et al. (2006) and the second is by Wu and Hsu [1998]. This nonlinear behavior occurs during compression due that the number of active coils. Apply the force, the biggest coil starts moving gradually to the bottom which causes an increasing stiffening of the spring. Paredes and Rodriguez (2008) studied the optimal design of conical springs. Rare work about the dynamic research of conical springs can be found, only Wu and Hsu propose a basic equation of motion, but do not give experimental verification of this model. Den Boer (2009) was the first to produce governing equations for a conical spring consisting of an initial linear plot and followed by a nonlinear plot. In his work, he tested the equations of motions analytically and experimentally and obtained that the governing equation produce the same results compared to the experimental tests.

The derivation of the load-deflection relation according to Rodriguez et al. is shown in section 3.4.2. The coil diameter d is 0.01 m, mean spring diameter of smallest initially active coil D_1 is 0.14 m, mean spring diameter of biggest initially active coil D_2 is 0.23 m, initial number of coils n is 4 coils, initial spring height H is 0.17 m and the modulus of rigidity G is $80*10^9$ Pa.

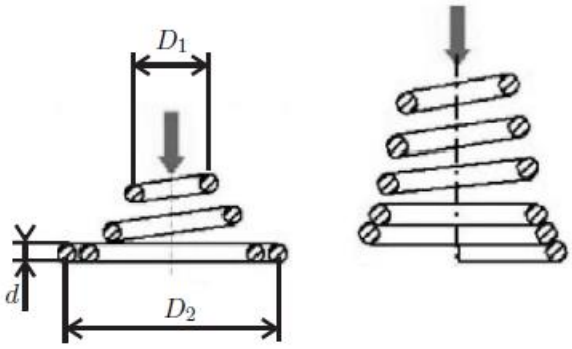

Figure 3.10 a) Telescoping Conical Spring. b) Nontelescoping Conical Spring.

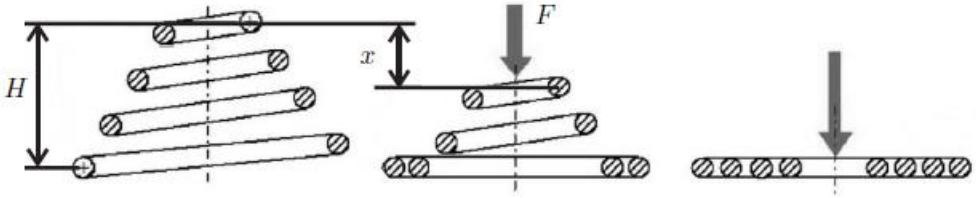

Figure 3.11 Compression of a Telescoping Conical Spring.

3.4.2 Linear Cylindrical Spring

Curvature and direct shear effects are neglected in this theory, also the assumption of that an element of an axially loaded helical cylindrical spring behaves essentially as a straight bar in pure torsion is taken into consideration. (Figure 3.12).

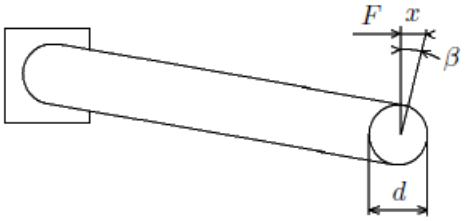

Figure 3.12 Spring Coil Behaves Essentially as a Straight Bar in Pure Torsion.

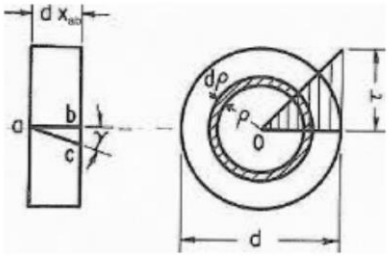

Figure 3.13 Cross-Sectional Element of Spring Under Torsion. (Wahl, 1963)

Each element of the spring coil is assumed to be subjected to a torque M = FD/2 acting about the spring center, where D is the mean spring diameter. A linear shear (τ) distribution along the bar radius is assumed, as shown in figure 3.13. At a distance ρ from the center O the shearing stress will be $\tau = 2\,\rho\,\tau\,\max/d$. The moment dM taken from a ring with width d ρ at a radius ρ will be $dM = 4\pi\,\tau\,\max\,\rho 3d\,\rho\,/d$. The total moment FD/2 then becomes

$$\frac{FD}{2} = \int_0^{\frac{d}{2}} dM = \int_0^{\frac{d}{2}} \frac{4\pi\tau_{max}\rho^3 d\rho}{d} = \frac{\pi d^3 \tau_{max}}{16} \tag{3.8}$$

and gives a maximum shear stress of

$$\tau_{max} = \frac{8FD}{\pi d^3} \tag{3.9}$$

An element ab (figure 3.13) on the surface of the bar and parallel to the coil axis is considered. After deformation, this element will rotate through a small angle (figure 3.13) to the position ac. From elastic theory, this angle γ will be

$$\gamma = \frac{\tau_{max}}{G} = \frac{8FD}{\pi d^3 G} \tag{3.10}$$

with G being the shear modulus. Since the distance $bc = \gamma\, dx_{ab}$ for small angles such as considered here, the elementary angle dβ through which one cross section rotates with respect to the other will be equal to $2\,\gamma\, dx_{ab}/d$. Again, if the spring may be considered as a straight bar of length L = πnD, the total angular deflection β (figure 3.12) of one end of the coil with respect to the other end becomes

$$\beta = \int_0^{\pi n D} \frac{2\,\gamma\,dx_{ab}}{d} = \int_0^{\pi n D} \frac{16FDdx_{ab}}{\pi d^4 G} = \frac{16FD^2 n}{Gd^4} \tag{3.11}$$

The effective moment arm of the load F is equal to D/2, so the total axial deflection of the spring at load F will be (figure 3.13).

$$x = \frac{\beta D}{2} = \frac{8FD^3 n}{Gd^4} \tag{3.12}$$

This is the commonly used formula for cylindrical spring deflections.

3.4.3 Linear Conical Spring

To study the linear part, conical helical springs without coil close will be considered. The formula for cylindrical helical springs will now be proven. Now the variable diameter of the spring as function of coil number n_D is (n_D being the continuous variable, running from 0 to n)

$$D(n_D) = D_1 + \frac{(D_2 - D_1)n_D}{n} \tag{3.13}$$

The total axial deflection of the spring will be obtained from (2.28) and (2.29) and gives

$$x = \frac{8F}{Gd^4}\int_0^n \left[D_1 + \frac{(D_2 - D_1)n_D}{n}\right]^3 dn_D = \frac{2Fn({D_1}^2 + {D_2}^2)(D_1 + D_2)}{Gd^4} \tag{3.14}$$

3.4.4 Nonlinear Conical Spring

In this subsection, telescoping conical springs with a constant pitch are considered. The total conical spring deflection (x) at a certain axial load (F), is an addition of the total axial deflection of the free coils (x_f) and the total axial deflection of the solid coils (x_s). This is approximated by an addition of all the elementary axial deflections of the free coils (δ_f) and the elementary axial deflections of the solid coils (δ_s). This gives a total deflection of

$$x = x_f + x_s = \int_0^{n_f} \delta_f(n_D) + \int_{n_f}^{n} \delta_s \tag{3.15}$$

Other algorithms use discretization of the coil into several angular parts. The deflection of the spring for a given load is determined by adding the individual deflections of each part of a cylindrical spring. Each individual deflection of each part is part of a cylindrical spring. Each individual deflection is limited to its maximum geometrical value. The method introduced in this chapter is based on the same principle as the other algorithms, but here discretization is replaced by an integral approach (see (3.24).

Every single elementary axial deflection of the free coils (δ_f) can be written as (taking the load deflection relation of the cylindrical spring (2.28), where mean spring diameter D is replaced with the variable diameter of the conical spring D(n_D) (2.29).

$$\delta_f(n_D) = \frac{8F[D(n_D)]^3}{Gd^4} dn_D \tag{3.16}$$

This derivation is based on a constant pitch, which implies that the axial distance between the coils is constant. Therefore, can be stated that, for every angular part, the elementary deflection of the solid coils (δ_s) corresponds to the maximum geometrical elementary deflection. This can be calculated as follows

$$\delta_s = \frac{H}{n} dn_D \tag{3.17}$$

F_T is the load for which the largest active coil (with local spring diameter D_2) reaches its maximum deflection δ_s. So, at the transition point T can be written

$$x_f(n) = x_s \tag{3.18}$$

Using (3.25) and (3.26), this can be written as

$$\frac{8F_T[D_2]^3}{Gd^4} = \frac{H}{n} \tag{3.19}$$

So

$$F_T = \frac{Gd^4 H}{8[D_2]^3 n} \tag{3.20}$$

On the conical spring load-deflection curve, the maximum point C defines the ultimate compression state of the spring. F_C is the load for which the smallest active coil (with local spring diameter D_1) reaches its maximum deflection H. So, like the transition point, this can be written as

$$F_C = \frac{Gd^4 H}{8[D_1]^3 n} \tag{3.21}$$

The elementary axial deflections of the free coils (δ_f) have a variable number of coils nD, running from 0 to n. Every single element reaches its maximum deflection at $n_D = n_f$ coils (with n_f is the number of free coils). This corresponds with the elementary axial deflection of the solid coils (δ_s), so

$$\delta_f(n_f) = \delta_s \tag{3.22}$$

Using (3.22), (3.25) and (3.26), this can be written as

$$\frac{8F\left[D(n_f)\right]^3}{Gd^4} = \frac{H}{n} \tag{3.23}$$

So that

$$n_f = \frac{n}{D_2 - D_1}\left[\left(\frac{Gd^4H}{8Fn}\right)^{1/3} - D_1\right] \tag{3.24}$$

As n_f is defined, the continues load-deflection relation can be written (using (3.24),

$$x(F) = \frac{2F[D_1]^4 n}{Gd^4(D_2 - D_1)}\left[\left\{1 + \left(\frac{D_2}{D_1} - 1\right)\frac{n_f}{n}\right\}^4 - 1\right] + H\left(1 - \frac{n_f}{n}\right) \tag{3.25}$$

The load-deflection relation for a conical spring with a constant pitch is derived, see (3.24) and (3.25). This relation will be used for the analysis of a nonlinear conical spring.

In compression, these springs show a two-regime load deflection relation (see figure 3.14), where the first regime is linear, and the second regime is nonlinear. In extension, the load-deflection relation for these springs is linear.

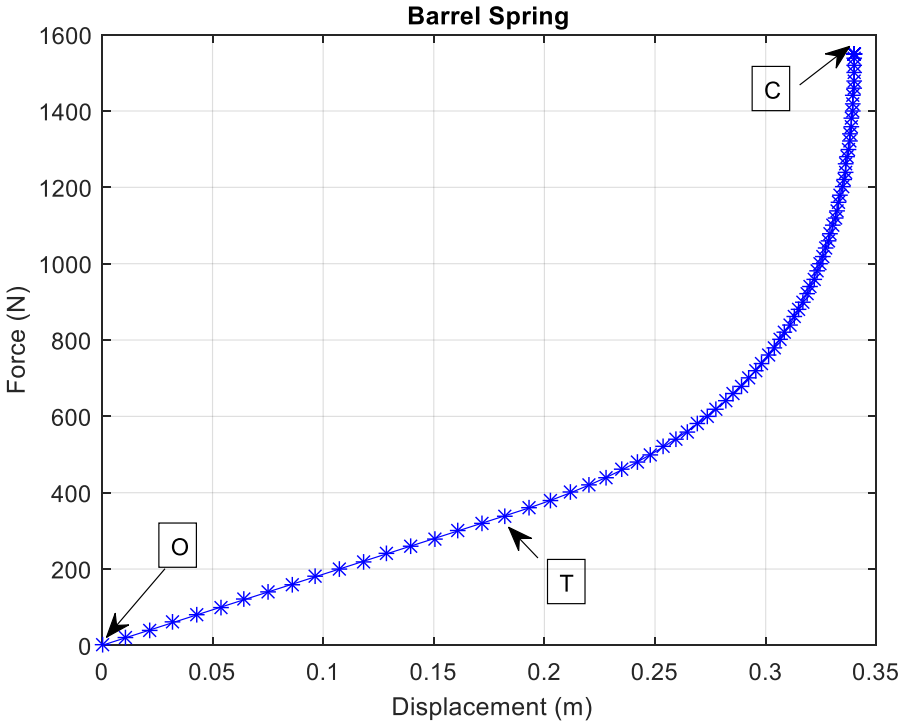

.

Figure 3.14 Telescoping Conical Spring Characteristic. Point O: No Compression. Transition Point T: Start of Active Coil-Ground Contact; Start of Nonlinear Behaviour. Point C: Maximal Compression (all active coils in contact with the ground).

In the linear regime of the deflection curve (from point O to T in figure 3.14), the largest coil is free so deflects, as all other coils of the spring. Thus, the load-deflection relation is linear according to (3.14).

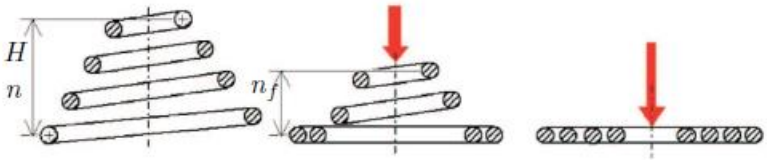

Figure 3.15 Telescoping Spring.
Left: Linear Behaviour, n Free Coils.
Middle: Nonlinear Behaviour, nf < n Free Coils.
Right: Maximum Deflection,
nf = 0. [Rodriguez et al., 2006]

Along the nonlinear regime (from point T to C in figure 3.14), the active coils are gradually compressed to the ground. During this regime, n_f coils are free and $n - n_f$ coils are compressed to the ground (these coils are called solid coils), see figure 3.15. The coil is considered as an infinitely number of elementary angular parts. When the first elementary part of the largest coil has reached its maximum physical deflection, it starts to be a nonactive element of the spring. This defines the transition point T. The first regime of compression

then stops and the second one begins. During the second regime of compression, n_f continuously decreases from n to 0 and leads to a gradual increase of the spring stiffness. This explains why this second regime shows a nonlinear load-deflection relation.

3.4.5 Conical Springs Constraints on Design Parameters

In this section, additional constraints on the design parameters of the experimental setup will be discussed. For manufacturing reasons of the spring, the minimal mean spring diameter (D_1) must be at least three times greater than the coil diameter (d).

$$D_1 > 3\text{d} \tag{3.26}$$

As stated before, in this project the telescoping conical spring is used. This means that during compression to the ground, every coil must fit in the following coil. When the spring is fully compressed to the ground, the distance from one coil to the next (heart to heart) is $\frac{D_2-D_1}{2n}$. The distance from one coil to the next (e) when the spring is fully compressed to the ground is e = $\frac{D_2-D_1}{2n} - d$. A spring is telescoping when e > 0 m, otherwise the spring is nontelescoping. So, the constraint can be written as

$$\frac{D_2 - D_1}{2n} - d > 0\ m \tag{3.27}$$

3.4.6 Experimental Design of Barrel Spring

The barrel spring was designed to meet the criteria of giving a nonlinear stiffness using the equation 3.23, 3.34. Considering that the barrel spring is two conical springs in series, therefore the displacement in each equation of motion has been multiplied by two. Also limited by the design of the car, the spring design parameter are given in figure 3.16. Diameter of the coil is 1 cm.

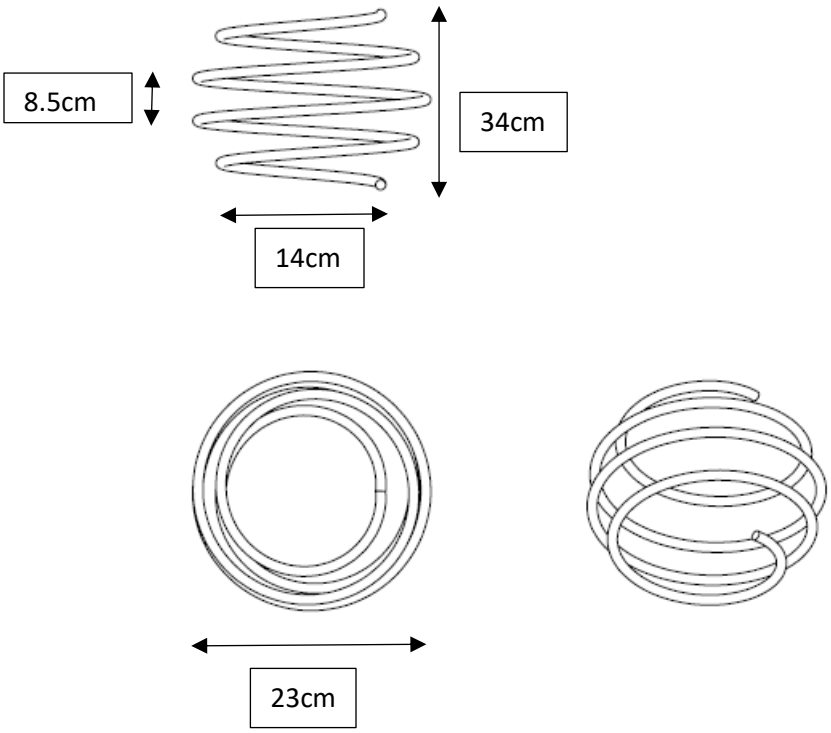

Figure 3.16 Parameters of Barrel Spring.

3.4.7 Conclusion

The spring theoretical design have been produced according to the barrel governing equation limited by the design parameters of the spring and the car it will be implemented into. Further experimental work will be applied on this design when the prototype is manufactured. Other prototypes will be designed and compared to the standard passive spring.

4 CHAPTER 4 MATHEMATICAL MODEL OF QUARTER CAR SUSPENSION SYSTEM

4.1 Introduction

Single-degree-of-freedom or two-degrees-of-freedom quarter-car models, subjected to road excitation, are commonly employed in many areas of the automotive industry. These areas include the prediction of dynamic response, identification, optimization and control of ground vehicles (e.g. Crosby et al. (1974), Harrison and Hammond (1986), Sharp and Hassan (1986), Hrovat (1993), Dixon (1996), Metallidis et al. (2003)). This is mostly due to the simplicity of the quarter-car models and the qualitatively correct information they provide,

After doing the literature review and confirming the efficiency of a nonlinear configuration, we will try to use on a practical application. Here we will introduce the theoretical model of a quarter car model which will be our practical application and further study the model with two different suspension configurations. First configuration will contain a normal linear spring and then compare with a nonlinear stiffness in the 2-DOF quarter car system.

4.2 Mathematical Model

Most practical vibrating systems are very complex, and it is impossible to consider all the details for mathematical analysis. Only the most important features are considered in the analysis to predict the behaviour of the system under specified input conditions. Often, the overall behaviour of the system can be determined by considering even a simple model of the complex system. The analysis of a vibrating system usually involves mathematical modelling, derivation of the governing equations, solution of the equations, and interpretation of the results. By using the equivalent values of the mass, stiffness, and damping of the system, a mathematical model for a certain application can be obtained.
The equations of motion of the two masses are given by:

$$\mathbf{m_1}\,\ddot{\mathbf{x}}_1 + \mathbf{k_1}(\mathbf{x_1} - \mathbf{x_2}) + \mathbf{b_1}(\dot{\mathbf{x}}_1 - \dot{\mathbf{x}}_2) = \mathbf{0} \tag{4.1}$$

$$\mathbf{m_2}\,\ddot{\mathbf{x}}_2 + \mathbf{k_2}(\mathbf{x_2} - \boldsymbol{\omega}) + \mathbf{b_2}(\dot{\mathbf{x}}_2 - \dot{\boldsymbol{\omega}}) - \mathbf{k_1}(\mathbf{x_1} - \mathbf{x_2}) - \mathbf{b_1}(\dot{\mathbf{x}}_1 - \dot{\mathbf{x}}_2) = \mathbf{0} \tag{4.2}$$

Where m_1 is the primary mass (consisting of the car seat and passenger) and m_2 is the tyre mass. k_1 is the suspension stiffness and k_2 is the tyre stiffness. Included also in the equations of motion, b_1 and b_2 are the

damper coefficients of the main mass and tyre mass. x_1 and $x_2$are the displacements of the main mass and tyre masses, respectively. While ω is the deformation of the ground.

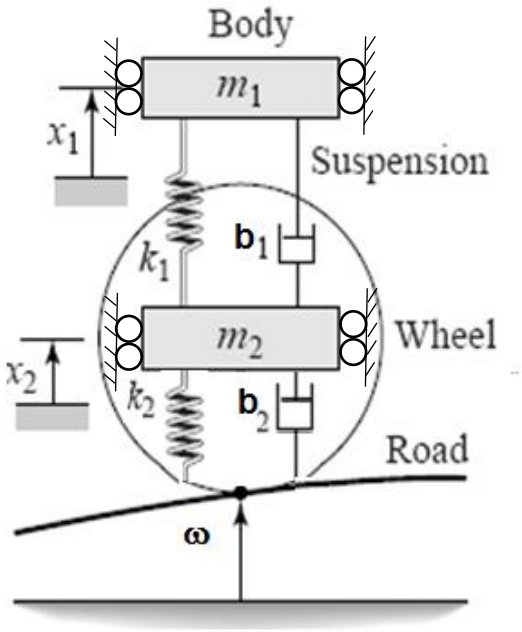

Figure 4.1 Quarter Car Model

The equations of motion of the two masses may be written as

$$\ddot{x}_1 = -\frac{k_1}{m_1}(x_1 - x_2) - \frac{b_1}{m_1}(\dot{x_1} - \dot{x_2}) \tag{4.3}$$

$$\ddot{x}_2 = \frac{k_2}{m_2}(\omega - x_2) + \frac{b_2}{m_2}(\dot{\omega} - \dot{x_2}) + \frac{k_1}{m_2}(x_1 - x_2) + \frac{b_1}{m_2}(\dot{x_1} - \dot{x_2}) \tag{4.4}$$

The equations of motion of the nonlinear suspension of two masses are given by:

$$m_1 \ddot{x}_1 + k_1(x_1 - x_2)^3 - b_1(\dot{x_1} - \dot{x_2}) = 0 \tag{4.5}$$

$$m_2 \ddot{x}_2 + k_2(x_2 - \omega) + b_2(\dot{x_2} - \dot{\omega}) - k_1(x_1 - x_2)^3 - b_1(\dot{x_1} - \dot{x_2}) = 0 \tag{4.6}$$

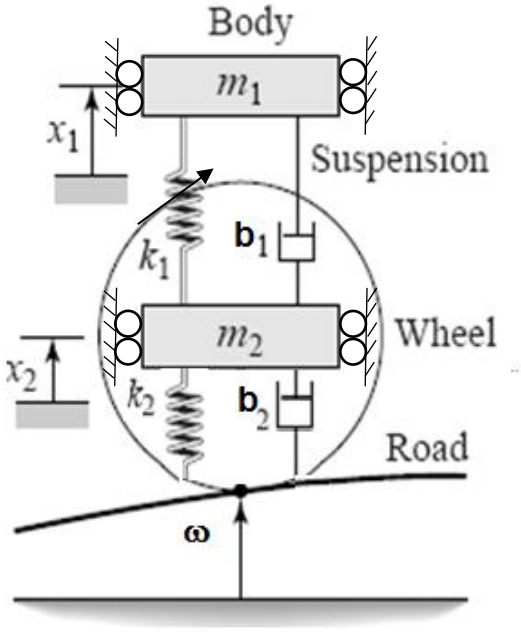

Figure 4.2 Quarter Car Model with Nonlinear Suspension

For the same model with a nonlinear suspension the equations of motion of the two masses may be written as

$$\ddot{x}_1 = -\frac{k_1}{m_1}(x_1 - x_2)^3 - \frac{b_1}{m_1}(\dot{x_1} - \dot{x_2}) \tag{4.7}$$

$$\ddot{x}_2 = \frac{k_2}{m_2}(\omega - x_2) + \frac{b_2}{m_2}(\dot{\omega} - \dot{x_2}) + \frac{k_1}{m_2}(x_1 - x_2)^3 + \frac{b_1}{m_2}(\dot{x_1} - \dot{x_2}) \tag{4.8}$$

Where m_1 is the primary mass (consisting of the car seat and passenger) and m_2 is the tyre mass. k_1 is the suspension stiffness and k_2 is the tyre stiffness. Included also in the equations of motion, b_1 and $b_2$are the damper coefficients of the main mass and tyre mass. x_1 and $x_2$are the displacements of the main mass and tyre masses, respectively. While ω is the deformation of the ground.

Equations 4.5, 4.6, 4.7 and 4.8 are solved using MATLAB SIMULINK as in Figure 4.3.

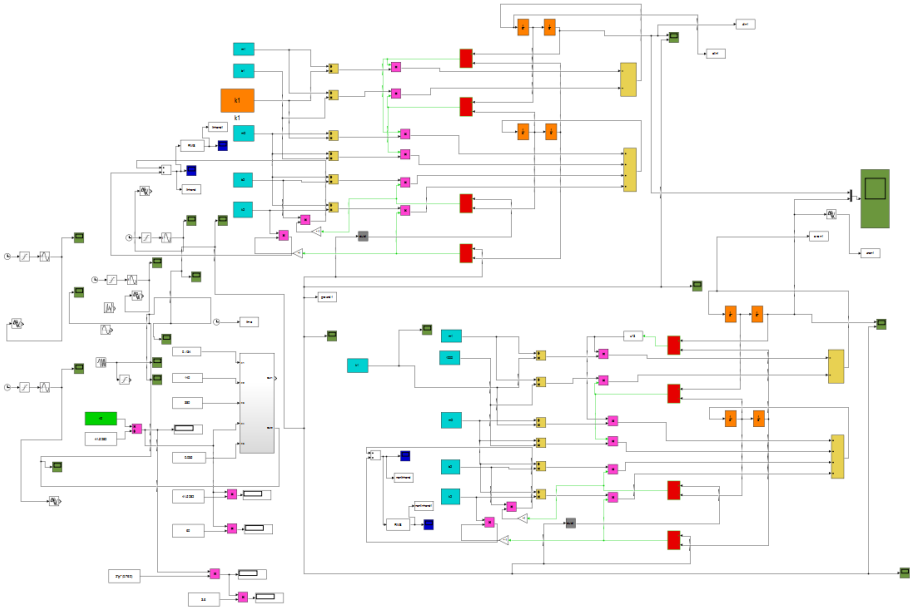

Figure 4.3 Simulink of Quarter Car Model

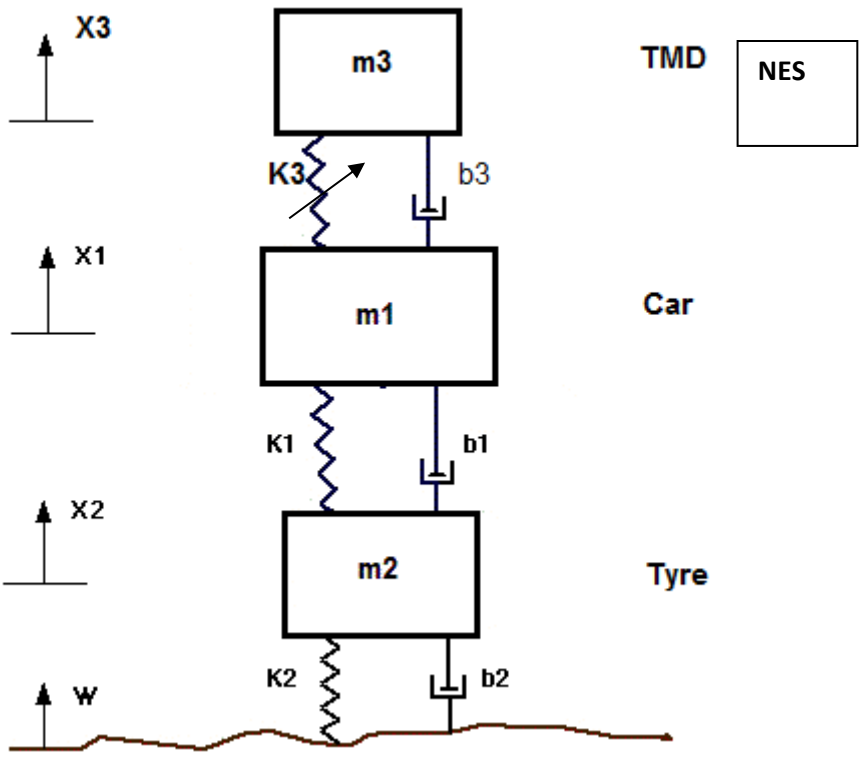

Figure 4.4 Quarter Car Mode Plus TMD.

The equations of motion of the three masses may be written as

$$\ddot{x}_3 = -\frac{k_3}{m_3}(x_3 - x_1)^3 - \frac{b_3}{m_3}(\dot{x}_3 - \dot{x}_1) \tag{4.9}$$

$$\ddot{x}_1 = -\frac{k_1}{m_1}(x_1 - x_2) - \frac{b_1}{m_1}(\dot{x}_1 - \dot{x}_2) - \frac{k_3}{m_1}(x_1 - x_3)^3 - \frac{b_3}{m_1}(\dot{x}_1 - \dot{x}_3) \tag{4.10}$$

$$\ddot{x}_2 = \frac{k_1}{m_2}(\omega - x_2) + \frac{b_2}{m_2}(\dot{\omega} - \dot{x}_2) + \frac{k_1}{m_1}(x_1 - x_2) + \frac{b_1}{m_1}(\dot{x}_1 - \dot{x}_2) \tag{4.11}$$

Where m_1 is the primary mass (consisting of the car seat and passenger) and m_2 is the tyre mass. k_1 is the suspension stiffness and k_2 is the tyre stiffness. Included also in the equations of motion, b_1 , b_2 and b_3 are the damper coefficients of the main mass and tyre mass and TMD damper coefficient. x_1 and x_2 are the displacements of the main mass and tyre masses, respectively. While ω is the deformation of the

ground. m_3 is the tuned mass damper (TMD) and k_3 is the non-linear suspension stiffness of the TMD and b_3 is the TMD damper coefficient.

Equations 4.9, 4.10 and4.11 are solved using MATLAB SIMULINK as in Figure 4.5.

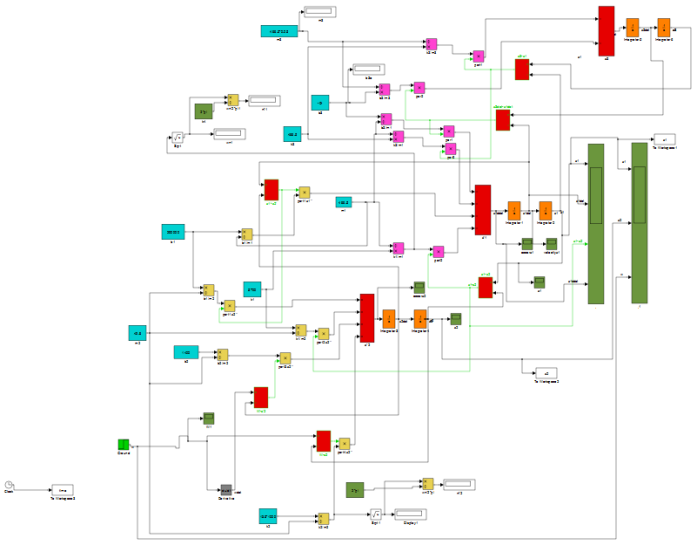

Figure 4.5 Simulink of Quarter Car Model Plus TMD

For the TMD model, various configurations of different masses for m_3 and b_3 and k_3 were researched. Most of the results show that the linear or nonlinear absorber has a minimal effect of car ride.

4.3 Modeling of the Road Hump

The most common hump shape is the rounded hump. The measurement of the hump is a replica of the ones used in our society used by the government in Egypt. The model of road hump is designed to consider the speed of car and the initial time of the start of the hump and then the model will calculate automatically the time end of the road hump as seen in Figure 4.6 by Abd el Salam et al. (2016). Also, the humps are considered to stay rigid and temperature-invariant through the tests.

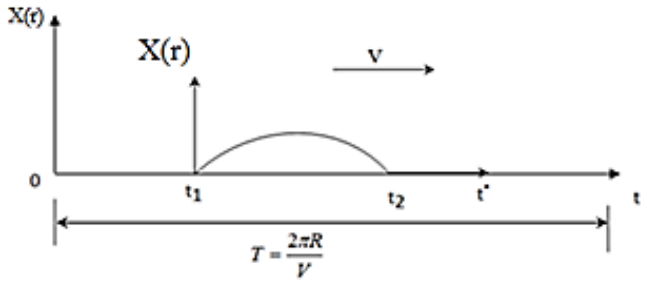

Figure 4.6 Schematic Diagram for Road Hump

Let $X(r) = \alpha + \beta t^* + \gamma t^{*2}$ (4.12)

At $t^* = 0, \quad X(r) = 0 \quad \alpha = 0$ (4.13)

$$X(r) = \beta t^* + \gamma t^{*2} \tag{4.14}$$

The model of the road hump has constant amplitude as shown in figure 4.7.

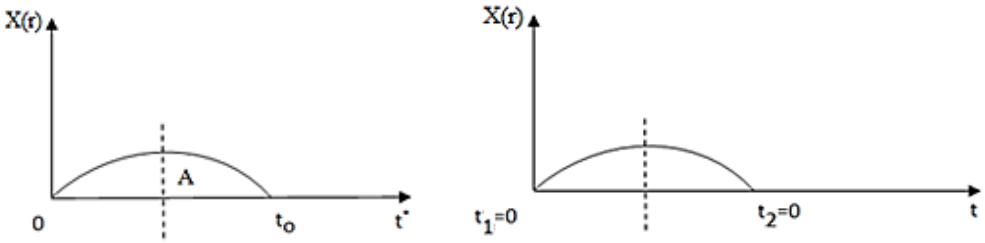

Figure 4.7 Amplitude of road hump at first boundary condition

At $t^* = t_o$, $X(r) = 0$ (4.15)

$$0 = \beta t_o^* + \gamma t_o^{*2} \quad \beta = -\gamma t_o \tag{4.16}$$

$$X(r) = (-\gamma t_o) t^* + \gamma t^{*2} \tag{4.17}$$

At $t* = \frac{1}{2} t_o \; X(r) = A$ (4.18)

$$A = -\gamma t_o \left(\frac{t_o}{2}\right) + \gamma \left(\frac{t_o^{\,2}}{4}\right) \qquad A = -\frac{1}{2}\gamma t_o^{\,2} + \frac{1}{4}\gamma t_o^{\,*}$$

(4.19)

$$4A = -2\gamma t_o^{\,2} + \gamma t_o^{\,2} = -\gamma t_o^{\,2} \tag{4.20}$$

$$\gamma = \frac{-4A}{t_o^{\,2}} \tag{4.21}$$

And $\beta = -\gamma t_o \qquad = \left(\frac{-4A}{t_o^{\,2}}\right) t_o \qquad = \left(\frac{4A}{t_o}\right)$ (4.22)

$$\beta = \frac{4A}{t_o} \tag{4.23}$$

$$X(r) = \left(-\gamma t_o\right) t^* + \gamma t^{*2} \tag{4.24}$$

To check the starting time zero and the end time as boundary conditions

At $t^* = 0 \qquad X(r) = 0$ (4.25)

At $t^* = t_o \qquad X(r) = \left(\frac{4A}{t_o}\right) to - \left(\frac{4A}{t_o^{\,2}}\right) t_o^{\,2} = 0$ (4.26)

At $t^* = \frac{1}{2} t_o \qquad X(r) = \left(\frac{4A}{t_o}\right)\left(\frac{t_o}{2}\right) - \left(\frac{4A}{t_o^{\,2}}\right)\left(\frac{t_o^{\,2}}{4}\right) = 2A - A = A$ (4.27)

$$X(r)=\left(\frac{4A}{t_o}\right)\left(1-\frac{t^*}{t_o}\right)t^*=\left(\frac{4A}{t_o}\right)\left(\frac{t_o-t^*}{t_o}\right)t^* \tag{4.28}$$

$$X(r)=\left(\frac{4A}{t_o^{\,2}}\right)\left(t_o-t^*\right)t^* \tag{4.29}$$

$$t^* = t-t_1 \tag{4.30}$$

then

$$X(r)=\frac{4A}{t_o^{\,2}}\left[t_o-\left(t-t_1\right)\right]\left(t-t_1\right) \tag{4.31}$$

$$=\frac{4A}{t_o^{\,2}}\left[t_o+t_1-t\right]\left(t-t_1\right) \tag{4.32}$$

$$X(r)=\frac{4A}{t_o^{\,2}}\left(t_2-t\right)\left(t-t_1\right) \tag{4.33}$$

$$=\frac{4A}{\left(t_2-t_1\right)^2}\left(t_2-t\right)\left(t-t_1\right) \tag{4.34}$$

$$X(r)=4A\frac{\left(t_2-t\right)\left(t-t_1\right)}{\left(t_2-t_1\right)^2} \tag{4.35}$$

$$\text{At}\quad t=0 \qquad X(r)=4A\frac{\left(t_o-o\right)\left(o-o\right)}{t_o^{\,2}}=0 \tag{4.36}$$

$$\text{At}\quad t=t_o \qquad X(r)=4A\frac{\left(t_o-t_o\right)\left(t_o-o\right)}{t_o^{\,2}}=0 \tag{4.37}$$

$$\text{At}\quad t=\frac{1}{2}to \qquad X(r)=4A\frac{\left(t_o-\frac{1}{2}t_o\right)\left(\frac{1}{2}t_o-o\right)}{t_o^{\,2}}=4A\frac{\frac{1}{4}t_o^{\,2}}{t_o^{\,2}}=A \tag{4.38}$$

$0\le t\le T$

$$0\le t<t_1 \qquad X(r)=0 \tag{4.39}$$

$$t_2 < t \le T \qquad X(r) = 0 \tag{4.40}$$

$$t_1 \le t \le t_2 \qquad X(r) = 4A\frac{(t_2 - t)(t - t_1)}{(t_2 - t_1)^2} \tag{4.41}$$

The geometry of the profile hump has been evaluated with second boundary condition as shown in figure 4.8.

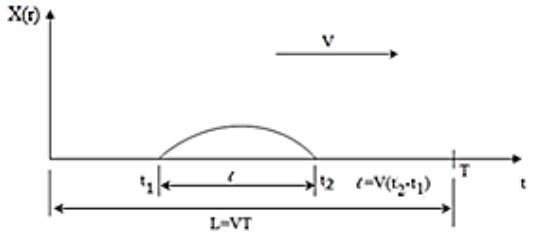

Figure 4.8 Road Hump at Second Boundary Condition

$$V = wR = 2\pi NR \tag{4.42}$$

$$T = \frac{L}{V} = \frac{2\pi R}{2\pi NR} = \frac{1}{N} \tag{4.43}$$

$$l = (\Delta\theta)R, \qquad L = 2\pi R \tag{4.44}$$

$$V(t_2 - t_1) = (\Delta\theta)R \tag{4.45}$$

$$t_2 - t_1 = \frac{(\Delta\theta)R}{V} = \frac{(\Delta\theta)RT}{V} = \frac{(\Delta\theta)RT}{2\pi R} \tag{4.46}$$

$$t_2 = t_1 + \left(\frac{\Delta\theta}{2\pi}\right)\frac{1}{N} \quad \text{or} \quad t_2 = t_1 + \left(\frac{l}{L}\right)\frac{1}{N} \tag{4.47}$$

The left and right side of the geometry of the road hump aero foil will be: (See fig 4.9 & 4.10)

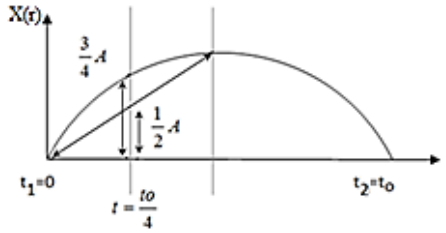

Figure 4.9 Geometry of Aerofoil Left Side Road Hump

$$X(r) = 4A\frac{(t_2 - t)(t - t_1)}{(t_2 - t_1)^2} \tag{4.48}$$

$$X(r) = 4A\left[\frac{\left(t_o - \frac{1}{4}t_o\right)\left(\frac{1}{4}t_o - 0\right)}{t_o{}^2}\right] \tag{4.49}$$

$$X(r) = \frac{3A}{4} \tag{4.50}$$

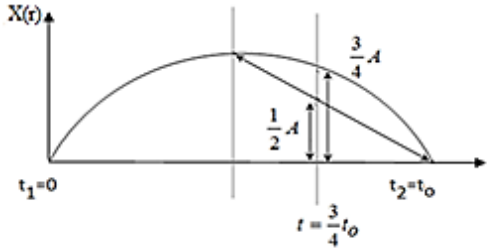

Figure 4.10 Geometry of Aerofoil Right Side Road Hump

$$X(r) = 4A\frac{(t_2 - t)(t - t_1)}{(t_2 - t_1)^2} \tag{4.51}$$

$$X(r) = \frac{4A}{t_o{}^2}\left[\left(t_o - \frac{3}{4}t_o\right)\left(\frac{3}{4}t_o - 0\right)\right] \tag{4.52}$$

$$X(r) = \frac{3A}{4} \tag{4.53}$$

Figure 4.11 described the simulation time during the modeling.

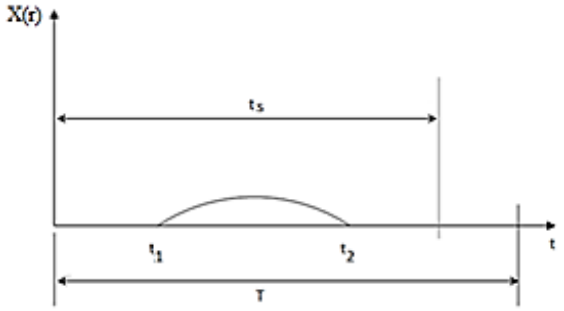

Figure 4.11 Simulation Time of Road Hump

$0 \le t \le t_s$

$$0 \le t \le t_1 \qquad X(r) = 0 \tag{4.54}$$

$$t_2 \le t \le t_s \qquad X(r) = 0 \tag{4.55}$$

$$t_1 \le t \le t_2 \qquad X(r) = 4A\frac{(t_2 - t)(t - t_1)}{(t_2 - t_1)^2} \tag{4.56}$$

Where

$$t_2 = t_1 + \left(\frac{l}{L}\right)\frac{1}{N} \quad \text{or} \quad t_2 = t_1 + \left(\frac{\Delta\theta}{2\pi}\right)\frac{1}{N} \tag{4.57}$$

This model was inserted into the 2-DOF model, which made it easier to simulate the bump considered in our study. The velocity of the car will be one of the parameters to be observed, it will vary in our test.

4.4 Parameters of Simulation Model

Objective of mathematical modeling of the suspension system in this work is to simulate the front quarter car suspension system in detail using MATLAB/SIMULINK representation of the model. The SIMULINK representation is derived based on the 2 degree of freedom equations of motion for the system. Ode5 (Dormand-prince) solver in MATLAB is used to observe the performance of the passive nonlinear and linear suspension system. On the present simulation, the simulation time was 10 second with 0.001 fixed step size. Table 4.1 shows the parameter for our simulation model.

Table 4.1 Parameter of Simulation Model

Definition	Symbol	Value
Car Body Mass	m_1	117 kg
Wheel Mass	m_2	36 kg
Spring Stiffness of Suspension	k_1	17.658 kN/m
Coefficient of Stiffness of Wheel	k_2	119.921 kN/m
Damping Coefficient of Damper	b_1	37.500 kN s/m
Damping Coefficient of Tyre	b_2	1447 N s/m
Irregular Excitation from the Road Surface	A	0.035 m
Length of The Road Hump	l	0.140
Radiance of The Drum Load	R	0.380 m
Frequency of Car Model System	N	Variable rps

4.5 Simulation Results and Discussion

The input of the irregularity of the road has been inputted into two models; the first is the quarter car model and the other the quarter car model with nonlinear suspension. Roads can have random roughness or standard humps to force drivers to reduce their vehicle speeds in residential areas. In this study, a speed hump is considered as an input to the quarter-car model. Standard humps have well known designs. They may be circular, parabolic or flat-topped. In our case, we entered a 0.035m high single hump with different widths therefore different frequencies (0.5Hz and 1Hz) to study the effect of the nonlinear suspension and the linear suspension.

4.5.1 Hump Road Input

In this section the simulation of the mathematical model will produce the displacement of the sprung mass and tyre. The input will be a hump with amplitude 0.035m with a frequency of 1Hz and 0.5z.

As we can see from figure 4.12 that the passenger displacement decreased by 51% and in figure 4.13 decreased by 35% therefore we concluded for different types of humps we can see that the nonlinear suspension always obtains a lower displacement than the normal suspension.

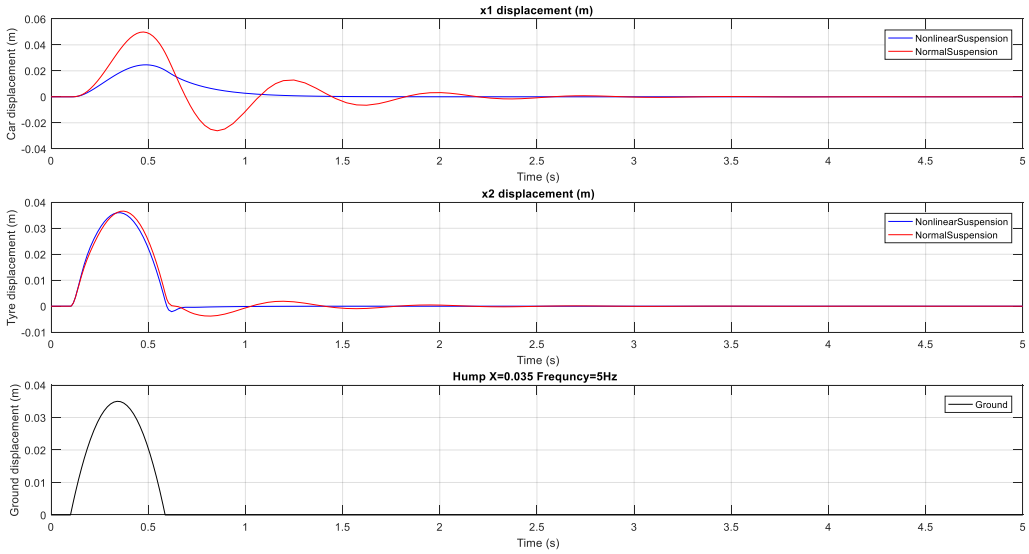

Figure 4.12 Hump Model 1: i) Car Displacement (m) ii) Tyre Displacement (m) iii) Ground Displacement Road Hump Amplitude 0.035 m Frequency: 1Hz

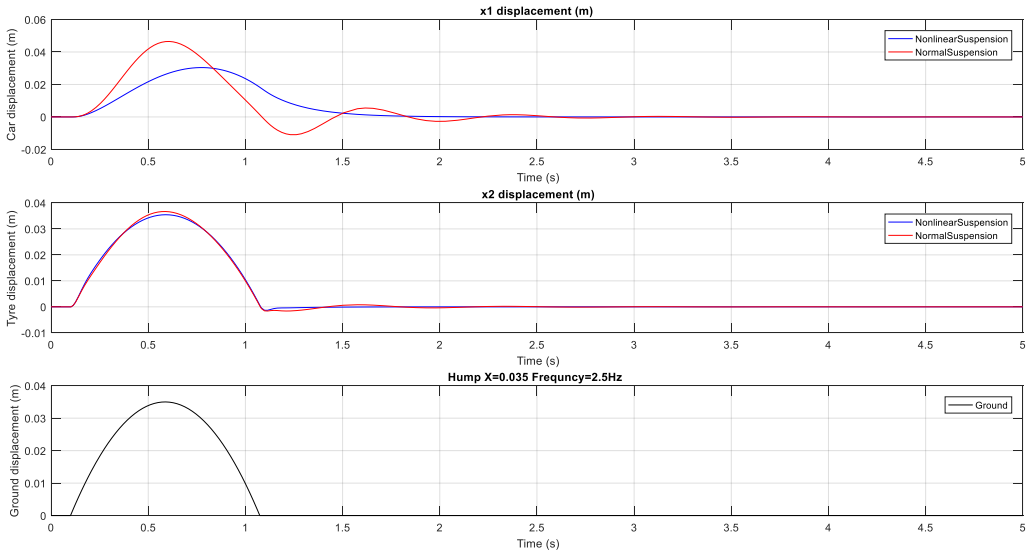

Figure 4.13 Hump Model 2: i) Car Displacement (m) ii) Tyre Displacement (m) iii) Ground Displacement Road Hump Amplitude 0.035 m Frequency: 0.5Hz

4.5.2 Sinusoidal Road Input

To further study the effect of the suspension we added a road input with a sinusoidal signal with different frequencies (0.5Hz, 1Hz) but with constant amplitude of 0.035 m acting as the road input. In this case, we investigated the displacement and acceleration of the passenger as seen in figure 4.14 to 4.20.

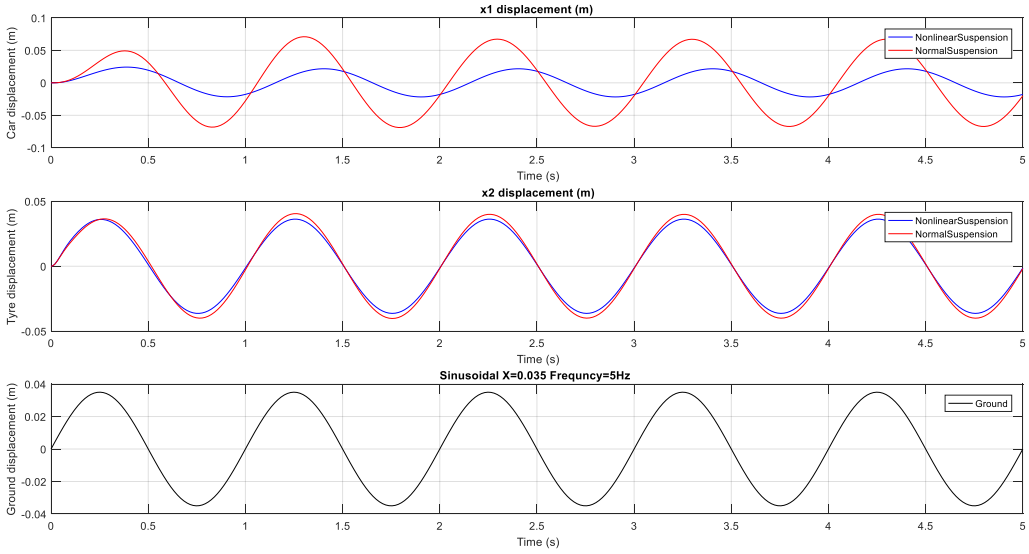

Figure 4.14 Sinusoidal Model 1: i) Car Displacement (m) ii) Tyre Displacement (m) iii) Ground Displacement Road Sinusoidal Amplitude 0.035 m Frequency: 1Hz

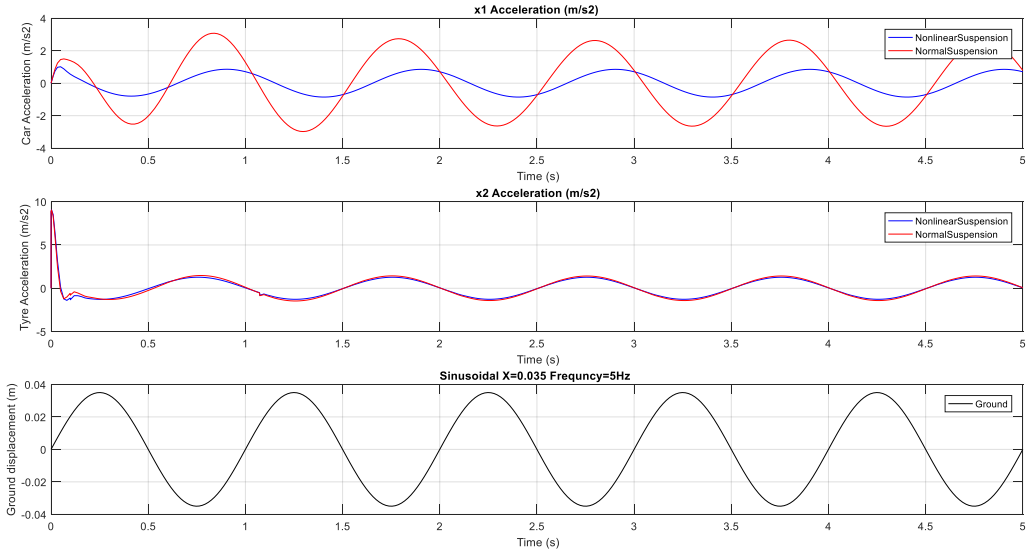

Figure 4.15 Sinusoidal Model 1: i) Car Acceleration (m/s^2) ii) Tyre Displacement (m) iii) Ground Displacement Road Sinusoidal Amplitude 0.035 m Frequency: 1Hz

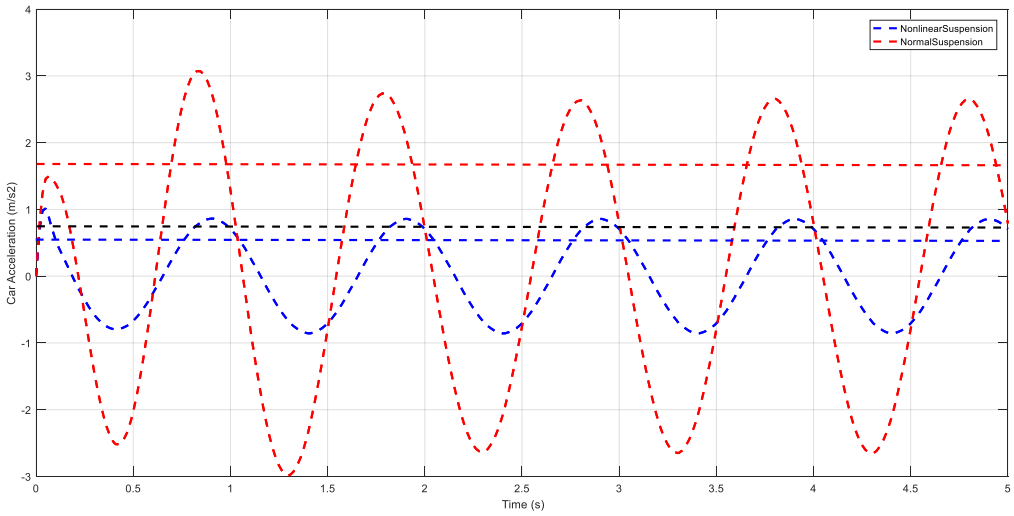

Figure 4.16 Sinusoidal Model 1: Car Acceleration (m/s^2) Road Sinusoidal Amplitude 0.035 m Frequency: 1Hz

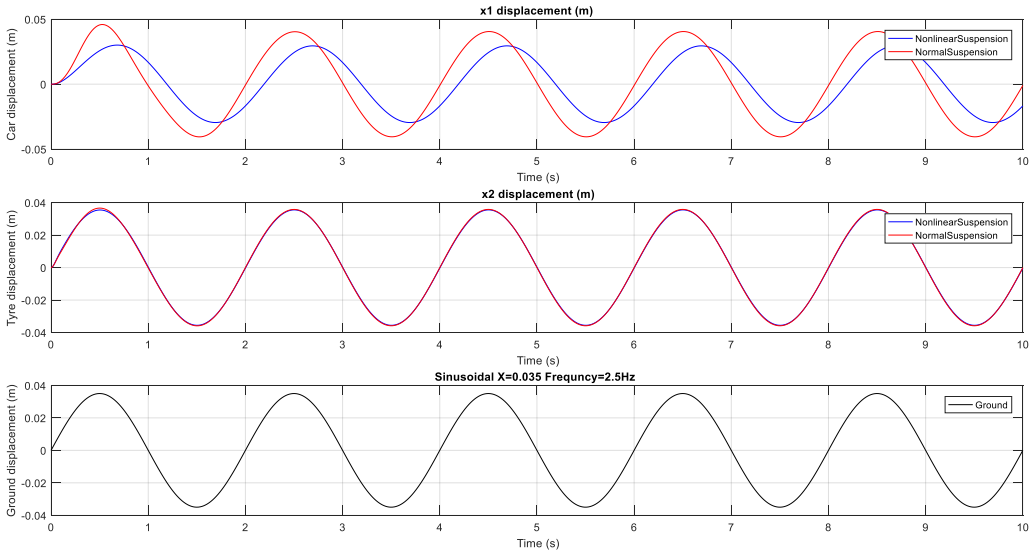

Figure 4.17 Sinusoidal Model 2: i) Car Displacement (m) ii) Tyre Displacement (m) iii) Ground Displacement Road Sinusoidal Amplitude 0.035 m Frequency: 0.5Hz

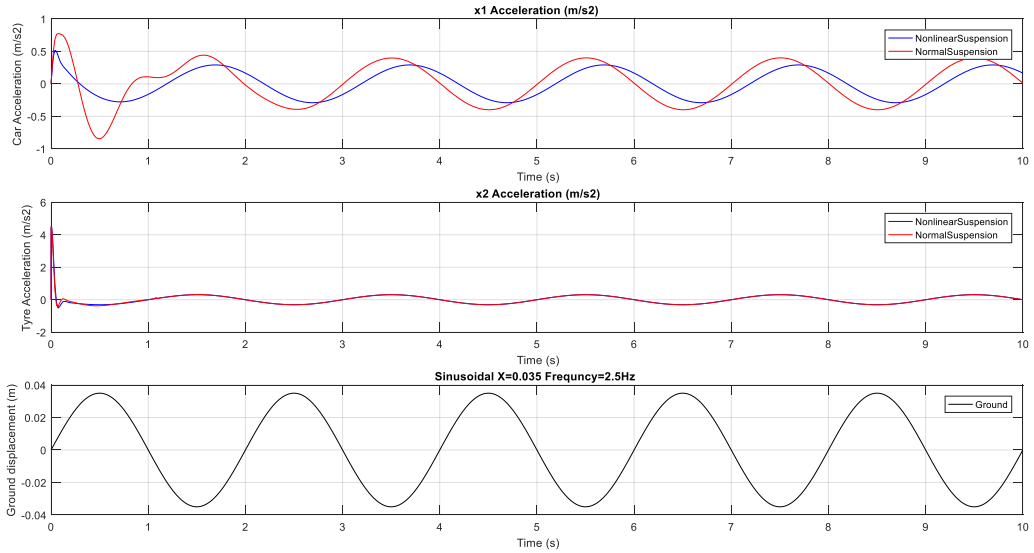

Figure 4.18 Sinusoidal Model 2: i) Car Acceleration (m/s^2) ii) Tyre Displacement (m) iii) Ground Displacement Road Sinusoidal Amplitude 0.035 m Frequency: 0.5Hz

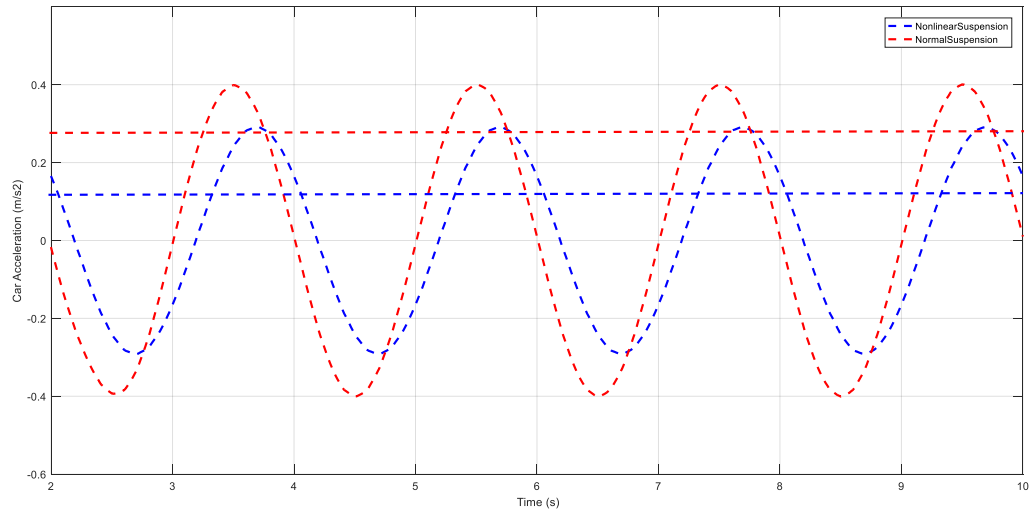

Figure 4.19 Sinusoidal Model 2: Car Acceleration (m/s^2) Road Sinusoidal Amplitude 0.035 m Frequency: 0.5Hz

Figure 4.14 shows that the displacement decreased by 56% from replacing a normal suspension with a nonlinear suspension. To ensure optimal ride comfort specified by British standards ISO 2631-1997 which states that the optimum weighted RMS of Vertical acceleration level must exceed 0.8m/s^2. We study the acceleration of the passenger as seen in figure 4.15, 4.16. The effect of the nonlinear suspension reduces the

acceleration of the passenger from 1.8m/s^2 to 0.6m/s^2 which is relatively close to the optimum ride comfort standard.

Figure 4.17 shows that the displacement decreased by 27% from replacing a normal suspension with a nonlinear suspension. We study the acceleration of the passenger as seen in figure 4.18, 4.19. The effect of the nonlinear suspension reduces the acceleration of the passenger from 0.3m/s^2 to 0.18m/s^2 which both are lower than the optimum ride comfort standard.

4.5.3 Random Road Input

In this section the road input will be a random signal with an average amplitude of 0.035 m, to analyse effect of the nonlinear spring on a coarse road.

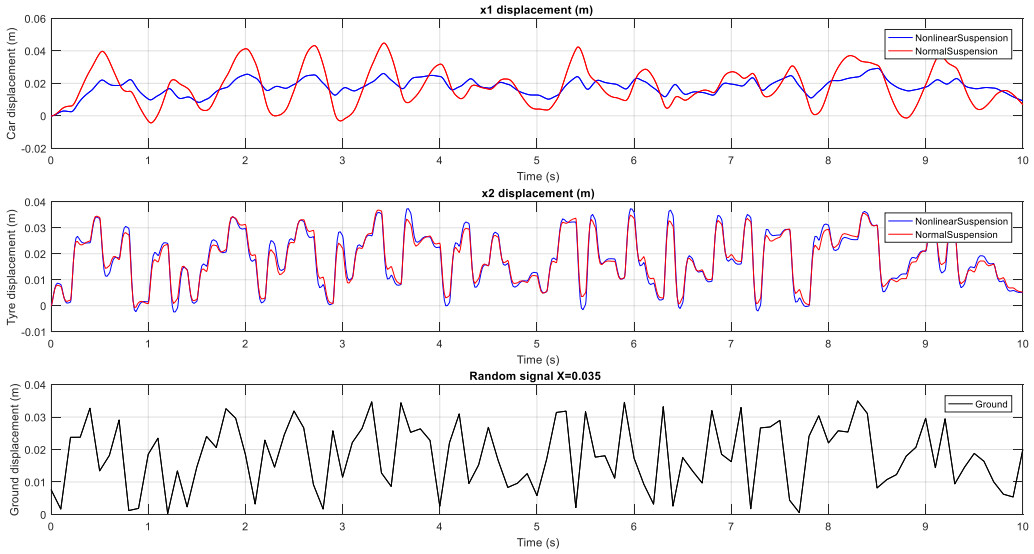

Figure 4.20 Random Model 1: i) Car Displacement (m) ii) Tyre Displacement (m) iii) Ground Displacement

Figure 4.20 shows that even in a random ground input that the nonlinear stiffness with no previous tuning can decrease the displacement of the passenger.

As we can see from the results we reach the conclusion that integrating nonlinear suspension in most cases increases the efficiency of the suspension and increases the comfort of the passenger.

The governing equations of the two degree-of-freedom quarter car model integrated with nonlinear suspension were developed using Matlab® and Simulink®. The integration of the nonlinear stiffness within the quarter model has been successfully achieved allowing for a decrease in vibration in all cases of road profiles. The criteria of road comfort are the RMS of the main mass acceleration and the results show that we reached this or got really close to it. It has been learnt that nonlinear suspension is verily suitable for vehicles.

4.5.4 Simulation Results with Linear Suspension for Different Masses

To further study our model, the vehicle speed is integrated into the simulation model. The simulation displacement of the sprung mass is compared for five different constant speeds (25 Hz, 27.5 Hz, 30 Hz, 35 Hz and 40 Hz) or in km/hr (5 km/hr, 6 km/hr, 6.3 km/hr, 7.3 km/hr and 8.3 km/hr) at four different sprung masses (100 kg, 150 kg, 200 kg and 250 kg) (See figures 4.21a, b, c and d respectively). By studying the effect of the speed of the car, it can be seen from the results of the four graphs that each given body mass, the amplitude of the displacement for the car body mass decreases as the speed increase.

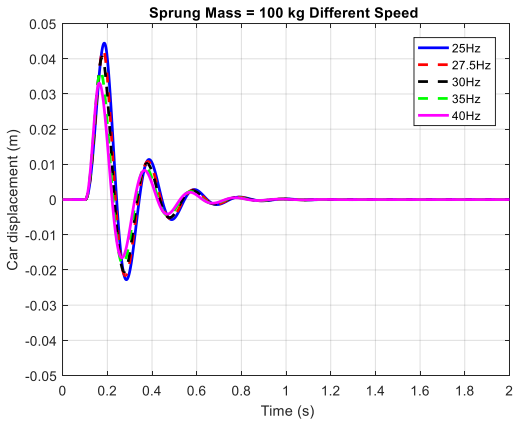

(a) Mass 100 kg

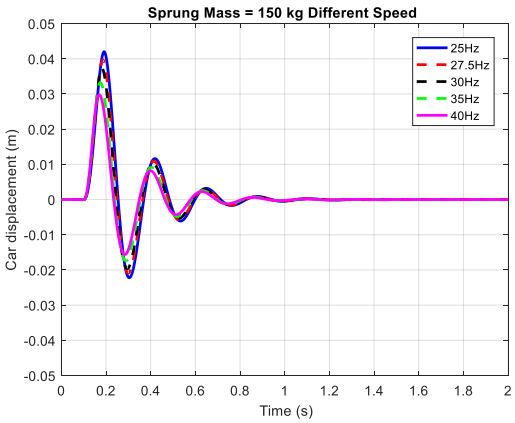

(b) Mass 150 kg

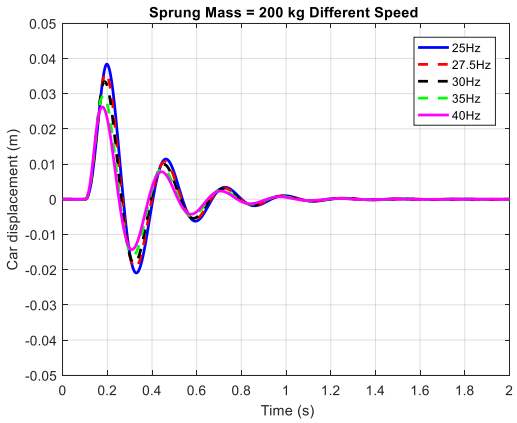

(c) Mass 200 kg

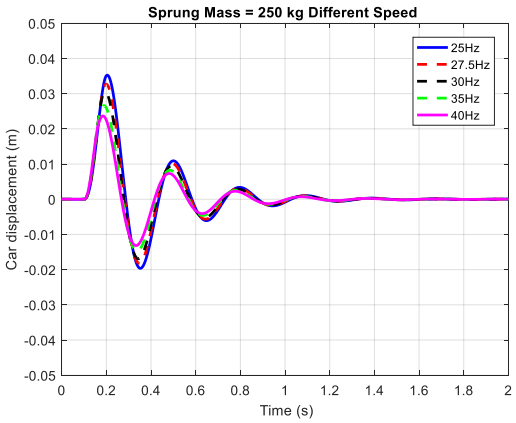

(d) Mass 250 kg

Figure 4.21 Simulation Amplitude of the Suspension System with Constant Car Mass for Different Speeds

4.5.5 Simulation Results with Linear Suspension for Different Speeds

The simulation displacement of the sprung mass is compared for four different masses (100 kg, 150 kg, 200 kg and 250 kg) at a constant speed therefore studying the effect of varying the mass. (See figures 4.22,23,24,25 & 26). By studying the effect of the car mass, it can be seen from the results of the five graphs that the amplitude of the displacement for the car body mass decreases as the car mass increases.

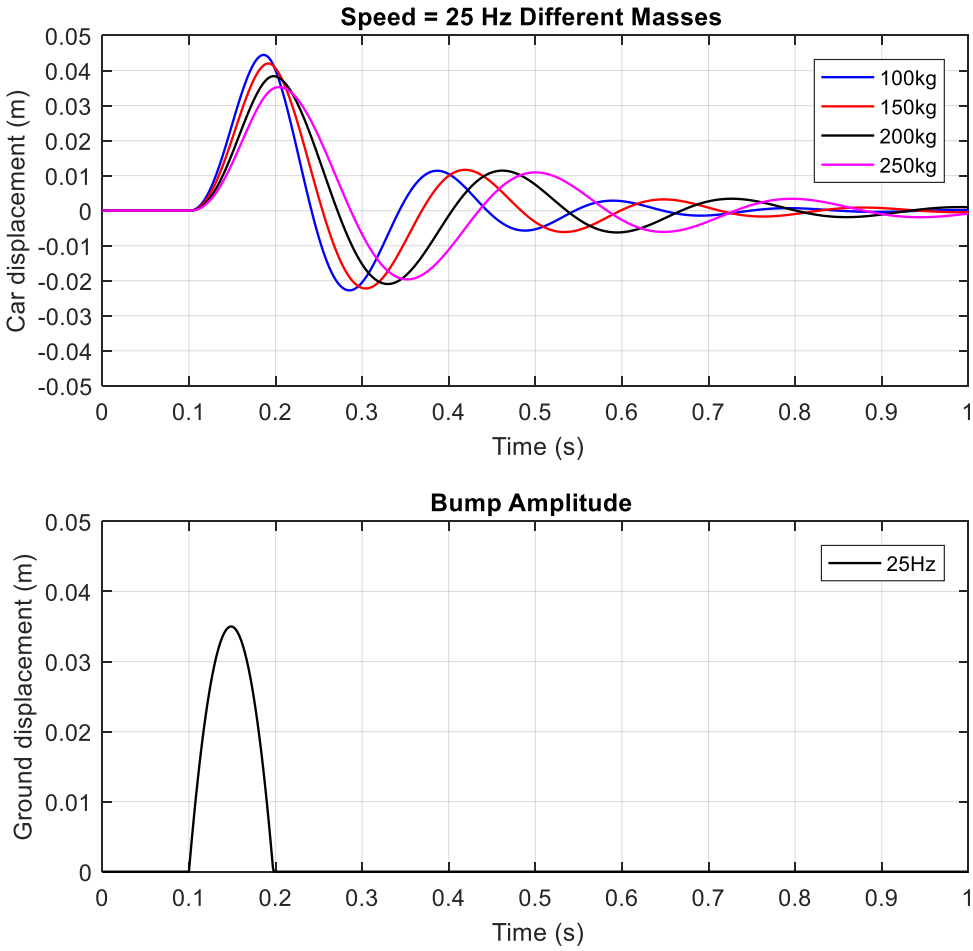

Figure 4.22 Simulation Amplitude of The Suspension System with Constant Speed 25 Hz, 5 km/hr for Different Car Mass

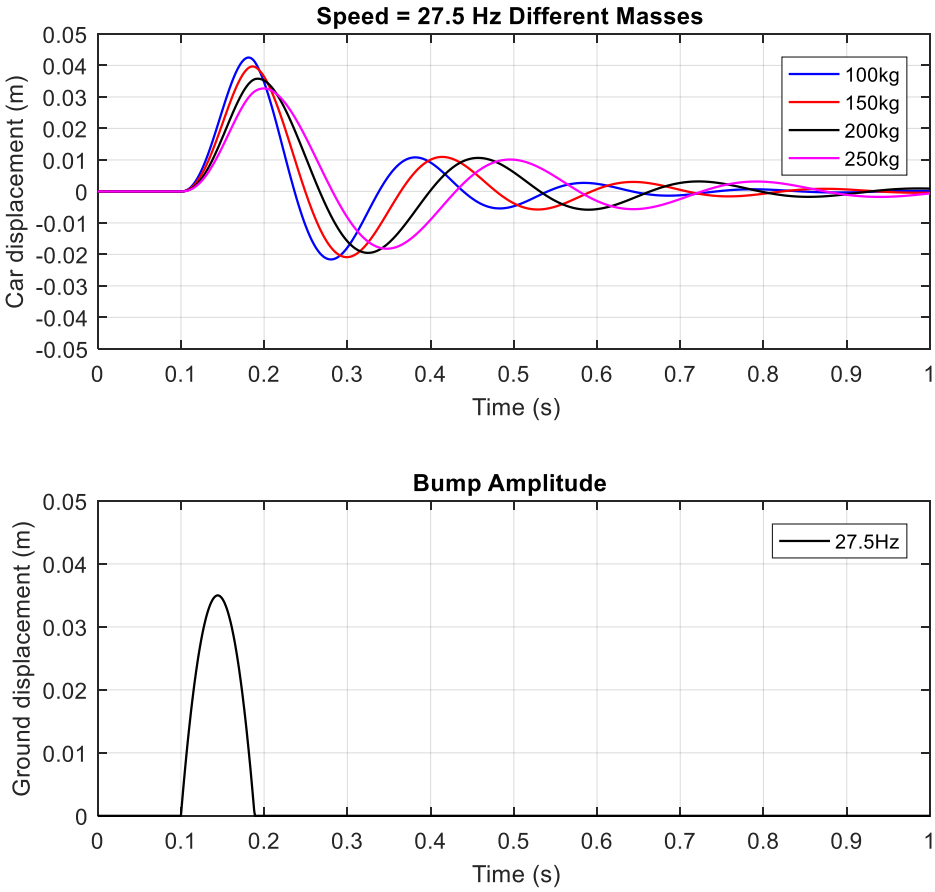

Figure 4.23 Simulation Amplitude of the Suspension System with Constant Speed 27.5 Hz,6 km/hr for Different Car Mass

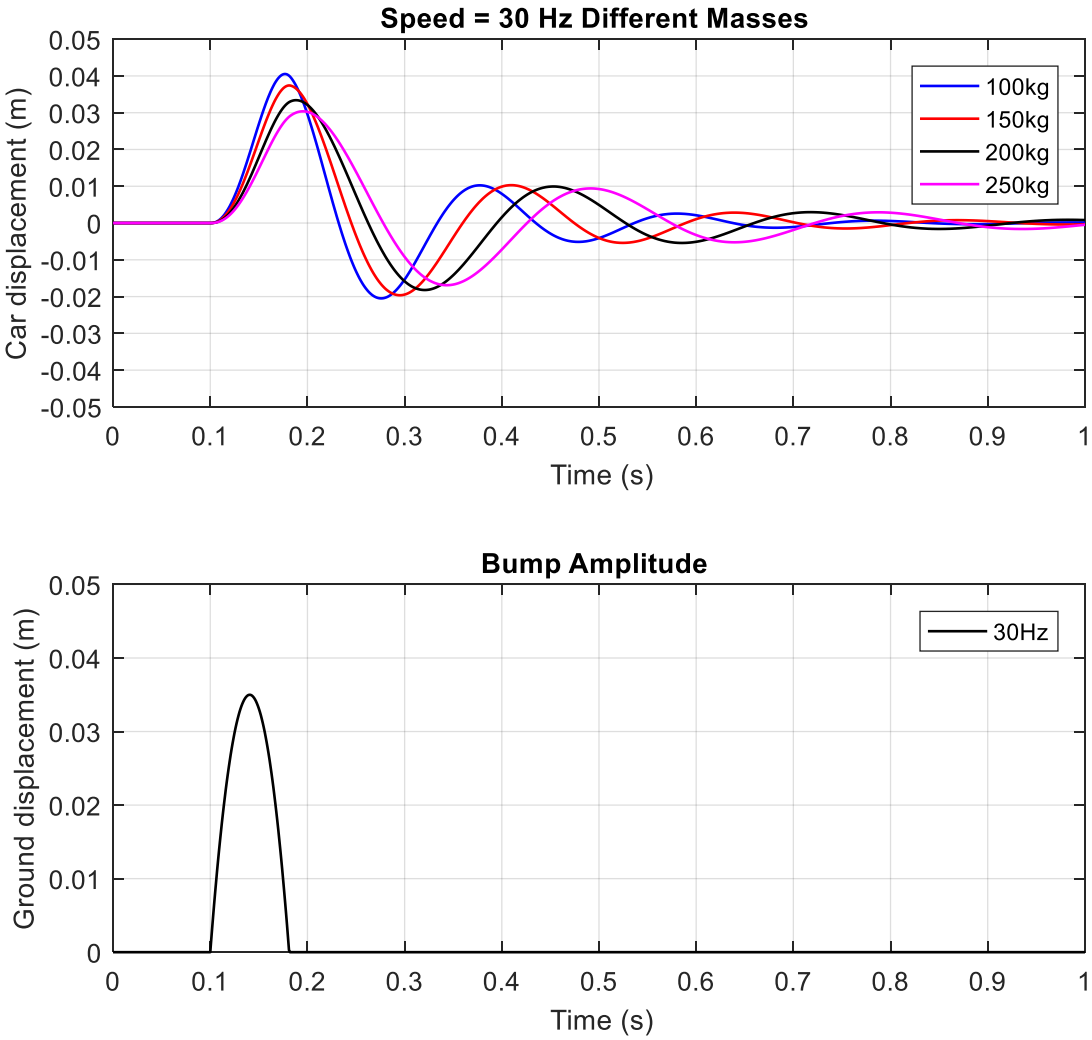

Figure 4.24 Simulation Amplitude of the Suspension System with Constant Speed 30 Hz,6.3 km/hr for Different Car Mass

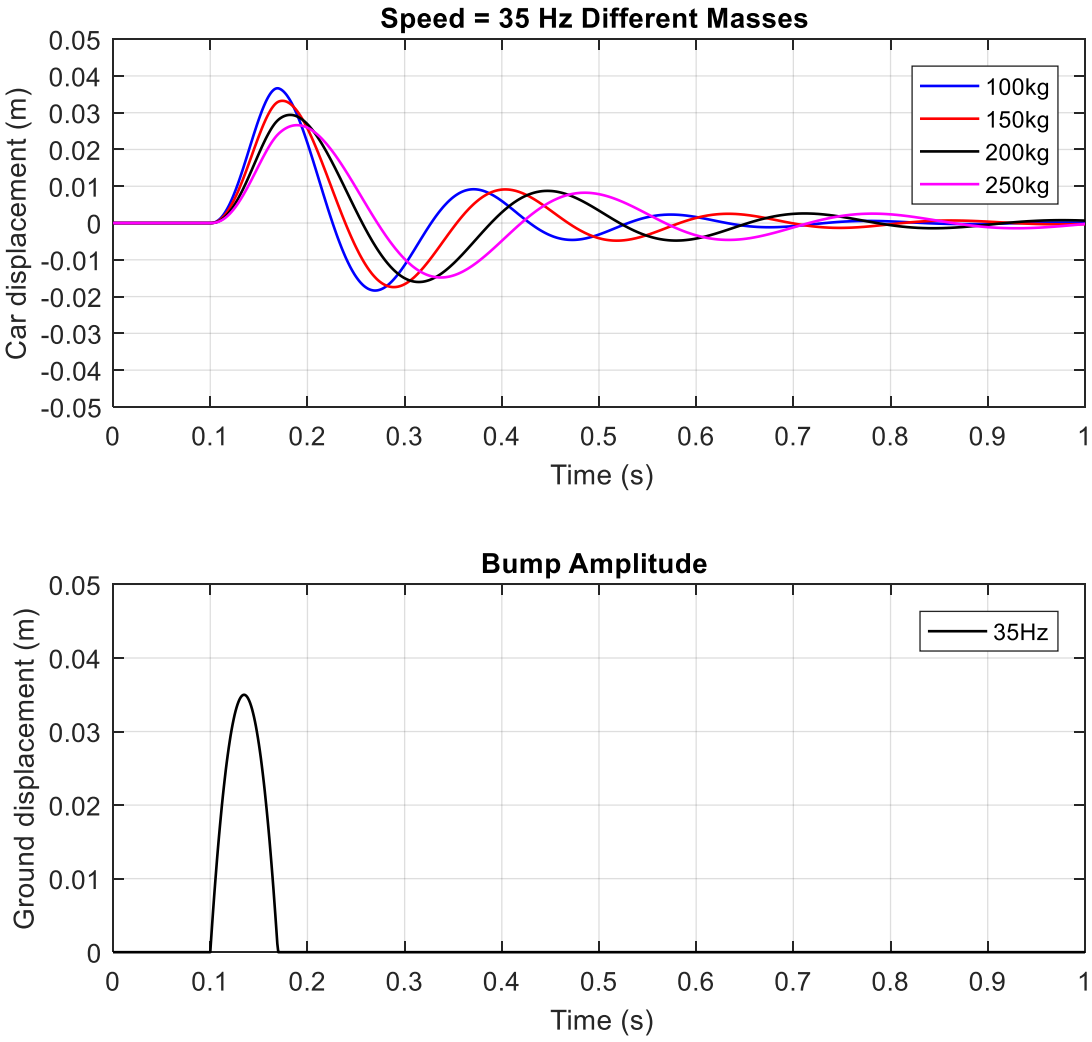

Figure 4.25 Simulation Amplitude of the Suspension System with Constant Speed 35 Hz,7.3 km/hr for Different Car Mass

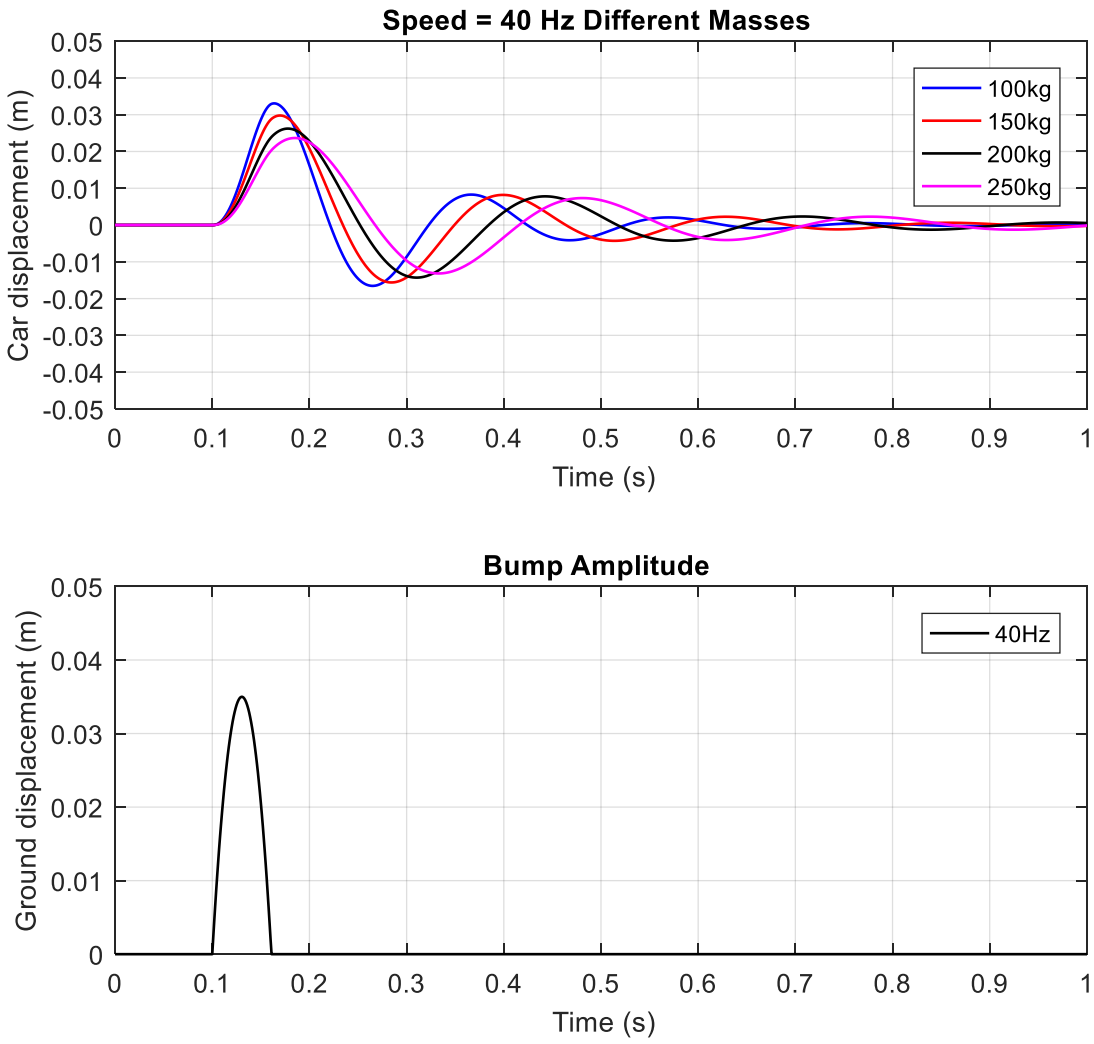

Figure 4.26 Simulation Amplitude of the Suspension System with Constant Speed 40 Hz,8.3 km/hr for Different Car Mass

4.5.6 Conclusion

A mathematical model of a quarter car has been derived, the governing equations have been simulated using Matlab/Simulink. The study consisted of applying different conditions to the model, first the model was given a sinusoidal input and a bump at different frequencies. Results showed that the nonlinear model obtained better results and performed much better than the linear passive model. The acceleration of the passenger clearly decreased entering in the domain of the comfort zone. To further investigate the model,

the two degree of freedom model was studied at different car speeds, studying the effect. Obtained data showed that by increasing the speed of the vehicle above the bump that the displacement of the passenger decreased. The same study was done by increasing the equivalent values of the main mass, results also showed that a decrease of displacement occurred. This data will help us investigate if this theoretical work corresponds to the experimental work in chapter 6.

5 CHAPTER 5 GENETIC ALGORITHM

5.1 Introduction

Obtaining an optimum suspension system is of great importance for automotive and vibration engineer involved in the vehicle design process. The suspension affects an automobile's comfort, performance, and safety. The suspension system suspended the automobile's body a short distance above the ground and maintains the body at relatively constant height to prevent it from pitching and swaying. To maintain effective acceleration, braking, and cornering the components of good handling, the suspension system must also keep all four tyres firmly in contact with the ground. In this work the optimization of suspension parameters which include the spring stiffness and damper coefficient is designed to compromise between the comfort and the road handling. The mathematical model of the quarter-car is derived, and the dynamics are evaluated in terms of the main mass displacement and acceleration. The approach starts with the development of a fast and accurate vehicle model in Matlab® and Simulink® combined for testing the parameters and concludes by automated optimization of suspension parameters using Genetic Algorithm, to meet performance requirements specified. Results show that by optimizing the parameters the vibration in the system decreases immensely.

To design vehicle suspensions engineers used to obtain results of the system by trial and error through replacing the stiffness and damper. This was of course costly, time consuming and tedious. Due to innovations in computational power and theoretical methods now it is possible to use optimization tools to determine the optimum suspension parameters. Y. He and J. McPhee (2007) researched Application of Optimization Algorithms and Multibody Dynamics to Ground Vehicle Suspension Design, there is more than one algorithm and numerous methods available. Genetic Algorithms (GAs) have been used in different applications such as function optimization and control systems. It is known that GAs offer significant advantages over traditional methods by using several principles simultaneously and heuristics, whose most important aspects are: a population-wide search, a continuous balance between exploitation (convergence) and exploration (maintained diversity), and the principle of building block combination D.E. Goldberg (1989). GAs are general-purpose stochastic optimization methods for solving search problems to seek a global optimum. However, GAs is characterized by a large number of function evaluations Y. He (2007).

Verros and Natsiavas (2005) presented optimization of suspension stiffness and damping based on a quarter car model travelling on a random road profile. Presented was a critical comparison of quarter car models with passive linear and dual-rate suspension dampers and semi-active sky-hook damping models. Gomes (2009) presented optimization of 2-DOF quarter car model travelling over a random road surface using

particle swarm optimization (PSO) algorithm. Minimization of dynamic vehicle load and minimization of suspension deflection were used as objective functions in two optimization examples.

Optimization of a light commercial vehicle to improve vehicle ride and handling was performed by Özcan et al. (2013) using a quarter car and the half car models in Matlab/Simulink. The performance criterions considered were RMS body acceleration, tyre forces, and body roll. The performance results of the optimized suspension unit were verified from the car manufacturer. Chi et al. (2008) had presented optimization of linear quarter car model using three different techniques namely genetic algorithm (GA), pattern search algorithm (PSA) and sequential quadratic program (SQP) subjected to body acceleration, suspension working space, and dynamic tyre load as design criterions.

Molina-Cristobal et al. (2006). had presented multi-objective optimization of a passive suspension system using quarter car model using meta-heuristic optimization with the multi objective genetic algorithm (MOGA) and bilinear matrix inequalities (BMI) techniques. Ride comfort using RMS body vertical acceleration and road holding criterions were used as objective functions during optimization.

Baumal et al. (1998) presented GA-based optimization of half car model with an objective to minimize acceleration of the passenger's seat, subject to constraints such as road holding and suspension working space. Kuznetsov et al. (2011) had presented optimization of quarter car model coupled with a driver using three types of models, a 3-DOF driver–car model, a quarter car having 2 DOF and a driver having 1 DOF. Ride comfort criteria as per ISO 2631-1997 were used for optimization using the algorithm for global optimization problems (AGOP).

Gundogdu (2007) optimized a quarter car suspension system including the seat model using the genetic algorithm. A 2-DOF linear quarter car model was developed including a 2-DOF lumped mass driver model. The objective function is formulated using head acceleration, crest factor, suspension deflection and tyre deflection objective functions then converted into a uni-objective function using non-dimensional expressions, giving equal importance to each of the objective functions.

Salah et al. (2010) presented optimization of a quarter car including the human bio-mechanical model using a genetic algorithm. Seat acceleration, head acceleration, and suspension working space were used as the optimization criterion. The objective function was converted into an uni-objective function using weighting parameters. Results are compared to step and sinusoidal road profile.
Also, the human bio-mechanical model considered for the study based upon either a 1 DOF (Kuznetsov et al. (2011)) or 2 DOF (Gundogdu (2007)).

On the other hand, genetic algorithms (GA) method increases the probability of finding the global optimal solution and avoids convergence to a local minimum which is a drawback of gradient-based methods as concluded by Baumal, A.E et al. and R. Alkhatib et al (1998). In any vehicle suspension system, there are a variety of performance parameters, which need to be optimized. There are three important parameters, which should be carefully considered in designing a vehicle suspension system as concluded by Zavadinka, P. and Krišśák, P., (2009). Ride Comfort is directly related to the acceleration sensed by passengers when traveling on a rough road. Road holding ability is associated with the contact forces of the tyres and the road surface. These contact forces are assumed to depend linearly on the tyre deflection. Suspension travel refers to the relative displacement between the sprung and the unsprung masses. It should always be lesser than the rattle space.

D. Hrovat, and M. Hubbard (1981) stated that the improvement of ride quality in vehicles can reduce the driver's fatigue resulting in an increased safety and vehicle control. The suspension system reduces the transmission of oscillations to the vehicle body from road surface disturbances. The chassis should be well isolated from the road surface with a minimal suspension travel yet provide good handling performance. Prolong exposure to vibrations during vehicle usage has adverse effects on the operator's health, task performance, and comfort. Further-more, frequent breaks may be necessary due to health regulations and excessive fatigue due to the vibration levels. Consequently, the attenuation of vibrations transmitted from the road surface to vehicle occupants is an important issue for the minimization of discomfort levels that effect operator efficiency.

5.2 Optimization

Fig 5.1 shows the general flow chart of GA and the main components that contribute to the overall algorithm. The operation of the GA starts with determining an initial population whether randomly or using some heuristics. The fitness function is used to evaluate the members of the population and then they are ranked based on the performances. Once all the members of the population have been evaluated, the lower rank chromosomes are omitted, and the remaining populations are used for reproduction. This is one of the most common approaches used for GA. Another possible selection scheme is to use pseudo-random selection, allowing lower rank chromosomes to have a chance to be selected for reproduction. The crossover step randomly selects two members of the remaining population (the fittest chromosomes) and exchanges and mates them. The final step of GA is mutation. In this step, the mutation operator randomly mutates on a gene of a chromosome. Mutation is a crucial step in GA since it ensures that every region of the problem space can be reached. Elitism is used to prevent the best solution of the population from being destroyed

during crossover and mutation operation. Elitism guarantees the fitness of new generation will be at least as good as current generation. The evaluation and generation of the new populations continue until the maximum number of generations is reached or the optimum solution is found. GA is advantageous in terms of requiring limited parameter settings and initializing itself from possible solutions rather than a single solution. One of the main drawbacks of GA is the lack of fast convergence towards the optimal values since the crossover and mutation process are random.

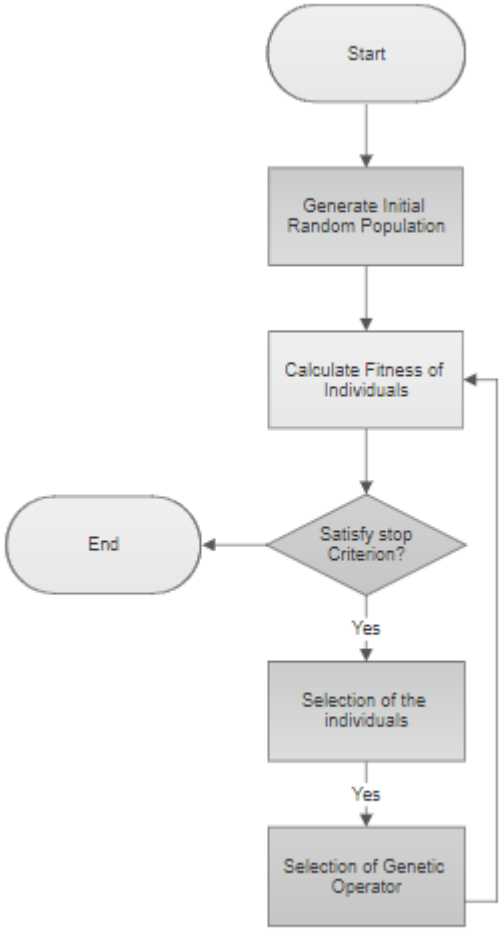

Figure 5.1 Flow Chart of Genetic Algorithm

Optimization objective is to minimize the sprung mass acceleration of the quarter car model. So, the required comfort is obtained from the system. For the above requirement, we use the objective function which is fitness function for Genetic Algorithm (GA) optimization process by D. A. HULLENDER (2001). According to James principal, the root mean square (RMS) of sprung mass acceleration can be expressed as:

$$\ddot{\alpha}(k_1, b_1) = \sqrt{\pi \, RV[\frac{k_2 \, b_1}{2 \, m_1 \left(\frac{3}{2}\right) k_1 \left(\frac{1}{2}\right)} + \frac{(m_1 + m_2) k_1^{(2)}}{2 \, b_1 \, m_1^{(2)}}]} \quad (5.1)$$

The optimization results are derived for a quarter car configuration, travelling at the speed of V=3 m/s on the road with an irregularity coefficient of power spectrum taking the value of R =6.5x10-6 m^3.

The total number of generations to study was not determined before testing began. Because of the complex nature of the genetic algorithm and time limitations for the number of possible generations run, it was decided to start the genetic algorithm and observe how the genetic algorithm progressed before convergence criteria were set. In the end, the algorithm was terminated at the 5th generation. Provided the lower and upper bounds for the variables as per shown in the table followed:

Table 5.1 Bounds for the Optimization Problem

Parameters	**Bounds**	
	Lower	**Upper**
k_1(N/m)	1000	70000
b_1(Ns/m)	0	6000

After running the GA Optimisation, the optimised values of the variables are as follows:

$k_1 = 10{,}000$ N/m.
$b_1 = 1000$ Ns/m.

The results that we are obtaining from GA optimization can be verified by checking the response of our Simulink® Model. First, we just take some arbitrary values from the ranges, and get the response for these values. Then we'll compare the results which we are getting from our GA optimized parameters.

The outputs to be studied of the nonlinear model with the new genetic parameters are the primary mass deflection, primary mass acceleration. They are compared with the normal suspension configuration and a nonlinear suspension configuration. It is shown by the plot represented as in Fig. 5.2 to 5.4.

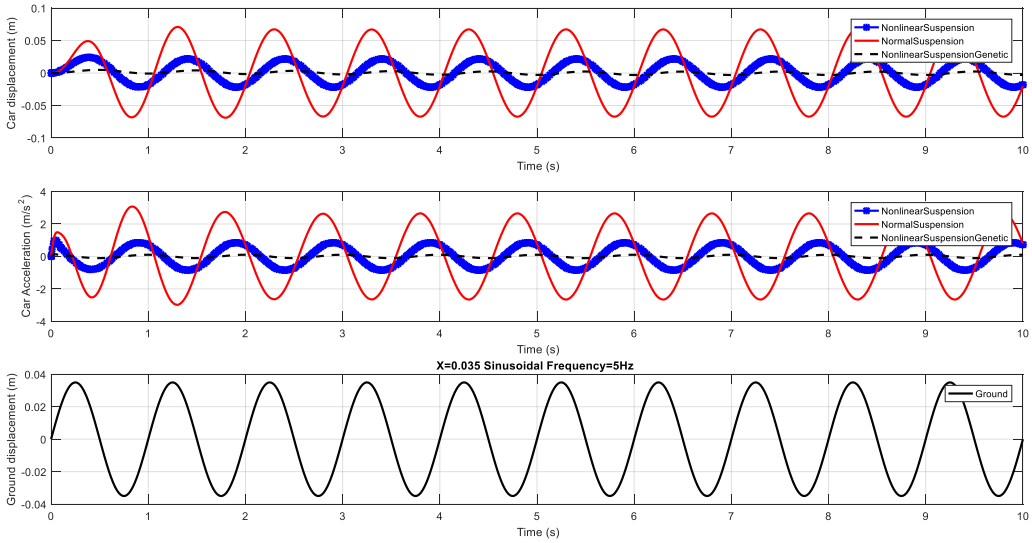

Figure 5.2 Sinusoidal Model 1: i) Car Displacement (m) ii) Car Acceleration (m/s^2) iii) Ground Displacement

Sinusoidal Model Amplitude 0.035 m Frequency: 1Hz

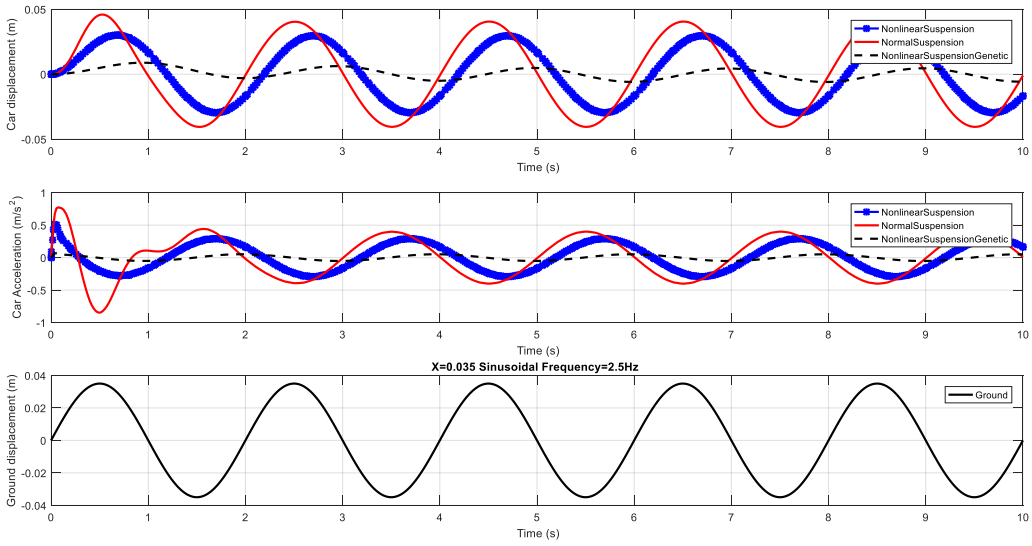

Figure 5.3 Sinusoidal Model 2: i) Car Displacement (m) ii) Car Acceleration (m/s^2) iii) Ground Displacement

Sinusoidal Model Amplitude 0.035 m Frequency: 0.5Hz

To further study the effect of the suspension we added a road input with a hump road input with different frequencies (0.5Hz, 1Hz) but with constant amplitude of 0.035 m. In this case, we investigated the displacement and acceleration of the passenger as seen in figure 5.4 and 5.5.

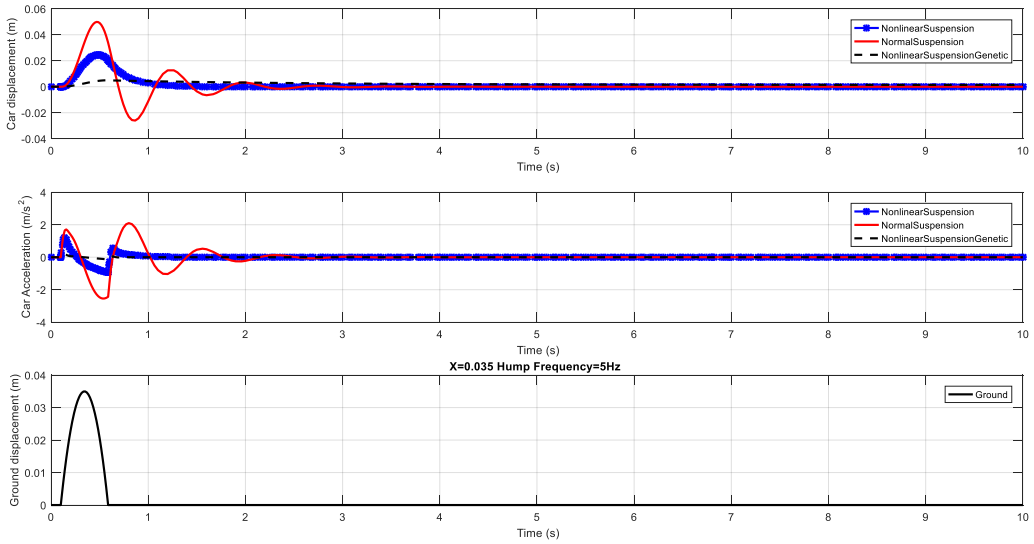

Figure 5.4 Hump Model 1: i) Car Displacement (m) ii) Car Acceleration (m/s^2) iii) Ground Displacement

Road Hump Amplitude 0.035 m Frequency: 1Hz

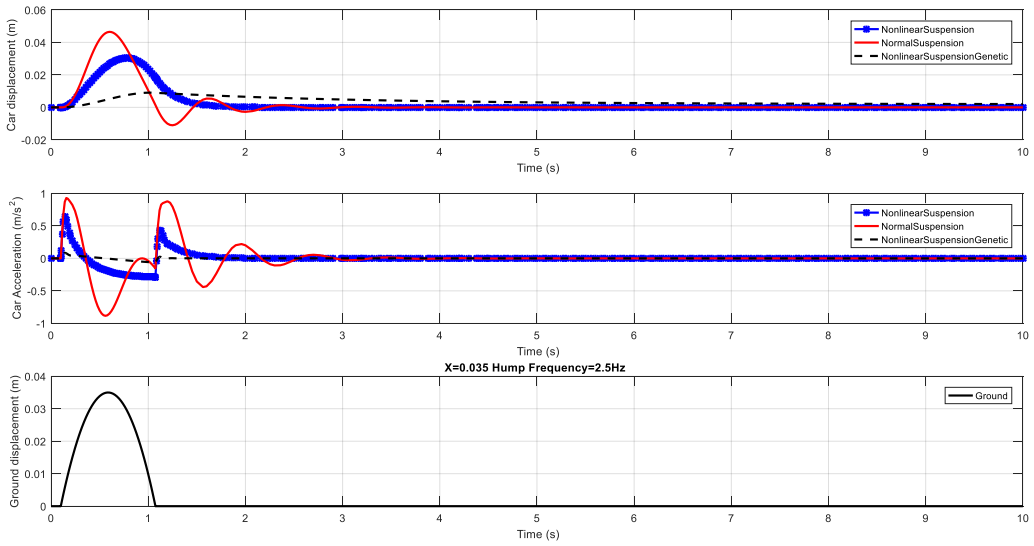

Figure 5.5 Hump Model 1: i) Car Displacement (m) ii) Car Acceleration (m/s^2) iii) Ground Displacement

Road Hump Amplitude 0.035 m Frequency: 0.5Hz

As we can see from Table 5.2 we conclude that the genetic algorithm parameters reduced the amplitude of vibration of the passenger in comparison to the Normal Suspension Model and a Nonlinear Suspension Model in the range of 80% to 95% also decreasing the acceleration.

Table 5.2 Results of Genetic Algorithm Model

Road Input	**Results of x_1 Displacement Amplitude**	
	Normal Suspension vs GA Suspension	**Nonlinear Suspension vs GA Suspension**
Sinusoidal Wave 1 Hz	Decreased by 90%	Decreased by 82%
Sinusoidal Wave 0.5 Hz	Decreased by 94.72%	Decreased by 81.96%
Hump Wave 1 Hz	Decreased by 92%	Decreased by 85.3%
Hump Wave 0.5 Hz	Decreased by 90.5%	Decreased by 81%

5.3 Conclusion

The integration of the optimization algorithms with the vehicle model has been successfully achieved allowing for an automated optimization process. It has been learnt that GA is verily suitable for such kind of iterative design problems. The number of parameters as applicable was appropriately selected by the algorithm for the optimized RMS of sprung mass acceleration. The parameters selected for optimization were in fact ideal. Usage of Matlab® for the application of the optimization algorithm i.e. GA made it very easy; else otherwise the massive amount of calculations to be carried for 'n' number of generations would have been practically impossible. It also gave the advantage of quickly adapting to the changes as per the algorithm to provide with the systems response. From the genetic algorithm, we note that for the nonlinear spring to work efficiently adding a smaller damping coefficient is needed.

6 CHAPTER 6 EXPERIMENTAL SET UP

6.1 Introduction

In this chapter, we will discuss the design and construction of the quarter-car test rig to be used in this work. It starts with a general discussion of the quarter-car rig's design. Details of how each major component was developed and/or specified are discussed. Calibration of different components of the rig are performed. The acceleration of the sprung mass is obtained for different suspension configurations, first with the passive linear suspension and secondly with the nonlinear suspension. Varying the speed and the sprung masses are the variables changed, to study their effect on the displacement of the sprung mass. Validation of the experimental set up with the simulated model is performed to ensure optimum parameter identification. At the end of this chapter the results are discussed.

6.2 General Description

An experimental rig was built from the ground up based on a Hyundai Verna 2014 car. It is designed so that testing different parameters with several configurations to attain all measurements required to study vehicle dynamics.

The rig is made up of various components which are the sprung mass, wheel and tyre, spring, vehicle suspension, damper, simulation land drum, base frame, linear guide as seen Figure 6.1 and 6.2. The tyre is a 195/50R15 type with a Center Bore: 54.1 mm, Wheel Fasteners: Lug nuts and Thread Size: M12 x 1.5. The torque of wheel bolts is 9~11 kg.m and the tyre pressure was set as 30 psi, which is the optimum pressure for this vehicle.

Figure 6.1 Quarter Car Experimental Test Rig

The body mass plate which carries the sprung mass are constrained with bearings to forcing it to only move in the vertical direction. Since the sprung mass is free to move in the vertical direction only, the vertical dynamic response of the specimen is to be tested because this is what the passenger will mainly feel when riding upon a road bump. To imitate a normal flat road the tyre is settled on the land drum which turns by the connected 7Horsepower motor.

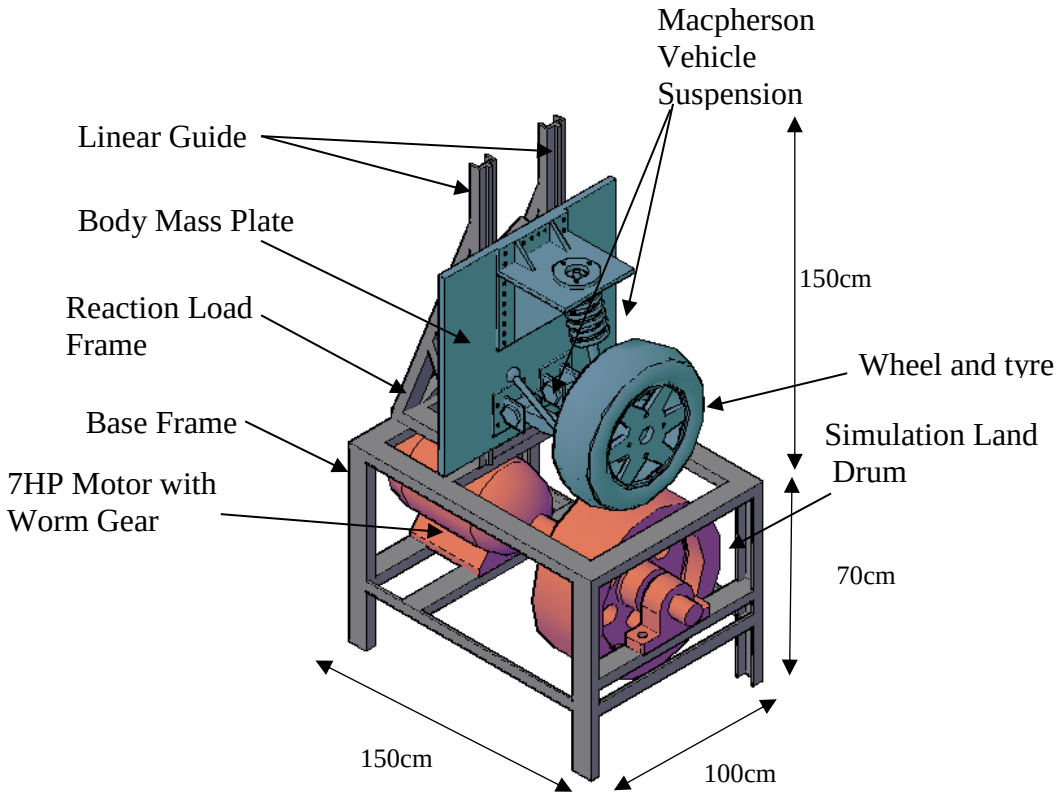

Figure 6.2 CAD Drawing for Suspension Test Rig

6.3 Base Frame and Foundation

The table frame is made of steel structure which damps any vibrations coming from the rig and carriers the whole rig consisting of reaction load frame with the body mass and suspension. On the other hand, the concrete base isolates our rig from any vibrations from for the floor building. (See Figure 6.3)

Figure 6.3 Concrete Base and Table Frame

6.4 Reaction Load Frame

For the same reasons as the base frame design the reaction load frame is also needed to be extremely robust. The reaction frame is the tall triangulated steel structure that is clamped to the table frame. The reaction frame and base frame are to provide a suitable rigid ground for the vibration experiment to work on. The reaction frame additional functionality lies in its ability to be move via small slots on the table frame allowing for a wide range of suspension designs and sizes. (See Figure 6.4)

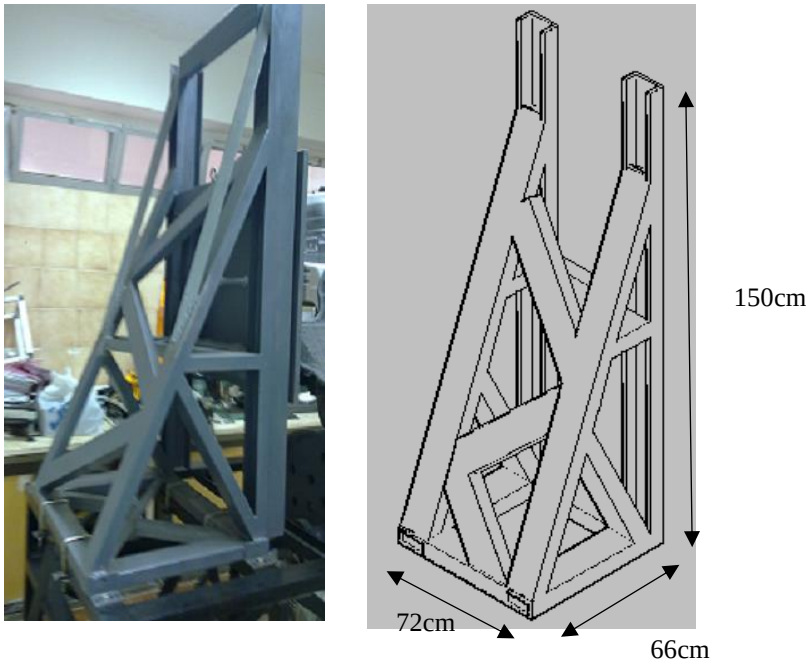

(a) **(b)**

Figure 6.4 (a) Reaction Load Frame (b) CAD design

6.5 Linear Guides

The base frame and reaction load frame are bolted together and will be the support structure for the entire rig. The linear guide is composed of eleven parts (See Figure 6.5). The frame of the linear guide holds the body mass plate with eight bolts. The linear two U shapes guide beams are bolted to the reaction load frame vertically. There are four rollers with slope each one with two bearing carries the frame of the linear guide and moves in one degree of freedom. There are four bearings at the back side of the U shapes beam to guide the frame in vertical direction only.

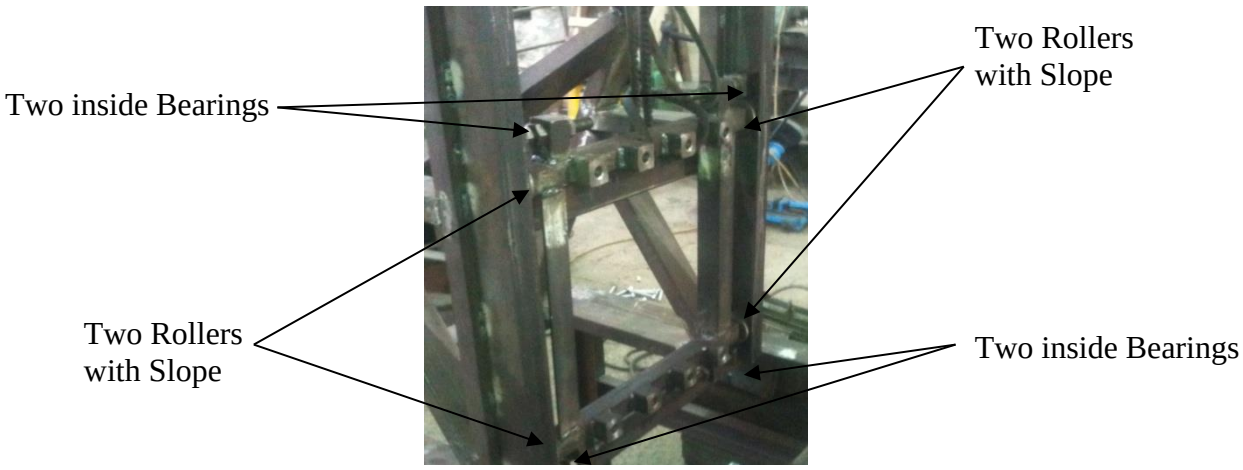

Figure 6.5 Linear Guide Chassis

6.6 Moving Mass

The moving mass is the part of the rig that replicates the vehicle's sprung mass, which includes the body and chassis. One design goal was to be able to attach different chassis designs to the same test rig without major modifications. To this end the moving mass was made into a modular two-piece design. A sprung mass plate was designed to be the permanently installed moving plate, while the sprung mass is bolted to the main moving mass carriers which are constrained by the linear guide chases. An adapter plate along with the appropriate fixtures is designed to be the interface between the sprung mass and the vehicle suspension. (See Figure 6.6)

Figure 6.6 Moving Mass Plate

6.7 Macpherson Suspension

The Macpherson strut suspension, designed in the late 1940s by Earl Steele Macpherson, was first used on the model 1949 Ford car. As such, it was a relatively new suspension configuration. Most current small and medium sized cars use this configuration. The MacPherson strut suspension configuration consists of a lower control arm and telescopic strut attached to the body of the car and to the wheel carrier, which is also called an upright. It is often the case that the primary spring and damper are co-linear with the strut's line of translation. The suspension, shown in Figure 6.7 is a typical variation of the Macpherson strut type independent suspension.

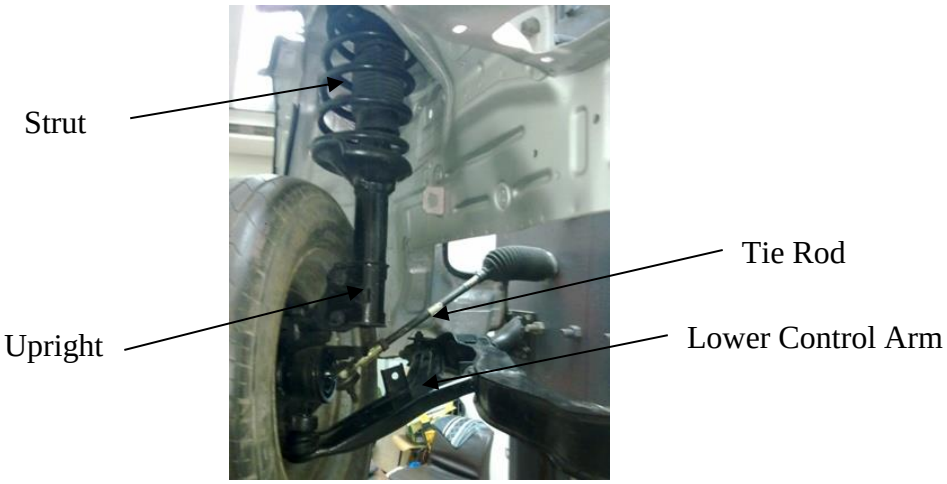

Figure 6.7 Macpherson Strut Type Suspension

6.8 Road Simulation

The road simulation drum has 0.75 m in diameter and a width of 0.3 m with the ability to add different types of humps, the one we will be using for our study is a half sin and its measurements are based upon the standard bumps found in all the roads, so it will provide the most realistic excitation and to include the effects of a rolling tyre. (See Figure 6.8)

Figure 6.8 Simulation Land Drum with Different Humps

6.9 Drive Motor with Inverter Controller

The base also houses the motor, motor controller, cams and gearing system. The motor is 3Hp and three phase electric motor (See Figure 6.9 a). The motor is run using a LS Inverter (See Figure 6.9 b).

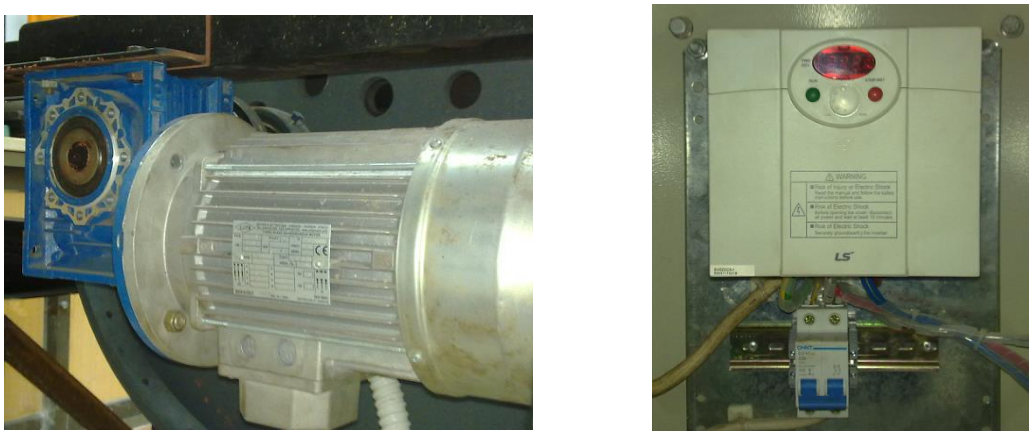

(a) Motor (b) Inverter

Figure 6.9 Three Phase Drive Motor and the LS Inverter

6.10 Electronic Drivers and Measuring Equipment

Figure 6.10 shows an overview of the electronics used to drive and sense the quarter-car output signals. PULSE Type 3560-C. Portable Data Acquisition Unit, is a portable data acquisition system with a battery/DC powered Type 2827 power supply unit. It can hold any combination of 1 Controller Module and 1 Input/output Module. The controller module handles communication with the PC while the input/output module handles measurement input and provides a sample clock. As an example, a Type 3560C fitted with a 5/1-ch.

Figure 6.10 Portable Data Acquisition Unit, Type 3560-C

An accelerometer is a device that measures acceleration. The proper acceleration measured by an accelerometer is not necessarily the coordinate acceleration (rate of change of velocity). Instead, the accelerometer sees the acceleration associated with the phenomenon of weight experienced by any test mass at rest in the frame of reference of the accelerometer device. In the present experiments two types of accelerometers are to be used, one of them is single axial accelerometer DYTRAN type 7027 and the other is a tri axial accelerometer B&K type 4506 with an accuracy of +5% or -5%. (See Figure 6.11)

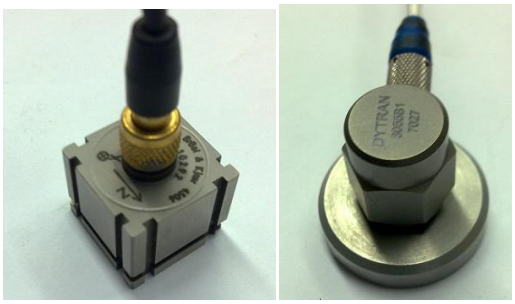

Figure 6.11 Tri axial and Single Axial Accelerometers

6.11 Data Acquisition Software

Data acquisition software allows exchanging information between the computer and the hardware. For example, typical software allows configuring the sampling rate of the kit and acquiring a predefined amount of data. B&K is the software used in the present experimental work. The data acquisition components and their relationship with each other are shown in Figure (6.12). Signals are input to a sensor, conditioned, converted into bits that a computer can read, and analyze to extract meaningful information. (See figure 6.13)

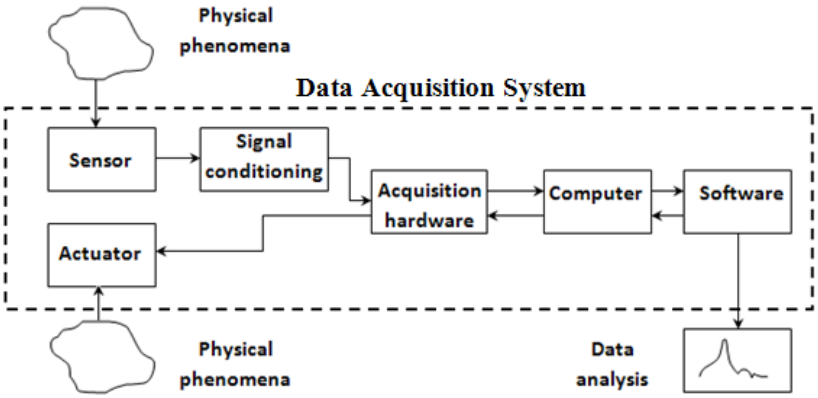

Figure 6.12 Process through Data Acquisition System

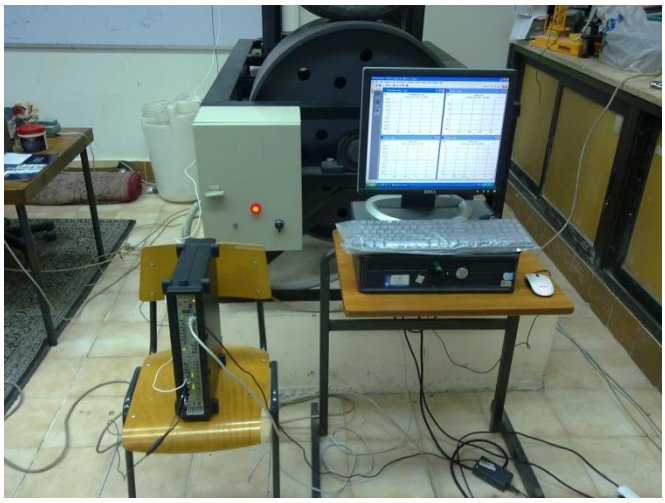

Figure 6.13 Data Acquisition System with the Computer Unit

6.12 Calibration of System Parameters

The calibration work was carried out in the laboratories to determine the stiffness of the spring using a Tensile/Compression Test Rig as seen in figure 6.14. Springs were inserted into the rig and using a load gauge and the deformation of the spring, a force vs displacement was plotted automatically using the data acquisition system of the rig. Four different Types of springs were tested, the normal linear spring, two variable pitched springs and a barrel spring. The linear spring consist of 5 coils having a 0.012 m wire diameter, 0.135 m outer diameter, 0.11 m inner diameter and spring height of 0.32 m. The two porotypes springs consist of 5 coils having a 0.014 m wire diameter, 0.135 m outer diameter, 0.11 m inner diameter and spring height of 0.32 m, while the smaller pitch is 0.0575m and the larger pitch 0.09 m as seen in figure 6.15.

Figure 6.14 Tensile/Compression Test Rig

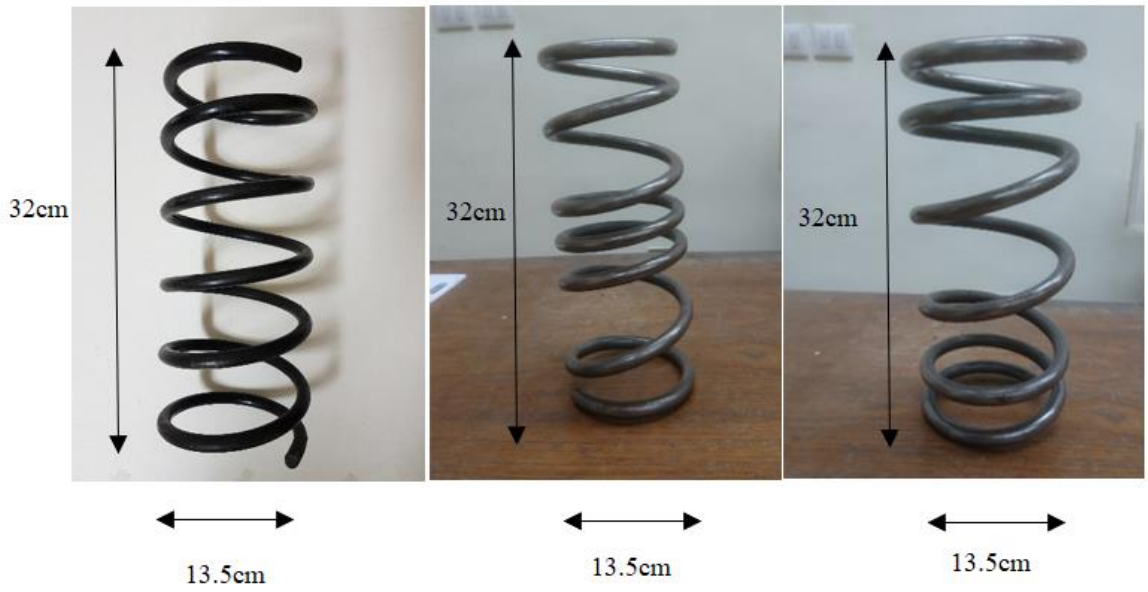

Figure 6.15 Left: Normal Spring Middle: Small Pitch in the Mid Length Right: Wide pitch in Mid Length

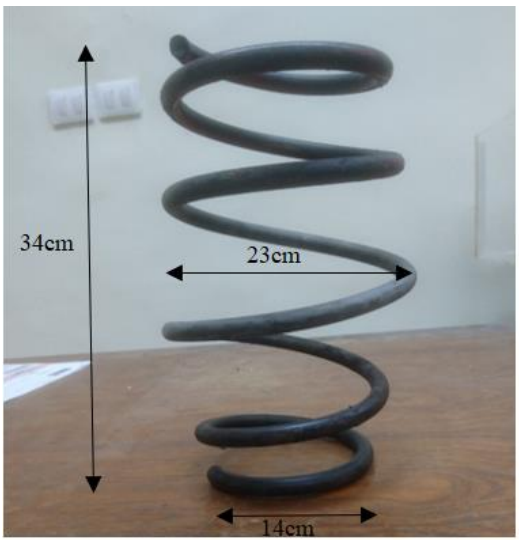

Figure 6.16 Barrel Spring

The procedure of calibration suspension system spring test:

1) Load the spring by a suitable weight and note the corresponding axial deflection.
2) Increase the load and take the corresponding axial deflection readings.
3) Plot a curve between load and deflection. The shape of the curve gives the stiffness of the spring.

The values obtained from the calibration of the spring, loading of masses and the deflection caused are listed in figure 6.17.

The normal spring produced a coefficient of stiffness of 17,458 N/m, as we can see from the figure that both prototype springs gave a linear coefficient of stiffness, therefore a barrel spring was used and calibrated as seen in figure 6.18. The barrel spring obtained a nonlinear load vs deflection graph and therefore can be used for our experimental rig. As seen in figure 6.22 the barrel spring has been inserted into the experimental rig.

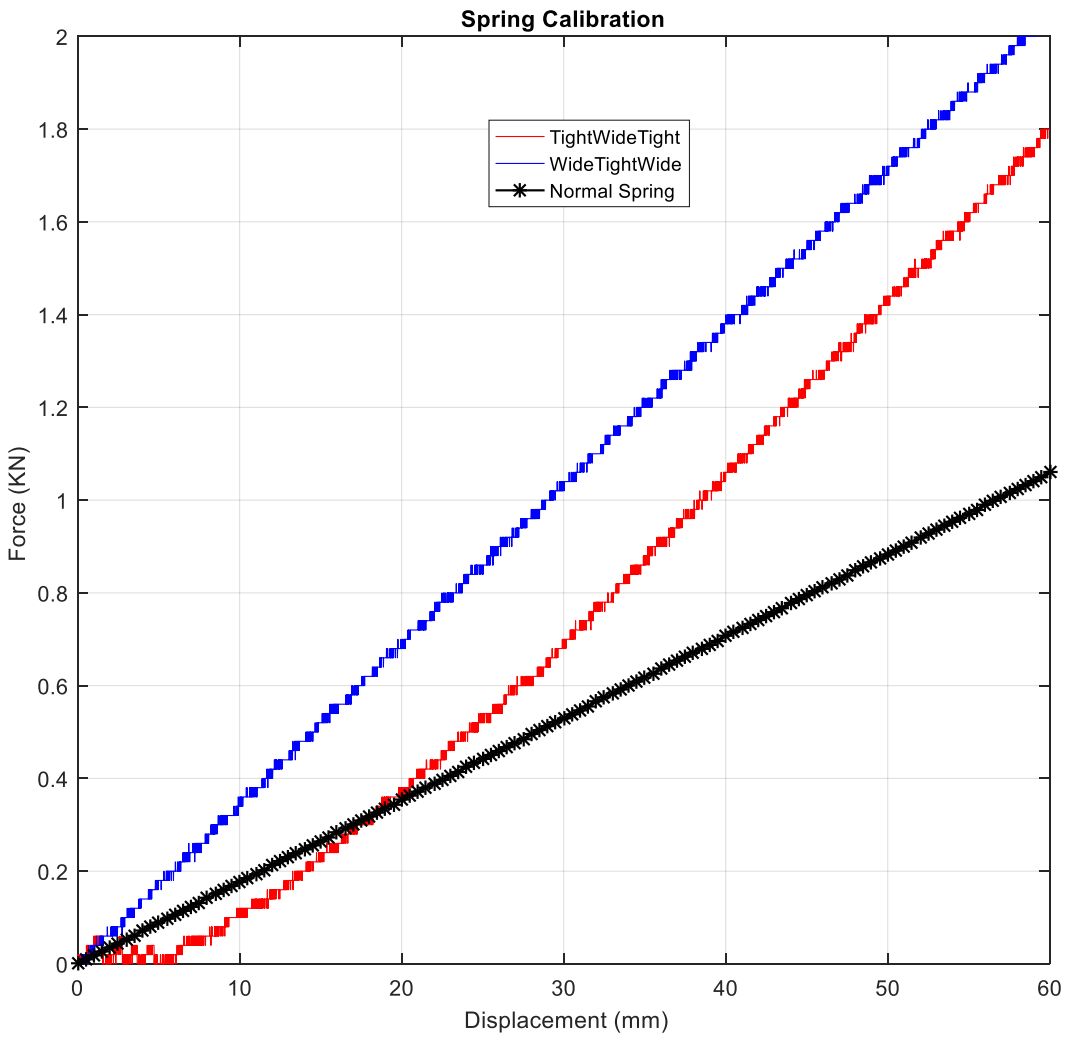

Figure 6.17 Force vs Displacement for the Two Prototype Springs.

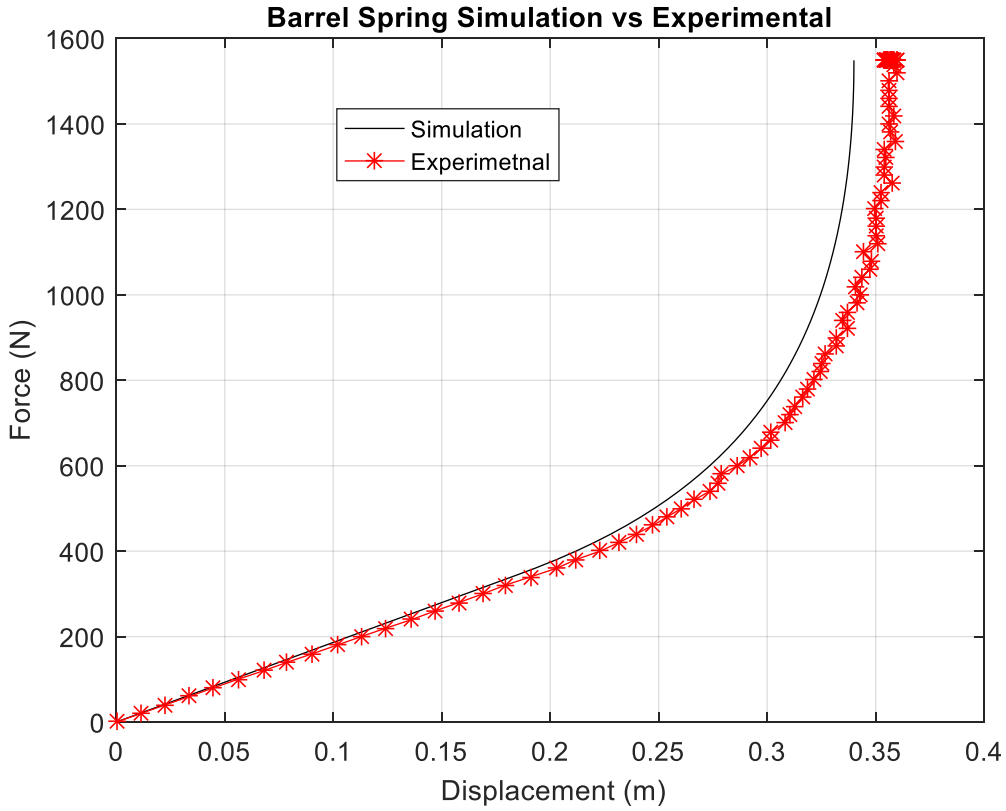

Figure 6.18 Barrel Spring Simulation vs Experimental

Fluid viscous dampers typically consist of a piston head with orifices contained in a cylinder filled with a highly viscous fluid, usually a compound of silicone or a similar type of oil. (See figure 6.19)

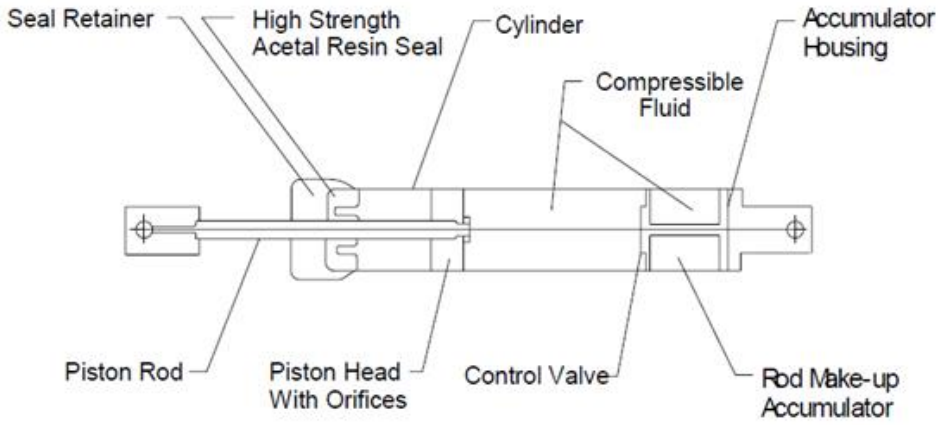

Figure 6.19 Fluid Viscous Damper Schematic Drawing

The procedure of calibration of the suspension system damper test:

1) Load the damper by a suitable weight and note the corresponding axial velocity in tension. (See Figure 6.20)
2) The length of the piston rod of the damper was marked at two positions. The closed damper when loaded the time was measured using a stop watch from the first position mark to the second position mark, therefore calculating the velocity because the length between the two positions is calculated beforehand.
3) Increase the load and take the corresponding axial velocity readings.
4) Plot a curve between load and velocity. The shape of the curve gives the damping coefficient of the damper. (See Figure 6.21)

The values obtained from the calibration of the damper, loading of masses and the velocity caused are listed in table 6.1

Figure 6.20 Calibration of Suspension System Damper Test Rig

Table 6.1 Damper Calibration Data

No.	Load (N)	Velocity (m/s)
1	39.24	0.00211
2	78.48	0.00292
3	122.997	0.005
4	164.877	0.00519
5	214.339	0.00653

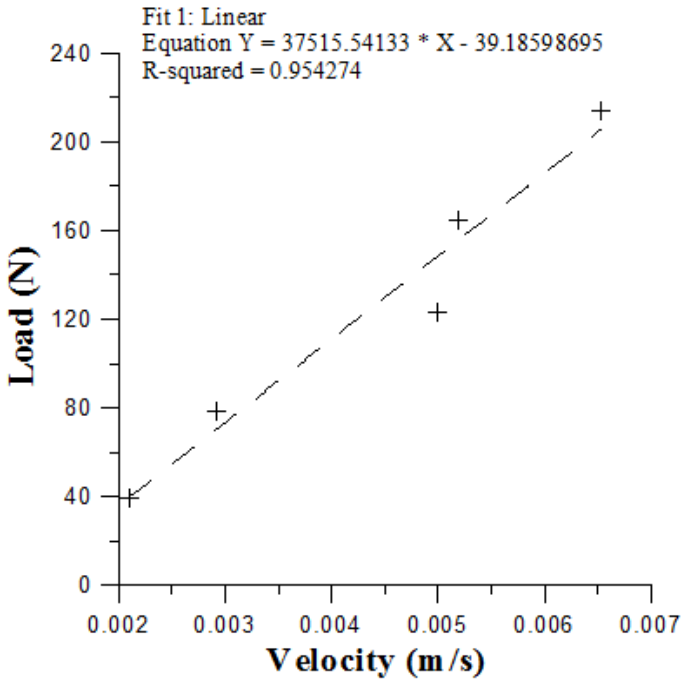

Figure 6.21 Calibration Curve of Suspension System Damper

Figure 6.22 Barrel Spring Inserted in Experimental Rig

6.13 Experimental Results of the Suspension System for Different Parameters

These preliminary experiments are carried out to identify the best locations on the test rig to measure the acceleration of the sprung mass. Multiple reading were taken at three points, and compared to the simulation model to obtain the best position for the accelerometer. Results show that the optimum position is to be situated in the middle of the main mass accelerations at point 2 as seen in figure 6.23.

The physical parameters to be investigated is divided into two sections, first at four different masses (100 kg, 150 kg, 200 kg and 250 kg) and then at five different constant speeds (25 Hz, 27.5 Hz, 30 Hz, 35 Hz and 40 Hz) or in km/hr (5 km/hr, 6 km/hr, 6.3 km/hr, 7.3 km/hr and 8.3 km/hr).

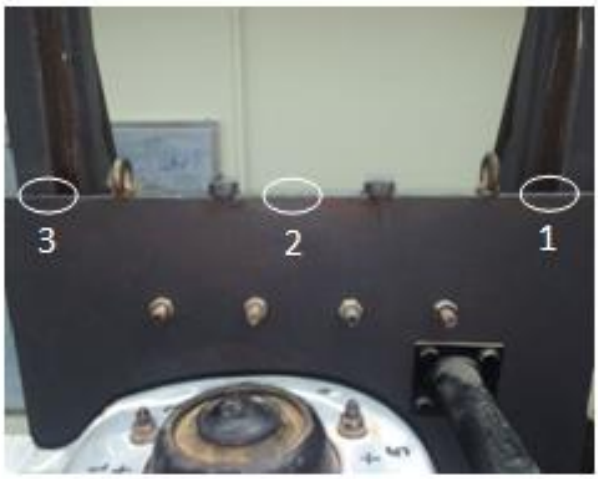

Figure 6.23 Location for Optimum Acceleration Sensor

6.13.1 Experimental Results with Linear Suspension for Different Masses

The experimental displacement of the sprung mass is compared for five different constant speeds (25 Hz, 27.5 Hz, 30 Hz, 35 Hz and 40 Hz) or in km/hr (5 km/hr, 6 km/hr, 6.3 km/hr, 7.3 km/hr and 8.3 km/hr) at four different masses (100 kg, 150 kg, 200 kg and 250 kg) (See figures 6.24 a, b, c and d respectively). By studying the effect of the speed of the car, it can be seen from the results of the four graphs, that the amplitude of the sprung mass decreases as the speed increases. The effect of increasing the sprung mass also shows that the amplitude will also decrease. Changing the speed and the sprung mass in the simulation model follows the same trend as the experimental data.

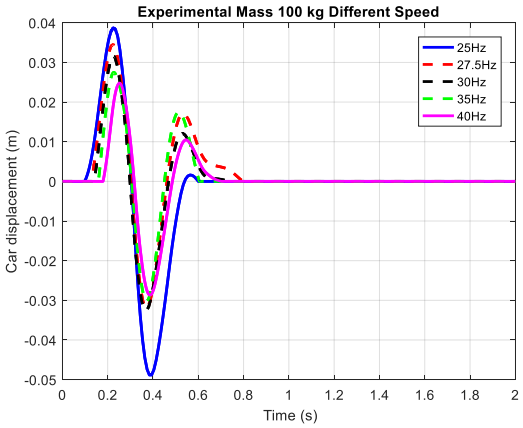

(a) Mass 100 kg

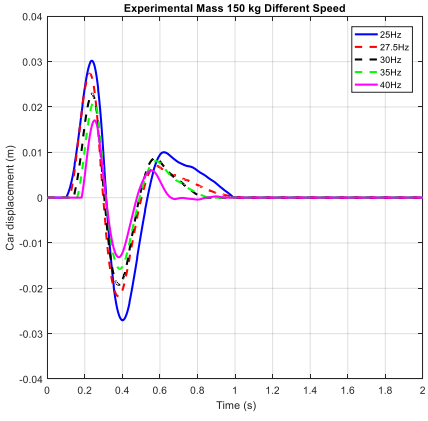

(b) Mass 150 kg

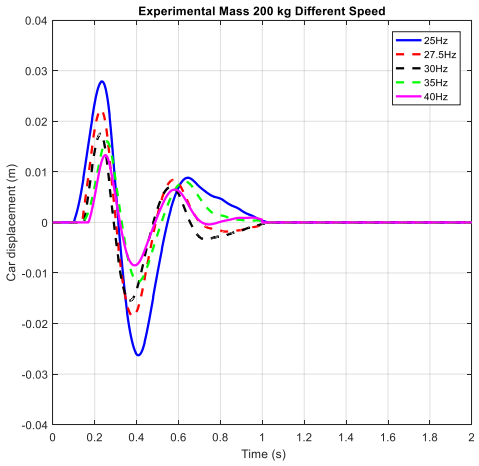

(c) Mass 200 kg

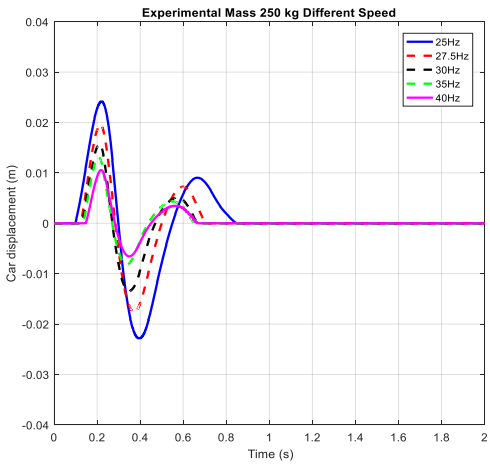

(d) Mass 250 kg

Figure 6.24 Experimental Amplitude of The Suspension System with Constant Car Mass for Different Speeds

6.13.2 Experimental Results with Linear Suspension for Different Speeds

The experimental displacement of the sprung mass is compared for four different masses (100 kg, 150 kg, 200 kg and 250 kg) at a constant speed therefore studying the effect of varying the mass. (See figures 6.25,26,27,28 & 29). By studying the effect of the car mass, it can be seen from the results of the five graphs that the amplitude of the displacement for the car body mass decreases as the car mass increases also following the same trend of the simulation.

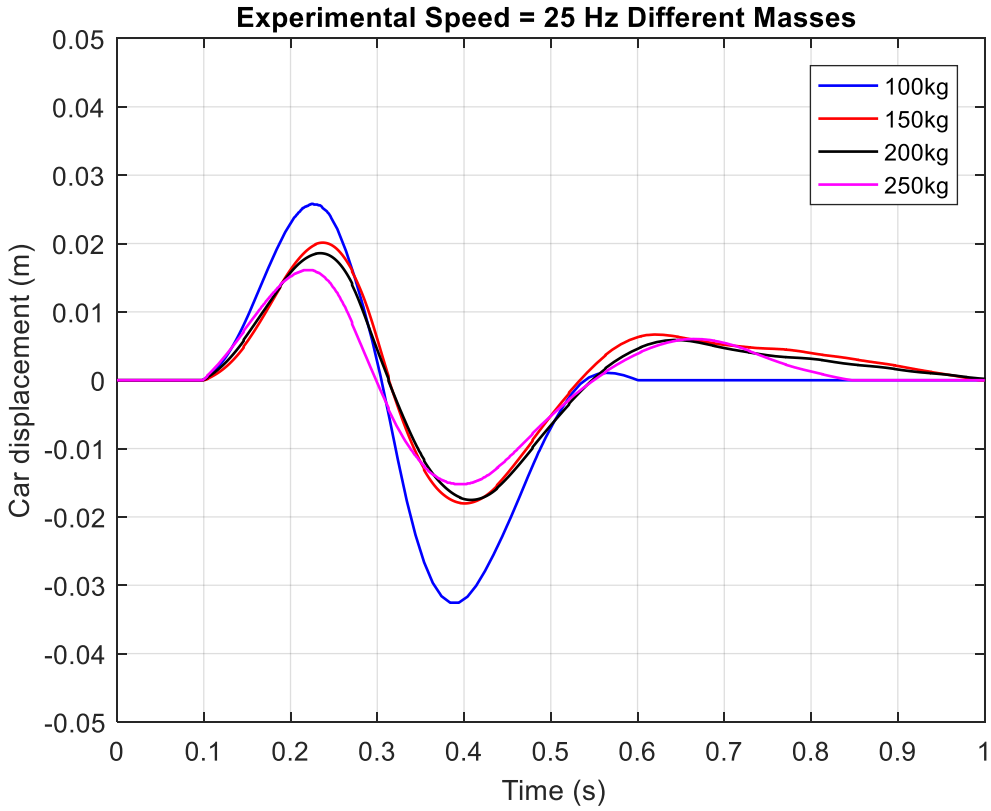

Figure 6.25 Simulation Amplitude of the Suspension System with Constant Speed 25 Hz,5 km/hr for Different Car Mass

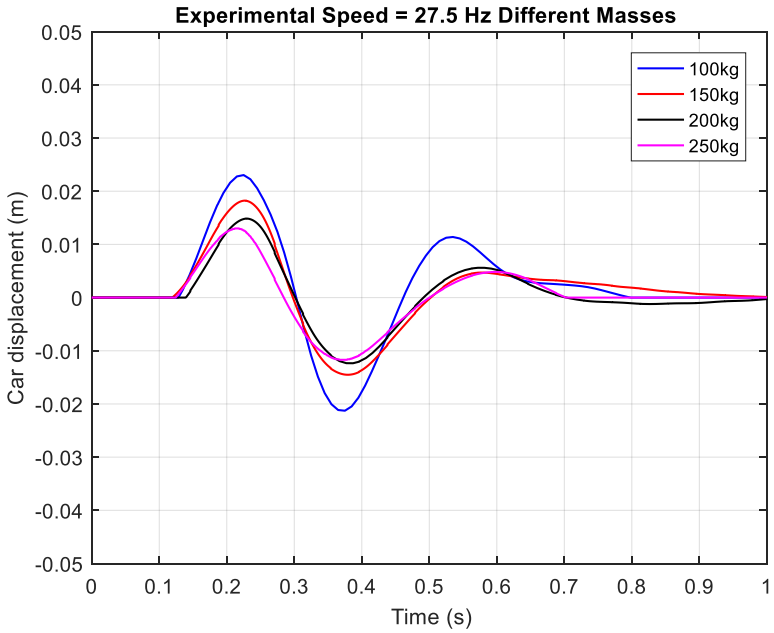

Figure 6.26 Simulation Amplitude of the Suspension System with Constant Speed 27.5 Hz,6 km/hr for Different Car Mass

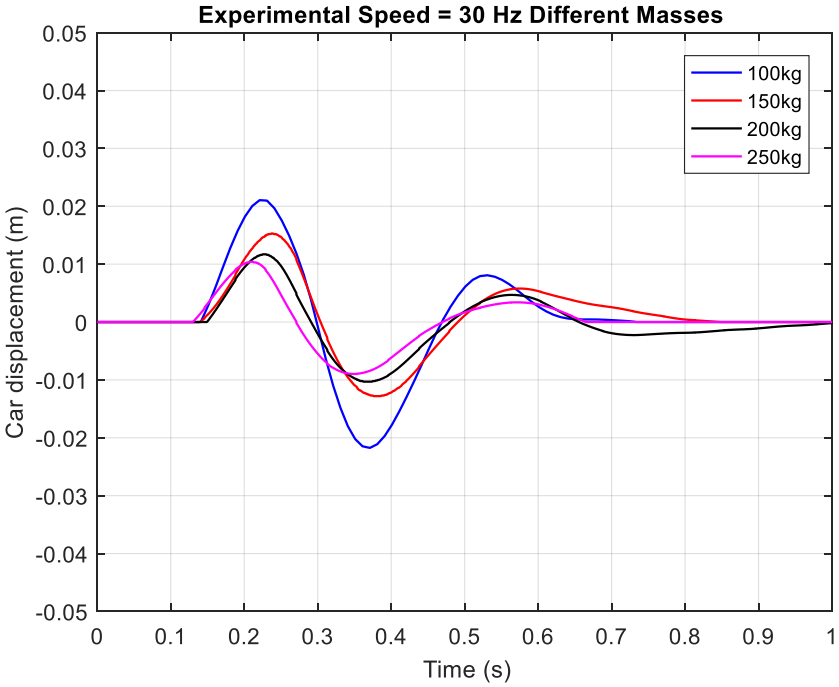

Figure 6.27 Simulation Amplitude of the Suspension System with Constant Speed 30 Hz,6.3 km/hr for Different Car Mass

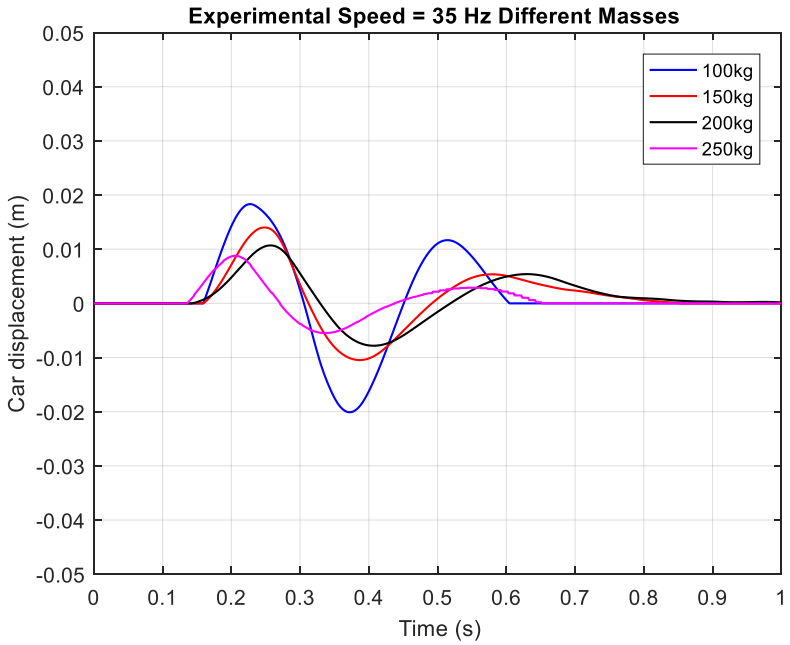

Figure 6.28 Simulation Amplitude of the Suspension System with Constant Speed 35 Hz,7.3 km/hr for Different Car Mass

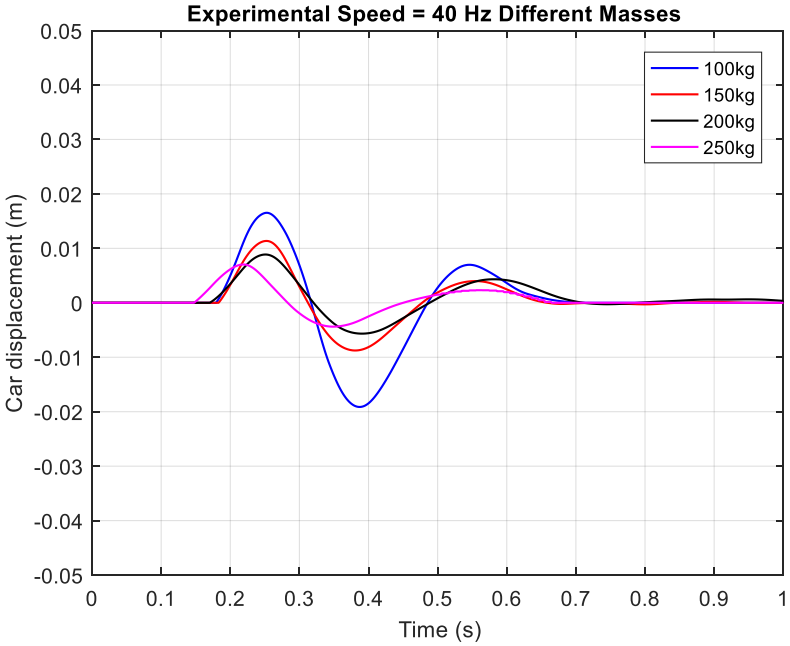

Figure 6.29 Simulation Amplitude of the Suspension System with Constant Speed 40 Hz,8.3 km/hr for Different Car Mass

6.13.3 Validation between Experimental and Simulation with Linear Suspension.

The simulation displacement of the sprung mass is validated by comparing it to the experimental data obtained at different speeds and different masses (See figures 6.30,31,32 & 33). Analyzing the results of the five graphs the amplitude follows the same trend with nearly the same amplitude size. The difference in the data is due to friction and that the car mass is supported and due to the simple quarter car model used in the simulation process.

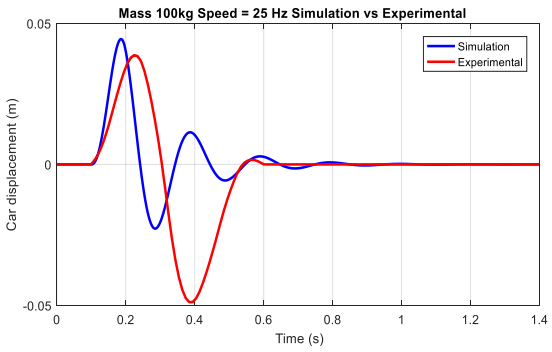

(a) Speed 25 Hz,5 km/hr

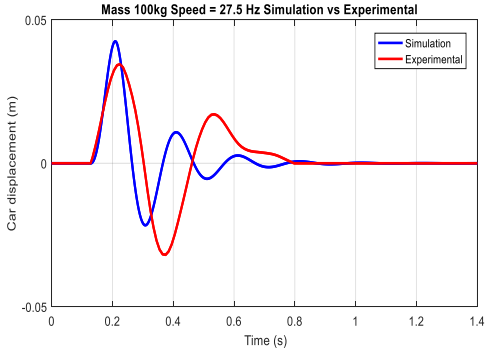

(b) Speed 27.5Hz,6 km/hr

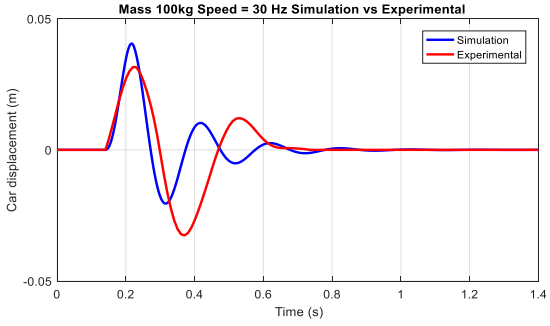

(c) Speed 30Hz,6.3 km/hr

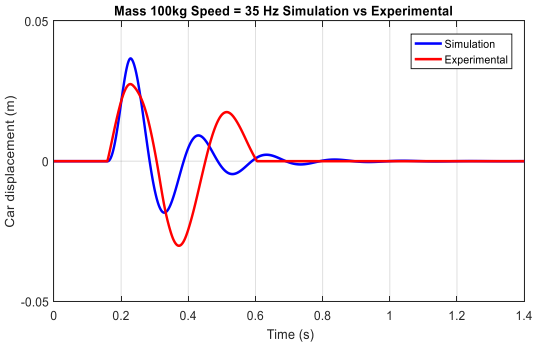

(d) Speed 35Hz,7.3 km/hr

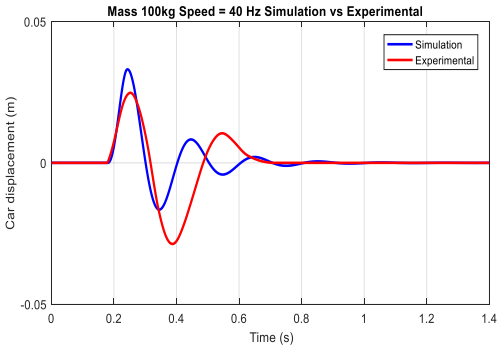

(e) Speed 40Hz,8.3 km/hr

Figure 6.30 Simulation Amplitude vs Experimental Amplitude of the Suspension System with Constant Mass 100kg at Different Speeds.

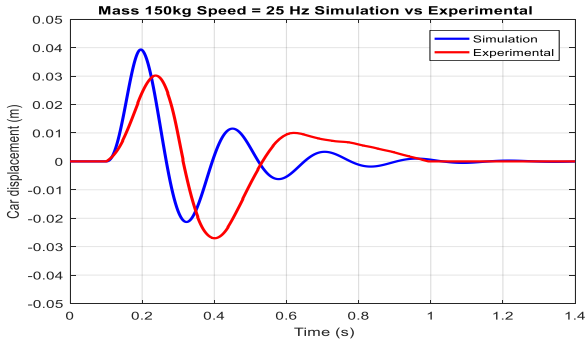

(a) Speed 25 Hz,5 km/hr

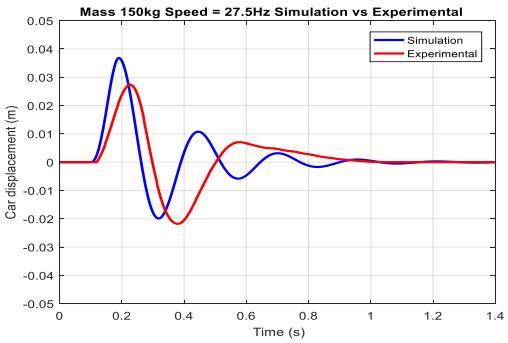

(b) Speed 27.5Hz,6 km/hr

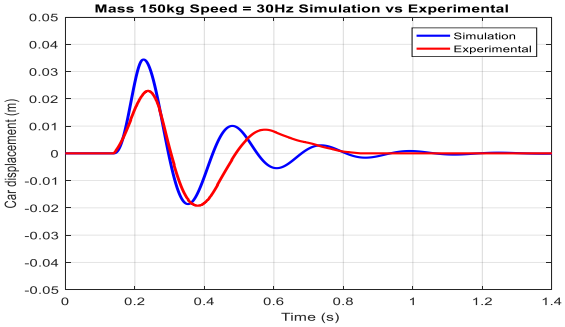

(c) Speed 30Hz,6.3 km/hr

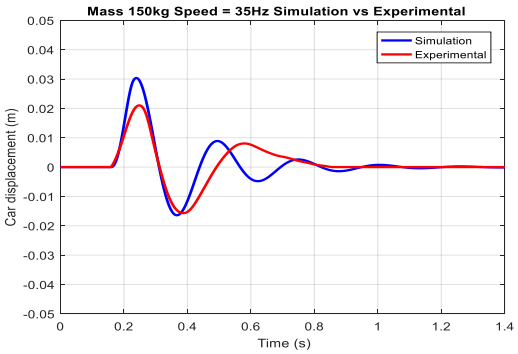

(d) Speed 35Hz,7.3 km/hr

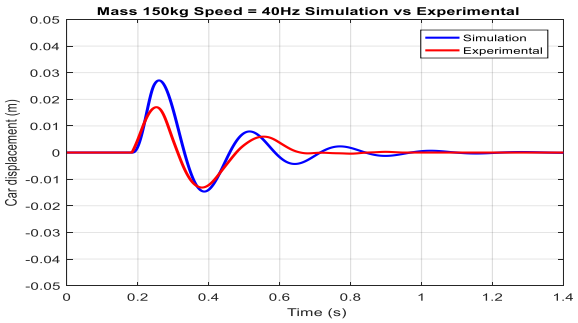

(e) Speed 40Hz,8.3 km/hr

Figure 6.31 Simulation Amplitude vs Experimental Amplitude of the Suspension System with Constant Mass 150kg at Different Speeds.

(a) Speed 25 Hz,5 km/hr

(b) Speed 27.5Hz,6 km/hr

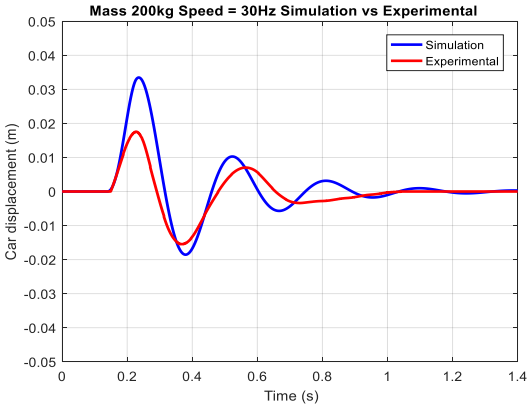

(c) Speed 30Hz,6.3 km/hr

(d) Speed 35Hz,7.3 km/hr

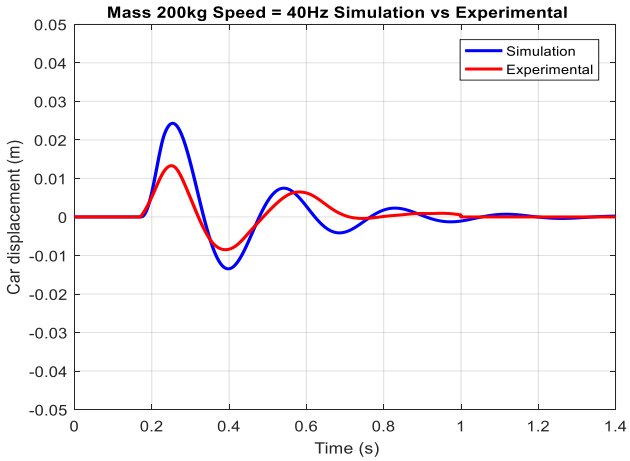

(e) Speed 40Hz,8.3 km/hr

Figure 6.32 Simulation Amplitude vs Experimental Amplitude of the Suspension System with Constant Mass 200kg at Different Speeds.

(a) Speed 25 Hz,5 km/hr

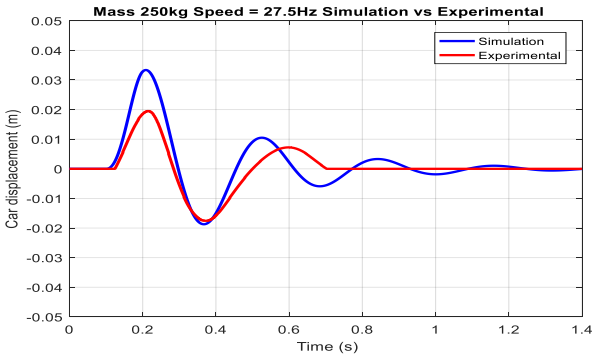

(b) Speed 27.5Hz,6 km/hr

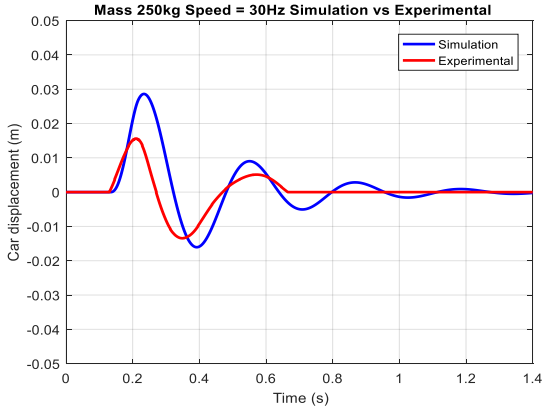

(c) Speed 30Hz,6.3 km/hr

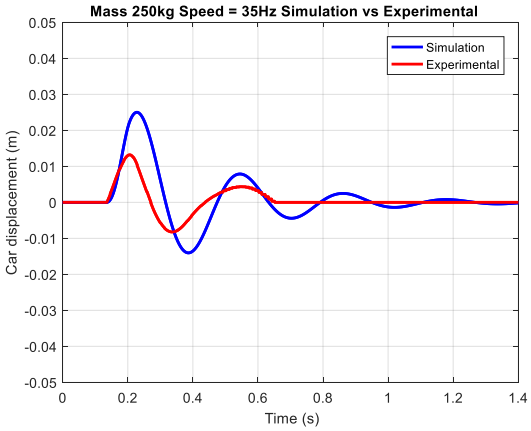

(d) Speed 35Hz,7.3 km/hr

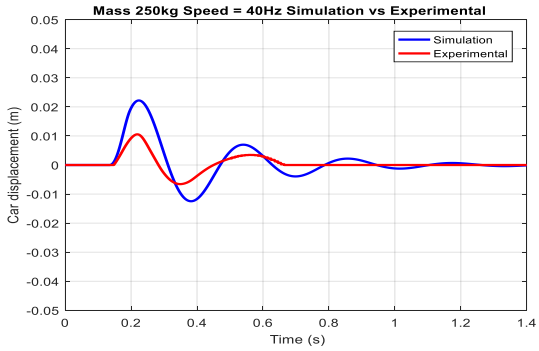

(e) Speed 40Hz,8.3 km/hr

Figure 6.33 Simulation Amplitude vs Experimental Amplitude of the Suspension System with Constant Mass 250kg at Different Speeds.

6.14 Nonlinear Suspension Experimental Results

6.14.1 Experimental Results with Nonlinear Suspension for Different Masses

The experimental displacement of the sprung mass with the nonlinear barrel spring with high damping is compared for five different constant speeds (25 Hz, 27.5 Hz, 30 Hz, 35 Hz and 40 Hz) or in km/hr (5 km/hr, 6 km/hr, 6.3 km/hr, 7.3 km/hr and 8.3 km/hr) at three different masses (100 kg, 150 kg and 200 kg) (See figures 6.34a, b and c respectively). By studying the effect of the speed of the car, it can be seen from the results of the three graphs that each amplitude and the given body mass, the amplitude of the displacement for the car body mass decreases as the speed increases.

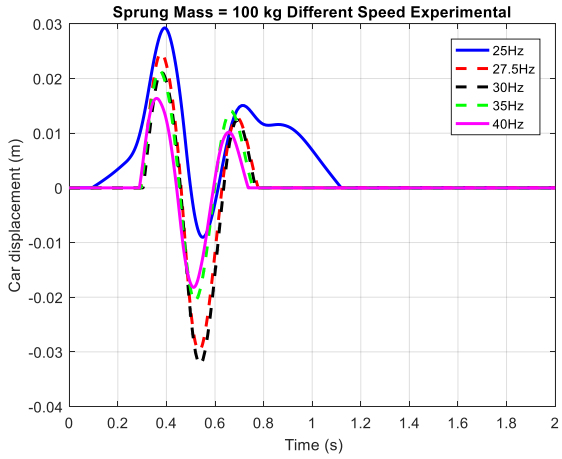

(a) Mass 100 kg

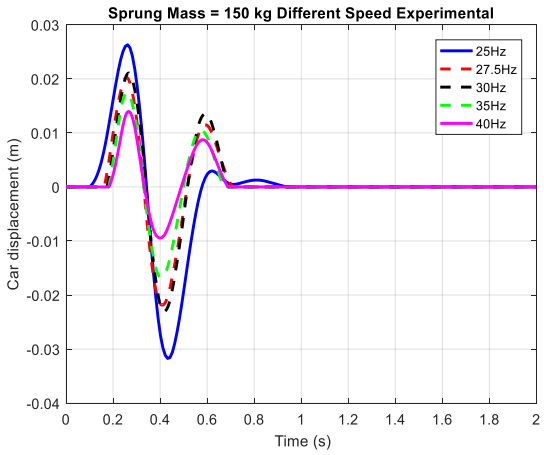

(b) Mass 150 kg

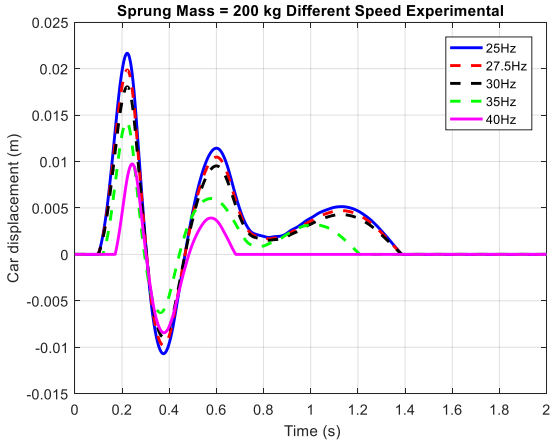

(c) Mass 200 kg

Figure 6.34 Experimental Amplitude of the Suspension System with Constant Car Mass for Different Speeds with Nonlinear Spring.

6.14.2 Experimental Results with Nonlinear Suspension for Different Speeds

The experimental displacement of the sprung mass is compared for three different masses (100 kg, 150 kg and 200 kg) at a constant speed therefore studying the effect of varying the mass. (See figures 6.35 a, b, c, d, e). By studying the effect of the car mass, it can be seen from the results of the five graphs that the amplitude of the displacement for the car body mass decreases as the car mass increases.

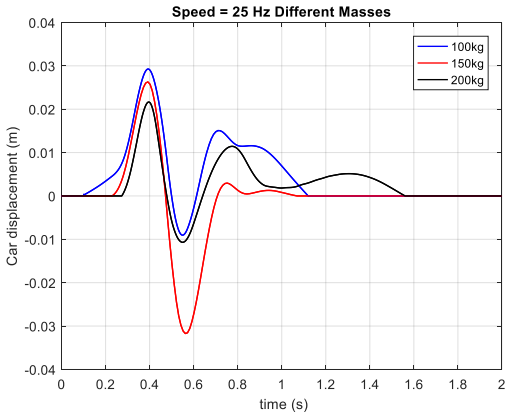

(a) Speed 25 Hz,5 km/hr

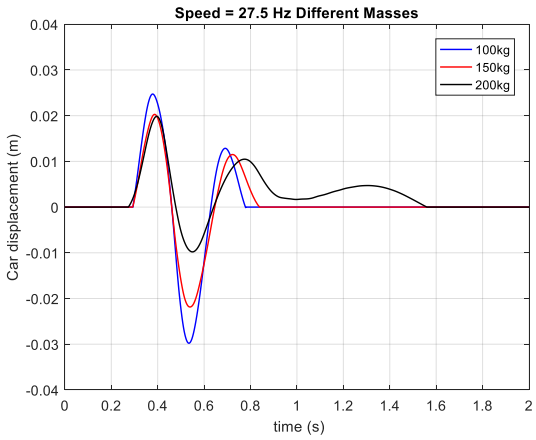

(b) Speed 27.5Hz,6.3 km/hr

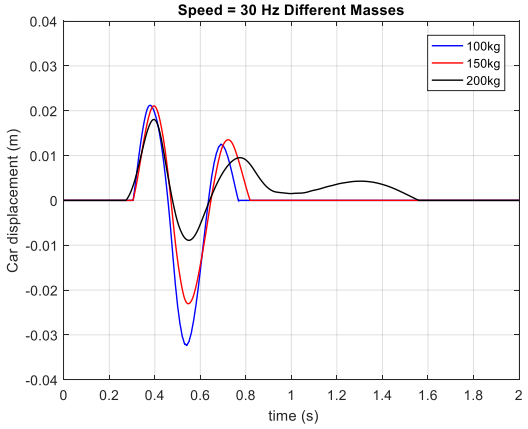

(c) Speed 30Hz,6.3 km/hr

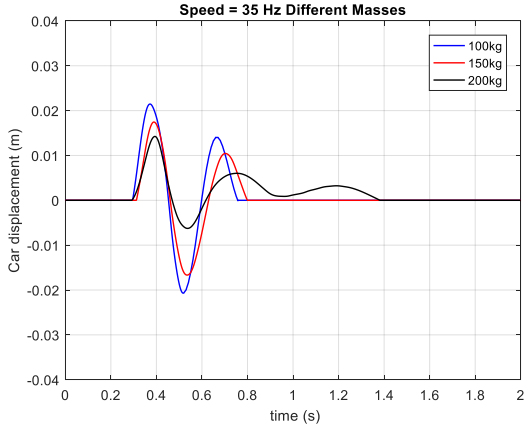

(d) Speed 35Hz,7.3 km/hr

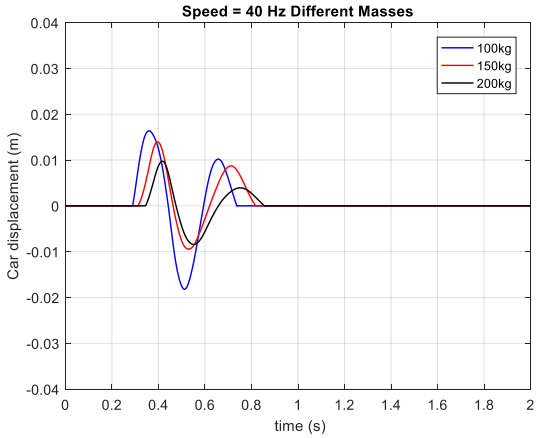

(e) Speed 40Hz,8.3 km/hr

Figure 6.35 Experimental Amplitude of the Suspension System with Constant Speeds for Different Car Mass with Nonlinear Suspension.

6.14.3 Experimental Results with Nonlinear Suspension for Different Masses with Low Damping.

The experimental displacement of the sprung mass with the nonlinear barrel spring is compared for five different constant speeds (25 Hz, 27.5 Hz, 30 Hz, 35 Hz and 40 Hz) or in km/hr (5 km/hr, 6 km/hr, 6.3 km/hr, 7.3 km/hr and 8.3 km/hr) at three different masses (100 kg, 150 kg and 200 kg) (See figures 6.36a, b and c respectively) with low damping. By studying the effect of the speed of the car, it can be seen from the results of the three graphs that each amplitude and the given body mass, the amplitude of the displacement for the car body mass decreases as the speed increases. At speed 25 Hz, 5 km/hr and sprung mass 100kg the amplitude of vibration of the sprung mass reacts abnormally this is explained due to the frequency of the inverter coinciding with frequency of the electrical input causing a deviation in the accelerometer readings.

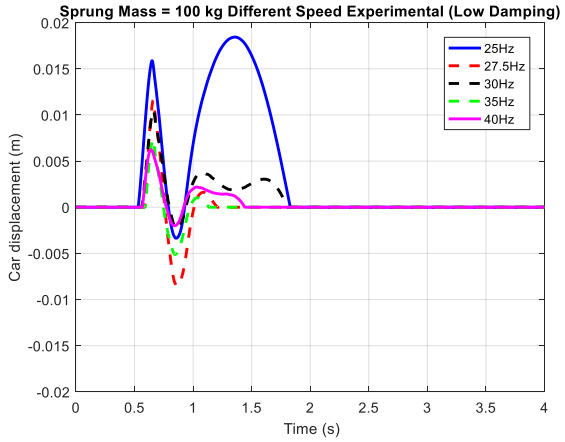

(a) Mass 100 kg

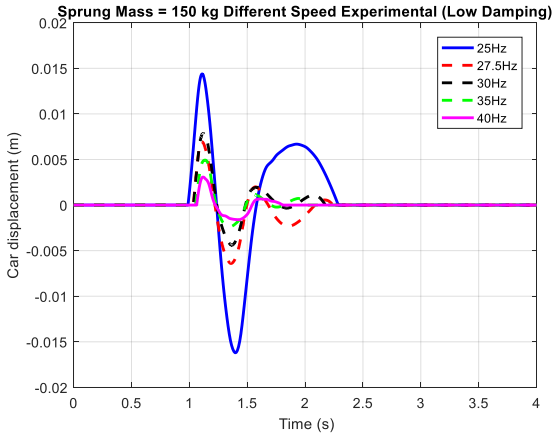

(b) Mass 150 kg

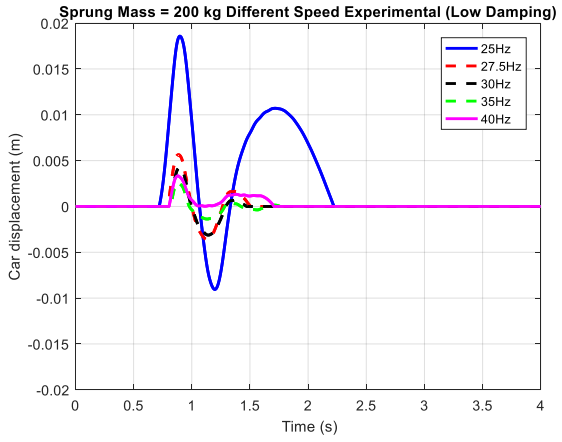

(c) Mass 200 kg

Figure 6.36 Experimental Amplitude of the Suspension System with Constant Car Mass for Different Speeds with Nonlinear Spring and Low Damping.

6.14.4 Experimental Results with Nonlinear Suspension for Different Speeds with Low Damping.

The experimental displacement of the sprung mass is compared for three different masses (100 kg, 150 kg and 200 kg) at a constant speed therefore studying the effect of varying the mass. (See figures 6.37a, b, c, d, and e). By studying the effect of the car mass, it can be seen from the results of the five graphs that the amplitude of the displacement for the car body mass decreases as the car mass increases.

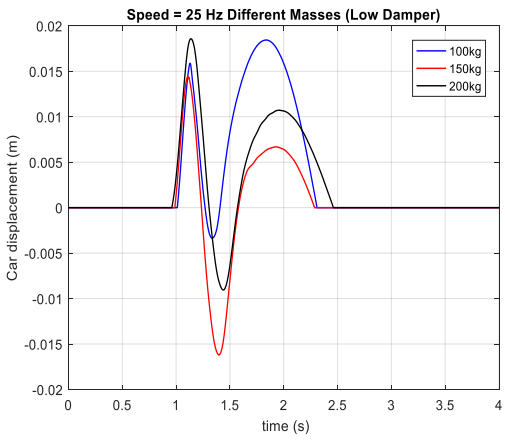

(a) Speed 25 Hz,5 km/hr

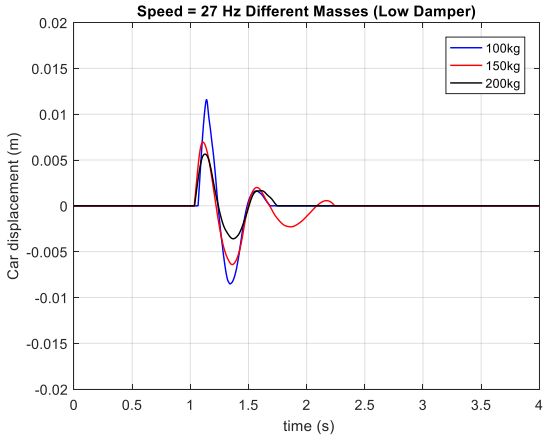

(b) Speed 27.5Hz,6.3 km/hr

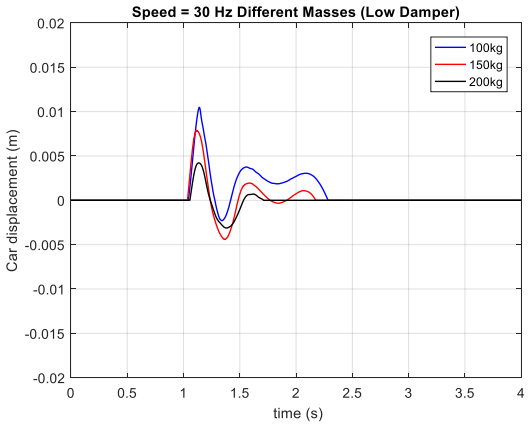

(c) Speed 30Hz,6.3 km/hr

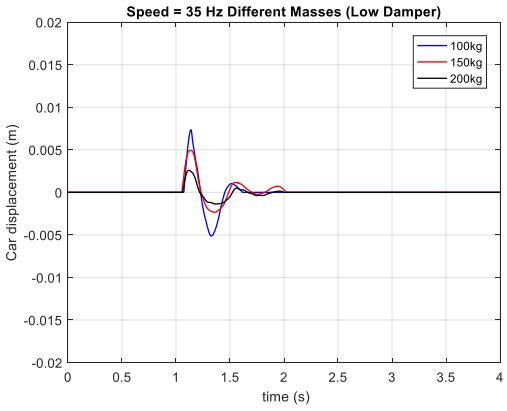

(d) Speed 35Hz,7.3 km/hr

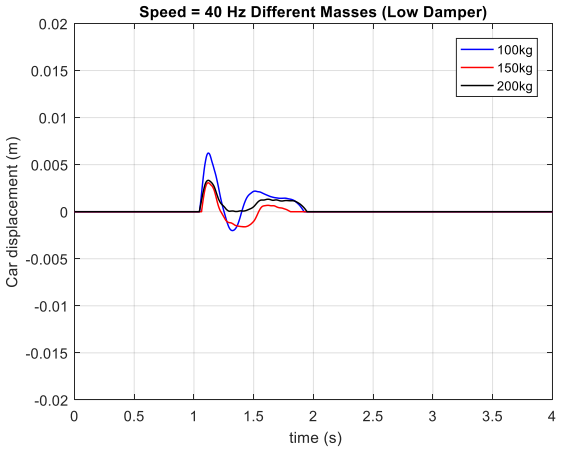

(e) Speed 40Hz ,8.3 km/hr

Figure 6.37 Experimental Amplitude of the Suspension System with Constant Speeds for Different Car Mass with Nonlinear Suspension and Low Damping.

6.14.5 Experimental Nonlinear Model with Low Damping Compared to Nonlinear Model.

The experimental displacement of the sprung mass of the model with a nonlinear model with a small value of coefficient of damping is compared to the experimental data of the nonlinear model with the stock damper at different speeds and masses (See figures 6.38,39& 40). After research, it shows us that adding a nonlinear spring is not enough to improve the system, a smaller value of coefficient of damping must be used in parallel as proven by the genetic algorithm. The results show a decrease of 60% to nearly 90% at different sprung mass conditions and at different speeds. Analyzing the results of the graphs concludes that adding the new nonlinear configuration decreases the vibration extensively. The real life experimental motion results in a much lower noise in the system and the vibration is much lower as compared to the normal suspension.

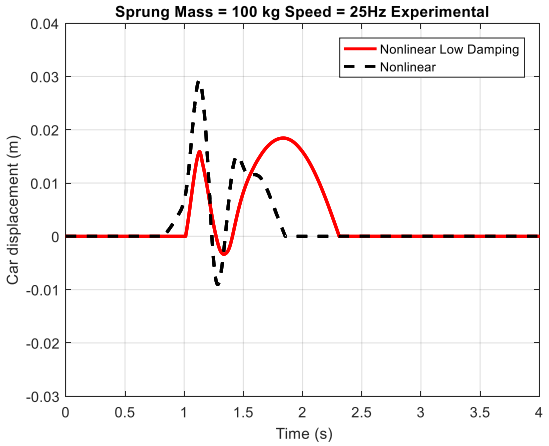

(a) Speed 25 Hz,5 km/hr

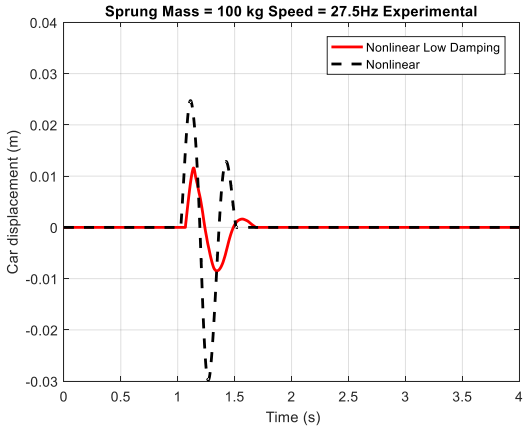

(b) Speed 27.5Hz,6.3 km/hr

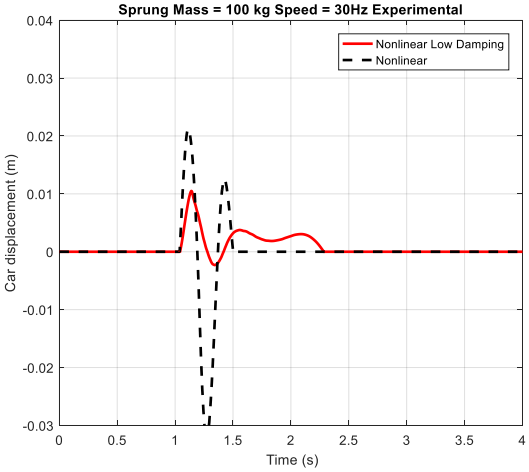

(c) Speed 30Hz,6.3 km/hr

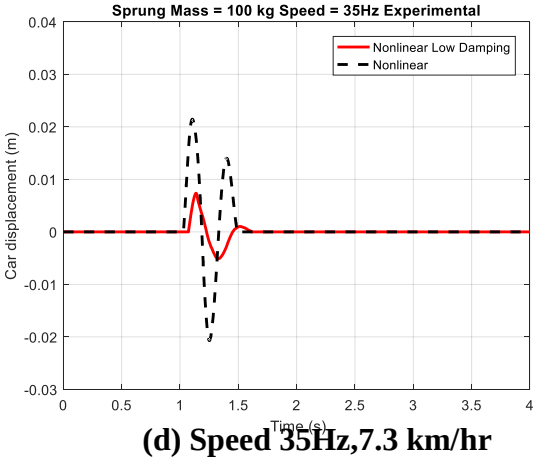

(d) Speed 35Hz,7.3 km/hr

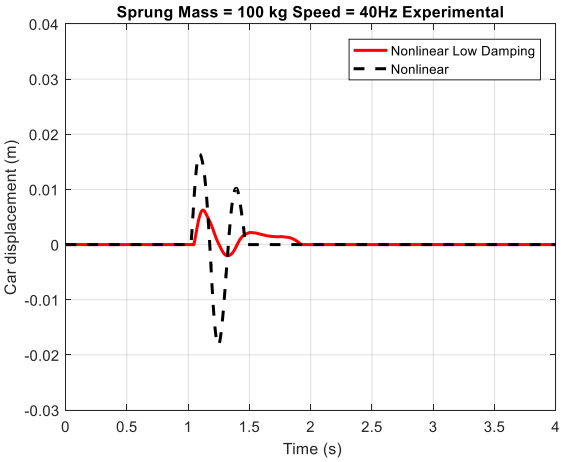

(e) Speed 40Hz,8.3 km/hr

Figure 6.38 Experimental Amplitude of the Suspension System for Nonlinear Model and Nonlinear Model with Low Damping for Mass=100kg at Different Speeds.

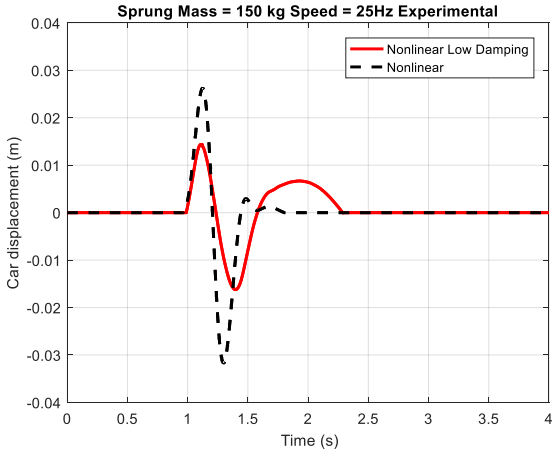

(a) Speed 25 Hz,5 km/hr

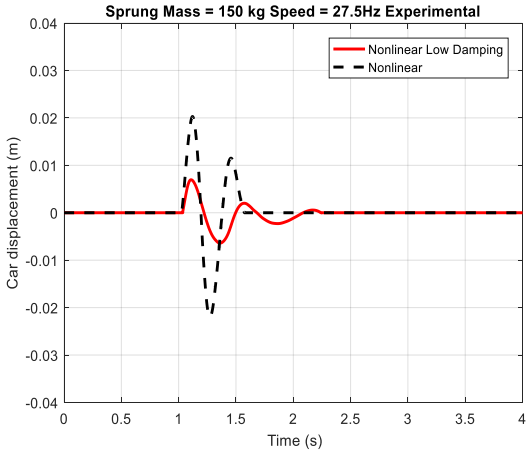

(b) Speed 27.5Hz,6.3 km/hr

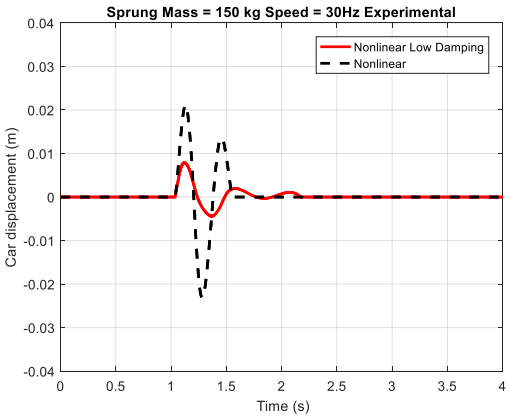

(c) Speed 30Hz,6.3 km/hr

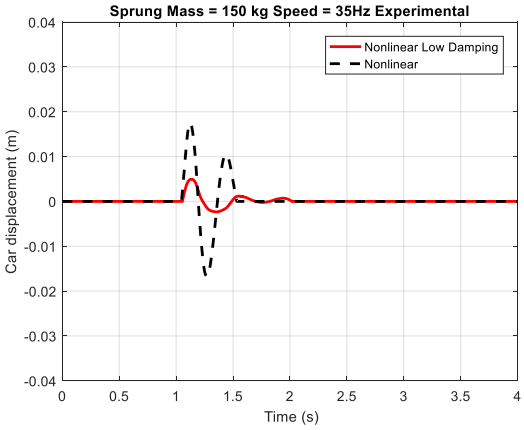

(d) Speed 35Hz,7.3 km/hr

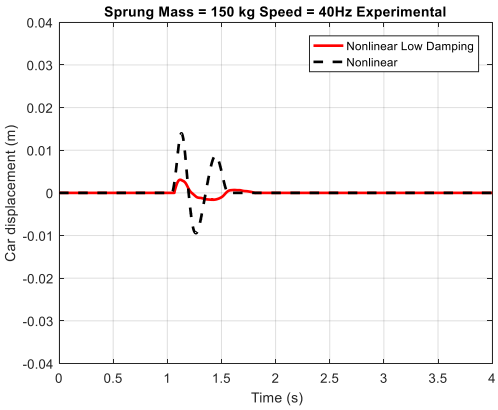

(e) Speed 40Hz,8.3 km/hr

Figure 6.39 Experimental Amplitude of the Suspension System for Nonlinear Model and Nonlinear Model with Low Damping for Mass=150kg at Different Speeds.

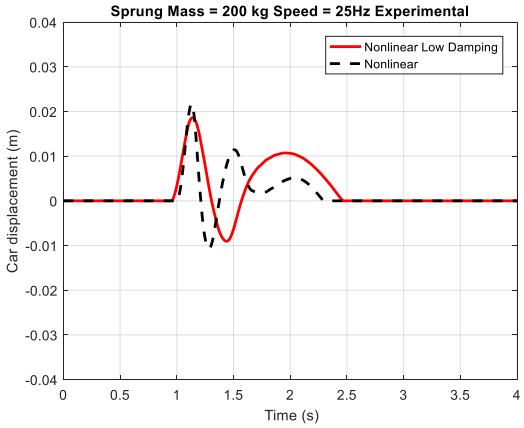

(a) Speed 25 Hz,5 km/hr

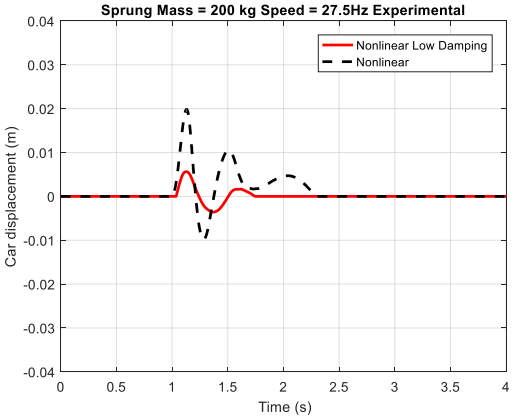

(b) Speed 27.5Hz,6.3 km/hr

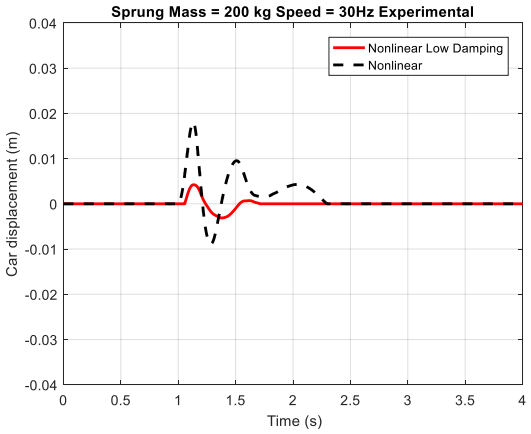

(c) Speed 30 Hz,6.3 km/hr

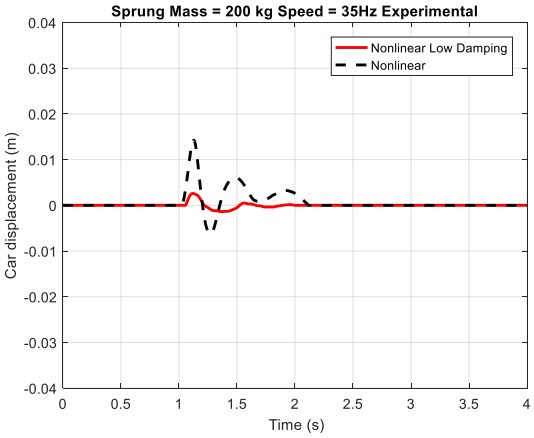

(d) Speed 35Hz,7.3 km/hr

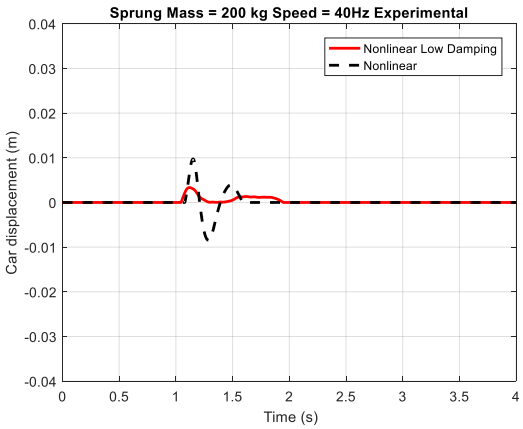

(e) Speed 40Hz,8.3 km/hr

Figure 6.40 Experimental Amplitude of the Suspension System for Nonlinear Model and Nonlinear Model with Low Damping for Mass=200kg at Different Speeds.

6.14.6 Conclusion

The experimental aspect of the work has been completed. The results show that by increasing the speed over the physical bump, the displacement amplitude decreases accordingly. The other parameter changed is the sprung mass, as seen in the results an increase of this parameter also causes a decrease in sprung mass displacement. This work is validated with the simulated model as it follows the same trend in both cases. A validation between is previewed to show how close a simple numerical model can simulate real dynamic motion. The nonlinear spring experimental results with low damping show a phenomenal change in behaviour and could decrease the sprung displacement by nearly 60% up to 90% at different speed conditions and sprung mass values compared to the conventional spring.

7 CHAPTER 7 CONCLUSION

7.1 Conclusions and Innovations of the Research

In this thesis, the effect of the attachment of a nonlinear stiffness spring in a quarter car model with different vehicle masses and at different vehicle speeds has been investigated. Compared to previous work the suspension spring is redesigned and tested. The realization of vibration reduction through one-way irreversible nonlinear energy localization which requires no pre-tuning in quarter car model is studied.

To start the research targeted energy transfer and nonlinear energy pumping was initially studied. The theory of energy transfer between a linear oscillator and an energy absorber using a nonlinear connection has been studied and showed a large energy transfer compared to a linear connection. From here the innovation of using the nonlinear spring in a quarter car model was invented. To avoid a complex model the two degree of freedom model was introduced.

The literature review has covered all the work done by previous researchers and introduce the methodology of using a nonlinear attachment, which offered the core theory of obtaining the theoretical model used in this thesis. Published studies of targeted energy transfer have been researched and showed that there is no practical work done in a quarter car setup.

The mathematical model of the quarter-car is derived, and the dynamics are evaluated in terms of the main mass displacement. The simulation of the car dynamics is performed using Matlab® and Simulink®. Different types of nonlinear springs have been researched and studied which offered an initial design of the nonlinear suspension and its corresponding equation of motion. The bump design to be integrated in the model was developed and introduced to simulate the actual speed in which the car will be approaching the bump.

The experimental rig of a quarter car suspension system has been designed and built from scratch to be used in the study of suspension model. Different types of nonlinear prototype springs have been designed and put to the test. To verify the experimental rig results it has been compared to simulated model done by MATLAB/SIMULINK. Experimental work is always essential to introduce new applied theories. The vehicle speeds of the experimental research are from 5 km/hr to 8.3 km/hr, imitating the usual speed a vehicle passing above a standard hump. Higher speeds can be simulated but as for the experimental work we were limited by the power of the motor connected to the drum.

Initially the simulated model results with the energy transfer theory have been recorded and in theory obtained remarkable results. To find the best parameters of the system, genetic algorithm has been introduced and used for picking the optimum parameter of the components. Finally, the new nonlinear spring was added and using the sensors on the main mass obtained nearly identical results, showing that the nonlinear spring was a success.

In the preliminary phase of designing the conventional suspension system, a validation of the experimental set up with the simulated model is required. The obtained sprung mass accelerometer data were compared and showed they coincide with the trends presented by the simulation model. Also, by increasing the sprung mass it was noted that the sprung mass amplitude decreased, while increasing the velocity of the vehicle also caused a decrease in values. This data is validated with the simulation governing equations. The results of this work show that integrating the nonlinear spring into the suspension will decrease the amplitude of the sprung mass by 50% to 60%. Upon further improvement using the new genetic parameters the amplitude would diminish to 60% to 90%.

Nonlinear attachment is fairly a new type of research therefore this work a new contribution to the car industry. The thesis work shows that by changing the design of the spring and optimizing the car parameters using genetic algorithm the sprung mass amplitude is always diminished at different road conditions at various sprung masses and different vehicle speeds. The advantage of using this configuration is that there is no prior tuning, does not require an external power supply or control theorems to optimize it. The future of the technology is in the use of a nonlinear suspension that could provide improvement in performance over that realized by the passive, semi active and active suspension.

7.2 Suggested Future Work

For the future work, designing a conical suspension spring, because this configuration will yield to more radical nonlinear slope thus obtaining better results. Study this model for different bumps and investigate how it will react.

To have a more accurate theoretical design, Macpherson modelling can be introduced, producing more accurate results but a more complex way to simulate the model. Trial of this new spring on a half-car model or full car model to study extensively its effect on a larger model. Apply this work to other types of cars for example racing cars, trucks and off-road vehicles. Finally combine a semi-active or active damper to further improve the study.

8 REFERENCES

[1] Ahmadabadi, Z.N. and Khadem, S.E., 2012. Nonlinear vibration control of a cantilever beam by a nonlinear energy sink. *Mechanism and Machine Theory*, *50*, pp.134-149.

[2] Ahmadian, M. and Pare, C.A., 2000. A quarter-car experimental analysis of alternative semiactive control methods. *Journal of Intelligent Material Systems and Structures*, *11*(8), pp.604-612.

[3] Abd_Elsalam, A., El-Gohary, M.A. and El-Gamal, H.A., 2016. Simulation of Nonlinear Quarter Car Suspension System with and without Tire Damping.

[4] Agharkakli, A., Sabet, G.S. and Barouz, A., 2012. Simulation and analysis of passive and active suspension system using quarter car model for different road profile. *International Journal of Engineering Trends and Technology*, *3*(5), pp.636-644.

[5] Alkhatib, R., Jazar, G.N. and Golnaraghi, M.F., 2004. Optimal design of passive linear suspension using genetic algorithm. *Journal of Sound and vibration*, *275*(3), pp.665-691.

[6] Amri, M., Basset, P., Cottone, F., Galayko, D., Najar, F. and Bourouina, T., 2011. Novel nonlinear spring design for wideband vibration energy harvesters. *Proceedings of the PowerMEMS*, pp.15-18.

[7] Andersen, E., 2007. Multibody dynamics modeling and system identification for a quarter-car test rig with McPherson strut suspension.

[8] Ando, B., Baglio, S., Trigona, C., Dumas, N., Latorre, L. and Nouet, P., 2010. Nonlinear mechanism in MEMS devices for energy harvesting applications. Journal of Micromechanics and *Microengineering*, *20*(12), p.125020.

[9] Baumal, A.E., McPhee, J.J. and Calamai, P.H., 1998. Application of genetic algorithms to the design optimization of an active vehicle suspension system. *Computer methods in applied mechanics and engineering*, *163*(1), pp.87-94.

[10] Bello, M.M., Akramin Shafie, A. and Khan, R., 2015. Active Vehicle Suspension Control Using Full State-Feedback Controller. In *Advanced Materials Research* (Vol. 1115, pp. 440-445). Trans Tech Publications.

[11] Bello, M.M., Shafie, A.A. and Khan, M.R., 2015. Electro-hydraulic pid force control for nonlinear vehicle suspension system. *International Journal of Engineering Research and Technology*, *4*(1), pp.517-524.

[12] Bououden, S., Chadli, M. and Karimi, H.R., 2016. A robust predictive control design for nonlinear active suspension systems. *Asian Journal of Control*, *18*(1), pp.122-132.

[13] Burton, A.W., Truscott, A.J. and Wellstead, P.E., 1995. Analysis, modelling-and control of an advanced automotive self-levelling suspension system. *IEE Proceedings-Control Theory and Applications*, *142*(2), pp.129-139.

[14] Cataldo, E., Bellizzi, S. and Sampaio, R., 2013. Free vibrations of an uncertain energy pumping system. *Journal of Sound and Vibration*, *332*(25), pp.6815-6828.

[15] Campos, J., Davis, L., Lewis, F.L., Ikenaga, S., Scully, S. and Evans, M., 1999, June. Active suspension control of ground vehicle heave and pitch motions. In *Proceedings of the 7th IEEE Mediterranean Control Conference on Control and Automation* (pp. 222-233).

[16] Chatterjee, S., 2010. Optimal active absorber with internal state feedback for controlling resonant and transient vibration. *Journal of Sound and Vibration*, *329*(26), pp.5397-5414.

[17] Chi, Z., He, Y. and Naterer, G.F., 2008. Design optimization of vehicle suspensions with a quarter-vehicle model. *CSME Transactions*, *32*(2), pp.297-312.

[18] Choi, S.B., Lee, H.K. and Chang, E.G., 2001. Field test results of a semi-active ER suspension system associated with skyhook controller. *Mechatronics*, *11*(3), pp.345-353.

[19] Choi, S.B. and Sung, K.G., 2008. Vibration control of magnetorheological damper system subjected to parameter variations. *International Journal of Vehicle Design*, *46*(1), pp.94-110.

[20] Cochelin, B., Herzog, P. and Mattei, P.O., 2006. Experimental evidence of energy pumping in acoustics. *Comptes Rendus Mécanique*, *334*(11), pp.639-644.

[21] Crosby, M.J., Harwood, R.A. and Karnopp, D., 1974. Vibration control using semi-active force generators. *Journal of engineering for industry*, *96*(2), pp.619-626.

[22] Cui, M., Geng, L. and Wu, Z., 2017. Random Modeling and Control of Nonlinear Active Suspension. *Mathematical Problems in Engineering*, *2017*.

[23] Daniels J., 1988. Car Suspensions *at Work: Theory & Practice of Steering, Handling, & Road holding: Motor Racing Publications*.

[24] Davis, L., Handbook of Genetic Algorithms, Van Nostrand Reinhold, New York, 1991. *Search PubMed*.

[25] Den Boer, L.J.A., 2009. *Nonlinear dynamic behavior of a conical spring with top mass* (Doctoral dissertation, Master Dissertation, Eindhoven University of Technology, Eindhoven, Netherlands).

[26] Den Hartog, J.P., 1934. Mechanical Vibrations McGraw-Hill Book Company. *New York*, pp.122-169.

[27] Dixon, J.C., 1996. Tires, suspension and handling. *Warrendale, PA: Society of Automotive Engineers, 1996. 636*.

[28] Elattar, Y.M., Metwalli, S.M. and Rabie, M.G., 2016, April. PDF Versus PID Controller for active vehicle suspension. In *Proceedings of the 17th Int. AMME Conference* (Vol. 19, p. 21).

[29] Faheem, A., Alam, F. and Thomas, V., 2006, December. The suspension dynamic analysis for a quarter car model and half car model. In *3rd BSME-ASME International Conference on Thermal Engineering, Dhaka* (pp. 20-22).

[30] Fayyad, S.M., 2012. Constructing control system for active suspension system. *Contemporary Engineering Sciences*, *5*(4), pp.189-200.

[31] Frahm, H., 1911. *Device for damping vibrations of bodies*. U.S. Patent 989,958.

[32] International Standards Organization. (1997). International standard mechanical vibration and shock – evaluation of human exposure to whole body vibration. 2nd ed., ISO 2631-1997:Part 1.

[33] Galal, A. H. (2014). 'Car Dynamics using Quarter Model and Passive Suspension,

[34] Part I: Effect of Suspension Damping and Car Speed.' International Journal of Computer Techniques, Volume 1 Issue 2, pp 1 - 9.

[35] Gameel, H. (2011). A Study of a Dynamic Vibration Absorber Using a Magneto-Rheological Damper, PhD Thesis, Arab Academy for Science and Technology University, Alexandria, Egypt.

[36] Garcia-Pozuelo, D., Gauchia, A., Olmeda, E. and Diaz, V., 2014. Bump modeling and vehicle vertical dynamics prediction. *Advances in Mechanical Engineering*, *6*, p.736576.

[37] Gendelman, O.V., 2001. Transition of energy to a nonlinear localized mode in a highly asymmetric system of two oscillators. *Nonlinear dynamics*, *25*(1-3), pp.237-253.

[38] Gendelman, O.V., 2004. Bifurcations of nonlinear normal modes of linear oscillator with strongly nonlinear damped attachment. *Nonlinear Dynamics*, *37*(2), pp.115-128.

[39] Gendelman, O., Manevitch, L.I., Vakakis, A.F. and M'closkey, R., 2001. Energy pumping in nonlinear mechanical oscillators: Part I—Dynamics of the underlying Hamiltonian systems. *Journal of Applied Mechanics*, *68*(1), pp.34-41.

[40] Gendelman, O., Manevitch, L.I., Vakakis, A.F. and Bergman, L., 2003. A degenerate bifurcation structure in the dynamics of coupled oscillators with essential stiffness nonlinearities. *Nonlinear Dynamics*, *33*(1), pp.1-10.

[41] Gendelman, O.V., Gorlov, D.V., Manevitch, L.I. and Musienko, A.I., 2005. Dynamics of coupled linear and essentially nonlinear oscillators with substantially different masses. *Journal of Sound and Vibration*, *286*(1), pp.1-19.

[42] Gilles, T., 2004. Automotive Chassis Brakes Steering & Suspension.

[43] Gillespie, T.D., 1992. Fundamentals of Vehicle Dynamics. Warrendale, PA: Society of Automotive Engineers.

[44] Gobbi, M. and Mastinu, G., 2001. Analytical description and optimization of the dynamic behaviour of passively suspended road vehicles. *Journal of sound and vibration*, *245*(3), pp.457-481.

[45] Goldberg, D.E., 1989. Genetic Algorithms in Search, Optimization, and Machine Learning, Addison-Wesley Professional. Reading, Massachusetts, US.

[46] Gomes, H.M., 2009. A swarm optimization algorithm for optimum vehicle suspension design. In *Proceedings of 20th international congress of mechanical engineering, Brazil* (pp. 1-10).

[47] Griffin, M.J., 2007. Discomfort from feeling vehicle vibration. *Vehicle System Dynamics*, *45*(7-8), pp.679-698.

[48] Gündoğdu, Ö., 2007. Optimal seat and suspension design for a quarter car with driver model using genetic algorithms. *International Journal of Industrial Ergonomics*, *37*(4), pp.327-332.

[49] Harrison, R.F. and Hammond, J.K., 1986. Approximate, time domain, non-stationary analysis of stochastically excited, non-linear systems with reference to the motion of vehicles on rough ground. *Journal of Sound and Vibration*, *105*(3), pp.361-371.

[50] He, Y. and McPhee, J., 2007. Application of optimization algorithms and multibody dynamics to ground vehicle suspension design. *International Journal of Heavy Vehicle Systems*, *14*(2), pp.158-192.

[51] Hessling, J., 2008. Analysis and synthesis of speed limiting road humps. In *Second Meeting on Analysis of Dynamic Measurements, London* (Vol. 18, No. 11).

[52] Holland, J.H., 1992. *Adaptation in natural and artificial systems: an introductory analysis with applications to biology, control, and artificial intelligence*. MIT press.

[53] Houck, C.R., Joines, J. and Kay, M.G., 1995. A genetic algorithm for function optimization: a Matlab implementation. *Ncsu-ie tr*, *95*(09), pp.1-10.

[54] Hrovat, D., 1993. Applications of optimal control to advanced automotive suspension design. *TRANSACTIONS-AMERICAN SOCIETY OF MECHANICAL ENGINEERS JOURNAL OF DYNAMIC SYSTEMS MEASUREMENT AND CONTROL*, *115*, pp.328-328.

[55] Hrovat, D., 1997. Survey of advanced suspension developments and related optimal control applications. *Automatica*, *33*(10), pp.1781-1817.

[56] Hrovat, D. and Hubbard, M., 1981. Optimum vehicle suspensions minimizing RMS rattle space, sprung-mass acceleration and jerk. *Journal of Dynamic Systems, Measurement, and Control*, *103*(3), pp.228-236.

[57] Hullender. D. A., Modeling and Simulation of Engineering Systems, Springer-Course Notebook for Dynamic Systems Modeling.

[58] Ikenaga, S., Lewis, F.L., Campos, J. and Davis, L., 2000. Active suspension control of ground vehicle based on a full-vehicle model. In *American Control Conference, 2000. Proceedings of the 2000* (Vol. 6, pp. 4019-4024). IEEE.

[59] Inman, D.J., 2017. *Vibration with control*. John Wiley & Sons.

[60] Jutte, C.V., 2008. *Generalized synthesis methodology of nonlinear springs for prescribed load-displacement functions*. ProQuest.

[61] Kerschen, G., Vakakis, A.F., Lee, Y.S., Mcfarland, D.M., Kowtko, J.J. and Bergman, L.A., 2005. Energy transfers in a system of two coupled oscillators with essential nonlinearity: 1: 1 resonance manifold and transient bridging orbits. *Nonlinear Dynamics*, *42*(3), pp.283-303.

[62] Kerschen, G., Lee, Y.S., Vakakis, A.F., McFarland, D.M. and Bergman, L.A., 2005. Irreversible passive energy transfer in coupled oscillators with essential nonlinearity. *SIAM Journal on Applied Mathematics*, *66*(2), pp.648-679.

[63] Kerschen, G., Gendelman, O., Vakakis, A.F., Bergman, L.A. and McFarland, D.M., 2008. Impulsive periodic and quasi-periodic orbits of coupled oscillators with essential stiffness nonlinearity. *Communications in Nonlinear Science and Numerical Simulation*, *13*(5), pp.959-978.

[64] Koz'min, A.Y., Mikhlin, Y.V. and Pierre, C., 2007. Localization of energy in nonlinear systems with two degrees of freedom. *International Applied Mechanics*, *43*(5), pp.568-576.

[65] Kozmin, A., Mikhlin, Y. and Pierre, C., 2008. Transient in a two-DOF nonlinear system. *Nonlinear Dynamics*, *51*(1-2), pp.141-154.

[66] Kumar, M.S. and Vijayarangan, S., 2007. Analytical and experimental studies on active suspension system of light passenger vehicle to improve ride comfort. *Mechanics*, *65*(3), pp.34-41.

[67] Kuznetsov, A., Mammadov, M., Sultan, I. and Hajilarov, E., 2011. Optimization of a quarter-car suspension model coupled with the driver biomechanical effects. *Journal of Sound and Vibration*, *330*(12), pp.2937-2946.

[68] Lauwerys, C., Swevers, J. and Sas, P., 2005. Robust linear control of an active suspension on a quarter car test-rig. *Control Engineering Practice*, *13*(5), pp.577-586.

[69] Lee, Y.S., Kerschen, G., Vakakis, A.F., Panagopoulos, P., Bergman, L. and McFarland, D.M., 2005. Complicated dynamics of a linear oscillator with a light, essentially nonlinear attachment. *Physica D: Nonlinear Phenomena*, *204*(1), pp.41-69.

[70] Lin, J.S. and Huang, C.J., 2004. Nonlinear back stepping active suspension design applied to a half-car model. *Vehicle system dynamics*, *42*(6), pp.373-393.

[71] Macpherson, E.S., Ford Motor Co, 1953. *Wheel suspension for motor vehicles*. U.S. Patent 2,660,449.

[72] Manevitch, L.I., Gourdon, E. and Lamarque, C.H., 2007. Parameters optimization for energy pumping in strongly nonhomogeneous 2 DOF system. *Chaos, Solitons & Fractals*, *31*(4), pp.900-911.

[73] Manevitch, L.I., Gourdon, E. and Lamarque, C.H., 2007. Towards the design of an optimal energetic sink in a strongly inhomogeneous two-degree-of-freedom system. *Journal of Applied Mechanics*, *74*(6), pp.1078-1086.

[74] Mántaras, D.A., Luque, P. and Vera, C., 2004. Development and validation of a three-dimensional kinematic model for the McPherson steering and suspension mechanisms. *Mechanism and Machine Theory*, *39*(6), pp.603-619.

[75] McFarland, D.M., Bergman, L.A. and Vakakis, A.F., 2005. Experimental study of non-linear energy pumping occurring at a single fast frequency. *International Journal of Non-Linear Mechanics*, *40*(6), pp.891-899.

[76] McFarland, D.M., Kerschen, G., Kowtko, J.J., Lee, Y.S., Bergman, L.A. and Vakakis, A.F., 2005. Experimental investigation of targeted energy transfers in strongly and nonlinearly coupled oscillators. *The Journal of the Acoustical Society of America*, *118*(2), pp.791-799.

[77] Metallidis, P., Verros, G., Natsiavas, S. and Papadimitriou, C., 2003. Fault detection and optimal sensor location in vehicle suspensions. *Modal Analysis*, *9*(3-4), pp.337-359.

[78] Michalewicz, Z., 1994. GAs: What are they? In *Genetic algorithms+ data structures= evolution programs* (pp. 13-30). Springer Berlin Heidelberg.

[79] Milliken, W.F. and Milliken, D.L., 1995. *Race car vehicle dynamics* (Vol. 400, p. 16). Warrendale: Society of Automotive Engineers.

[80] Molina-Cristobal, A., Papageorgiou, C., Parks, G.T., Smith, M.C. and Clarkson, P.J., 2006, April. Multi-objective controller design: evolutionary algorithms and bilinear matrix inequalities for a passive suspension. In *13th IFAC Workshop on Control Applications of Optimization, Cachan-Paris, France* (pp. 386-391).

[81] Moran, A. and Nagai, M., 1994. Optimal active control of nonlinear vehicle suspensions using neural networks. *JSME international journal. Ser. C, Dynamics, control, robotics, design and manufacturing*, *37*(4), pp.707-718.

[82] Musienko, A.I., Lamarque, C.H. and Manevitch, L.I., 2006. Design of mechanical energy pumping devices. *Journal of vibration and control*, *12*(4), pp.355-371.

[83] Nagarkar, M.P., Patil, G.J.V. and Patil, R.N.Z., 2016. Optimization of nonlinear quarter car suspension–seat–driver model. *Journal of advanced research*, *7*(6), pp.991-1007.

[84] Omar, M., El-kassaby, M.M. and Abdelghaffar, W., 2017. A universal suspension test rig for electrohydraulic active and passive automotive suspension system. *Alexandria Engineering Journal*.

[85] Ormondroyd, J., 1928. Theory of the dynamic vibration absorber. *Transaction of the ASME*, *50*, pp.9-22.

[86] Oueslati, F. and Sankar, S., 1994. A class of semi-active suspension schemes for vehicle vibration control. *Journal of Sound and Vibration*, *172*(3), pp.391-411.

[87] Özcan, D., Sönmez, Ü. and Güvenç, L., 2013. Optimization of the nonlinear suspension characteristics of a light commercial vehicle. *International Journal of Vehicular Technology*, *2013*.

[88] Ozdalyan, B., Blundell, M.V. and Phillips, B., 1998. Comparison of suspension rig measurements with computer simulation.

[89] Panagopoulos, P.N., Gendelman, O. and Vakakis, A.F., 2007. Robustness of nonlinear targeted energy transfer in coupled oscillators to changes of initial conditions. *Nonlinear Dynamics*, *47*(4), pp.377-387.

[90] Paredes, M. and Rodriguez, E., 2009. Optimal design of conical springs. *Engineering with computers*, *25*(2), p.147.

[91] Park, J., Guenther, D.A. and Heydinger, G.J., 2003. *Kinematic suspension model applicable to dynamic full vehicle simulation* (No. 2003-01-0859). SAE Technical Paper.

[92] Patil, M.K. and Palanichamy, M.S., 1985. Minimization of human body responses to low frequency vibration: Application to tractors and trucks. *Mathematical Modelling*, *6*(5), pp.421-442.

[93] Patil, S.A. and Joshi, S.G., 2014. Experimental analysis of 2 DOF quarter-car passive and hydraulic active suspension systems for ride comfort. *Systems Science & Control Engineering: An Open Access Journal*, *2*(1), pp.621-631.

[94] Patil, V.R. and Jadhav, P.V., 2016, December. Development of Prototype of Light Passenger Quarter Car for Improved Vehicle Ride Characteristics. In *Techno-Societal 2016, International Conference on Advanced Technologies for Societal Applications* (pp. 855-867). Springer, Cham.

[95] Pazooki, A., Rakheja, S. and Cao, D., 2012. Modeling and validation of off-road vehicle ride dynamics. *Mechanical systems and signal processing*, *28*, pp.679-695.

[96] Rao, L.G. and Narayanan, S., 2008. Preview control of random response of a half-car vehicle model traversing rough road. *Journal of Sound and Vibration*, *310*(1), pp.352-365.

[97] Rahnejat, H., 1998. *Multi-body dynamics: vehicles, machines, and mechanisms*. Wiley.

[98] Renn, J.C. and Wu, T.H., 2007. Modeling and control of a new 1/4T servo-hydraulic vehicle active suspension system. *Journal of Marine Science and Technology*, *15*(3), pp.265-272.

[99] Rodriguez, E., Paredes, M. and Sartor, M., 2006. Analytical behavior law for a constant pitch conical compression spring. *Journal of Mechanical Design*, *128*(6), pp.1352-1356.

[100] Salaani, M.K., Heydinger, G.J. and Grygier, P.A., 2001. *Parameter determination and vehicle dynamics modeling for the NADS of the 1998 Chevrolet Malibu* (No. 2001-01-0140). SAE Technical Paper.

[101] Salah, A., Abbas, W. and Abouelatta, O.B., 2010. Design of optimal linear suspension for quarter car with human model using genetic algorithms.

[102] Sharp, R.S. and Hassan, S.A., 1986. The relative performance capabilities of passive, active and semi-active car suspension systems. *Proceedings of the Institution of Mechanical Engineers, Part D: Transport Engineering*, *200*(3), pp.219-228.

[103] Shirahatti, A., Prasad, P.S.S., Panzade, P. and Kulkarni, M.M., 2008. Optimal design of passenger car suspension for ride and road holding. *Journal of the Brazilian Society of Mechanical Sciences and Engineering*, *30*(1), pp.66-76.

[104] Simon, D.E., 1998. Experimental evaluation of semiactive magnetorheological primary suspensions for heavy truck applications.

[105] Spencer, B.F., Dyke, S.J., Sain, M.K. and Carlson, J., 1997. Phenomenological model for magnetorheological dampers. *Journal of engineering mechanics*, *123*(3), pp.230-238.

[106] Taffo, G.K., Siewe, M.S. and Tchawoua, C., 2016. Stability switches and bifurcation in a two-degrees-of-freedom nonlinear quarter-car with small time-delayed feedback control. *Chaos, Solitons & Fractals*, *87*, pp.226-239.

[107] Tanese, R., 1989. Distributed genetic algorithms for function optimization.

[108] Thite, A.N., Coleman, F., Doody, M. and Fisher, N., 2017. Experimentally validated dynamic results of a relaxation-type quarter car suspension with an adjustable damper. *Journal of Low Frequency Noise, Vibration and Active Control*, *36*(2), pp.148-159.

[109] Timoshenko, Stephen P., and James M. Gere. "Théorie de la stabilité élastique." *Paris: Dunod,| c1966, 2eme ed.* (1966).

[110] Trom, J.D., Lopez, J.L. and Vanderploeg, M.J., 1987. Modeling of a mid-size passenger car using a multibody dynamics program. *Journal of Mechanisms, Transmissions, and Automation in Design*, *109*(4), pp.518-523.

[111] Tsakirtzis, S., Kerschen, G., Panagopoulos, P.N. and Vakakis, A.F., 2005. Multi-frequency nonlinear energy transfer from linear oscillators to mDOF essentially nonlinear attachments. *Journal of Sound and Vibration*, *285*(1), pp.483-490.

[112] Quinn, D.D, Vakakis, A.F., Gendelman, O.V., Bergman, L.A., Kerschen, G. and. Sapsis, T.P., 2009. Efficiency of targeted energy transfers in coupled nonlinear oscillators associated with 1: 1 resonance captures: Part II, analytical study. *Journal of Sound and Vibration*, *325*(1), pp.297-320.

[113] Watts, P., 1883. On a method of reducing the rolling of ships at sea. *Trans. INA*, *24*.

[114] Wahl, A. 1963. Mechanical springs. McGraw=Hill book company, Inc.

[115] Wu, M.H. and Hsu, W.Y., 1998. Modelling the static and dynamic behavior of a conical spring by considering the coil close and damping effects. *Journal of Sound and Vibration*, *214*(1), pp.17-28.

[116] Unaune, D., Pawar, M. and Mohite, S., 2011, November. Ride analysis of quarter vehicle model. In *Proceedings of the First International Conference on Modern Trends in Industrial Engineering, Surat, Gujarat, India*.

[117] Vakakis, A.F., 2001. Inducing passive nonlinear energy sinks in vibrating systems. *Journal of Vibration and Acoustics*, *123*(3), pp.324-332.

[118] Vakakis, A.F. and Gendelman, O., 2001. Energy pumping in nonlinear mechanical oscillators: part II—resonance capture. *Journal of Applied Mechanics*, *68*(1), pp.42-48.

[119] Vakakis, A.F. and Rand, R.H., 2004. Non-linear dynamics of a system of coupled oscillators with essential stiffness non-linearities. *International Journal of Non-Linear Mechanics*, *39*(7), pp.1079-1091.

[120] Vakakis, A.F., Gendelman, O.V., Bergman, L.A., McFarland, D.M., Kerschen, G. and Lee, Y.S., 2009. Nonlinear Targeted Energy Transfer in Discrete Linear Oscillators with Single-DOF Nonlinear Energy Sinks. *Nonlinear Targeted Energy Transfer in Mechanical and Structural Systems*, pp.93-302.

[121] Venkateswarulu, E. and Ramesh, N., 2014. raju., Seshadri G. The active suspension system with hydraulic actuator for half car model analysis and self-tuning with PID controllers. *International Journal of Research in Engineering and Technology*, *3*, p.415.

[122] Verros, G., Natsiavas, S. and Papadimitriou, C., 2005. Design optimization of quarter-car models with passive and semi-active suspensions under random road excitation. *Modal Analysis*, *11*(5), pp.581-606.

[123] Vetturi, D., Gadola, M., Cambiaghi, D. and Manzo, L., 1996. *Semi-active strategies for racing car suspension control* (No. 962553). SAE Technical Paper.

[124] Yao, G.Z., Yap, F.F., Chen, G., Li, W. and Yeo, S.H., 2002. MR damper and its application for semi-active control of vehicle suspension system. *Mechatronics*, *12*(7), pp.963-973.

[125] Zavadinka, P. and Krišśák, P., 2009. Modeling and simulation of mobile working machine powertrain. *Technical Computing Prague*, *19*, p.2009.

[126] Zhao, D., 2016. *Investigation and modelling of tremor reducer with the technology of targeted energy transfer* (Doctoral dissertation, Aston University).

[127] Zhao, L., Zhou, C., Yu, Y. and Yang, F., 2017. An analytical formula of driver RMS acceleration response for quarter-car considering cushion effects. *Vehicle System Dynamics*, *55*(9), pp.1283-1296.